U.S. Department
of Transportation
National Highway
Traffic Safety
Administration

NHTSA

DOT HS 813 518

November 2023

Pedestrian Safety: Assessment of Crashworthiness Test Procedures

DISCLAIMER

This publication is distributed by the U.S. Department of Transportation, National Highway Traffic Safety Administration, in the interest of information exchange. The opinions, findings, and conclusions expressed in this publication are those of the authors and not necessarily those of the Department of Transportation or the National Highway Traffic Safety Administration. The United States Government assumes no liability for its contents or use thereof. If trade or manufacturers' names or products are mentioned, it is because they are considered essential to the object of the publication and should not be construed as an endorsement. The United States Government does not endorse products or manufacturers.

NOTE: This report is published in the interest of advancing motor vehicle safety research. While the report may provide results from research or tests using specifically identified motor vehicle models, it is not intended to make conclusions about the safety performance or safety compliance of those motor vehicles, and no such conclusions should be drawn.

Suggested APA Format Citation:

Hu, J., Lin, Y.-S., Boyle, K., Bonifas, A., Reed, M. P., Gupta, V., & Lin, C.-H. (2023, November). *Pedestrian safety: Assessment of crashworthiness test procedures* (Report No. DOT HS 813 518). National Highway Traffic Safety Administration.

Technical Report Documentation Page

1. Report No.	2. Government Accession No.	3. Recipient's Catalog No.
DOT HS 813 518		

4. Title and Subtitle	5. Report Date
Pedestrian Safety: Assessment of Crashworthiness Test Procedures	November 2023
	6. Performing Organization Code

7. Authors	8. Performing Organization Report No.
Jingwen Hu (https://orcid.org/0000-0001-6477-0360), Yang-Shen Lin, Kyle Boyle, Anne Bonifas, Matthew P. Reed, Vishal Gupta, Chin-Hsu Lin	UMTRI 2023-XXUMTRI 2023-XX

9. Performing Organization Name and Address	10. Work Unit No.
University of Michigan Transportation Research Institute Ann Arbor, MI 48109 General Motors, Warren, MI 48092	11. Contract or Grant No. 693JJ9-21-F-000160 (21-D-000021) pr_21-RQ-000507

12. Sponsoring Agency Name and Address	13. Type of Report and Period Covered
National Highway Traffic Safety Administration 1200 New Jersey Avenue SE Washington, DC 20590	Final
	14. Sponsoring Agency Code

15. Supplementary Notes

16. Abstract

The objective of this study is to use finite element (FE) pedestrian and vehicle models to evaluate pedestrian interactions with vehicles equipped with pop-up hoods. To do so, we generated a virtual database of pedestrian impacts with a wide range of vehicle front-end geometries; developed prediction models for pedestrian head impact time (HIT) which is important to evaluate the response time of pop-up hood designs; and investigated effects of pop-up hood design parameters on pedestrian head injury responses.

The generic vehicle (GV) models used in Euro NCAP originally developed based on European vehicles were morphed into 20 U.S. vehicle front-end geometries across a wide range of vehicle types and characteristics. A total of 240 pedestrian impact simulations were conducted using the 20 morphed GV models with four sizes of pedestrian human body models (6-year-old, small female, midsize male, and large male) at three impact speeds (30, 40, and 50 kph). A set of predictors were selected based on the literature to predict HIT, head contact velocity, and head contact angle. High correlations and good model accuracies were achieved in the prediction models.

Simulations with the pop-up hood design found that a deployed hood could potentially collapse due to kinetic energy of a pedestrian under certain circumstances. Among the selected design parameters, actuator stiffness at the time of head contact with a pop-up hood is the biggest contributor for the pop-up hood design to avoid hood collapse. Due to the variations of kinetic energy provided by different sizes of the pedestrian, the deployment system of a pop-up hood needs to be designed for the highest pedestrian stature for avoiding hood collapse. With deployment system design as per the highest pedestrian stature, head injury criterion (HIC) for a smaller pedestrian may slightly increase, but it is still lower compared to an undeployed hood for the vehicles used in this study.

This study is not intended to suggest that a pop-up hood is the only way for every vehicle to meet pedestrian safety requirements. Passive hoods can also be designed to meet pedestrian safety requirements.

17. Key Words	18. Distribution Statement
Pedestrian safety, pop-up hood, finite element model, vehicle front-end geometry, head impact time, virtual pedestrian crash database, hood collapse, mesh morphing	This document is available to the public from the DOT, BTS, National Transportation Library, Repository & Open Science Access Portal, https://rosap.ntl.bts.gov.

19. Security Classif. (of this report)	20. Security Classif. (of this page)	21. No. of Pages	22. Price
		91	

Form DOT F 1700.7 (8-72) Reproduction of completed page authorized

Table of Contents

Introduction **1**
Pedestrian Injuries and Pop-Up Hood Design 1
Regulated or Consumer Information Testing Protocols on Pop-Up Hood Designs 1
Research Gap 2
Research Objectives 3

Task 1: Literature Review **4**
Potential Variables That May Affect HIT 4
Recent Testing and Modeling Studies on HIT and Associated Variables in Pedestrian Impacts 8
Discussion and Summary 14

Task 2: Simulations and Prediction Model to Determine HIT **16**
Generic Vehicle (GV) and Pedestrian Models 16
U.S. Vehicle Front-End Geometries 17
GV Models Morphed Into Different U.S. Vehicle Geometries 18
HIT Comparison Between the Morphed GV Models and Vehicle Models 20
Simulation Matrix and Setup 20
Assessment of Simulation Results 21
Virtual Database of Pedestrian Impacts 22
Simulation Matrix 22
Simulation Results 22
Data Trends on HIT, HeadV, and HVAng 24
Development of HIT Prediction Models 26
Prediction Models for Head Contact Velocity 29
Prediction Models for Head Velocity Angle 29

Task 3: Simulations for Hood Edge Impact With a Pop-Up Hood **31**
Pop-Up Hood Model 31
Simulation in a Hood Edge Impact Scenario 33

Task 4: Simulations in a Hood Collapse Scenario **35**
Selection of a Hood Collapse Case 35
Parametric Simulations in the Hood Collapse Scenario 35

Summary **37**

References **38**

Appendix A: Simulation Results (HIT, WAD, HeadV, HVAng) **A-1**

List of Figures

Figure 1. Fatality risk as a function of impact speed in vehicle-to-pedestrian crashes (Rosen et al., 2011) 5
Figure 2. Distributions of pedestrian injuries and injury sources by vehicle type (data from Longhitano et al., 2005) 6
Figure 3. Fatality risk per crash as a function of pedestrian age (Kim et al., 2008) 7
Figure 4. Headform test zones based on wrap around distance (Euro NCAP 2012b) 8
Figure 5. Head contact time (HC1 and HC2) and contact locations in (Kerrigan et al., 2012) 8
Figure 6. Exemplar impact locations and WAD values under 40 km/h pedestrian impact (Peng et al., 2012) 9
Figure 7. Exemplar impact locations and HIT values under various impact conditions (Watanabe et al., 2012) 10
Figure 8. HIT values reported in (Elliott et al., 2012) 10
Figure 9. Relationship between impact speed and HIT (Peng et al., 2013) 11
Figure 10. Model-predicted HIT values and simulation conditions (Chen et al., 2015) 12
Figure 11. Pedestrian impact simulations and prediction model of HIT by (Bhattacharjee et al., 2017) 12
Figure 12. HIT values reported in (Song et al., 2017), TIR 01-05: SUV, TIR 06-08: Van, TIR 09-11: Sedan 13
Figure 13. Effects from impact speed, vehicle type, and pedestrian size on HIT values (Decker et al., 2019) 13
Figure 14. Simplistic view of HIT and associated variables 14
Figure 15. GV models from https://cloud.tugraz.at/index.php/s/ehzfzo3CIoZLy0c 16
Figure 16. GHBMC simplified pedestrian models and latest versions 17
Figure 17. Process to scan a vehicle front-end geometry and reconfigure/morph a GV model to the scanned vehicle geometry 18
Figure 18. Morphed GV models representing the U.S. vehicle front-end geometries 19
Figure 19. PCA results for the U.S. vehicle front-end geometries (Bounds of the figures on the right represent geometries with PC scores of mean ± 2 standard deviations.) 20
Figure 20. HIT comparison between the morphed GV models and FE vehicle models (Delta HIT = $HIT_{morphed\text{-}GV} - HIT_{vehicle\text{-}model}$) 21
Figure 21. Exemplar pedestrian kinematic comparisons between morphed GV models and vehicle models 22
Figure 22. Examples of pedestrian simulation results with varied vehicle geometry, pedestrian size, and impact speed 23
Figure 23. An example of automated simulation results for pedestrian simulations 23
Figure 24. Factor effects on HIT and WAD ranges by pedestrian 24
Figure 25. Factor effects on HeadV 25
Figure 26. Factor effects on HVAng 25
Figure 27. Definitions of hood height, hood length, and hood angle 26
Figure 28. Error analysis for the HIT prediction models 27
Figure 29. Error analysis for the HIT prediction models (without pedestrian stature) 27

Figure 30. Error analysis for the HeadV prediction models 29
Figure 31. Error analysis for the HeadVAng prediction models 30
Figure 32. Error analysis for the HeadVAng prediction models with only the adult pedestrians..... 30
Figure 33. Pop-up hood model validation results against headform impact tests at different hood locations 31
Figure 34. Headform acceleration comparison between tests and simulations of the GM pop-up hood design..... 32
Figure 35. CT4 pop-up hood model actuator system and exemplar simulation with GHBMC pedestrian model 33
Figure 36. Two hood edge impact scenarios with M50 GHBM at 40 kph..... 34
Figure 37. Pop-up hood design #8 evaluation results with varied HBM size..... 36

List of Tables

Table 1. Sources of IHRA pedestrian AIS 2+ injuries by body region, adults (age>15) (Mizuno, 2005) 6
Table 2. Sources of IHRA pedestrian AIS 2+ injuries by body region, children (age≤15) (Mizuno, 2005) 6
Table 3. HIT/pop-up hood deploying time(Pal et al., 2014) 11
Table 4. Variables and their effects on HIT prediction 15
Table 5. Category mapping between GV models and U.S. vehicles 18
Table 6. Model coefficients and significant levels for the four HIT prediction models 28
Table 7. HIT comparison of a future BEV between the FE simulations and prediction models 28
Table 8. Pedestrian simulation results by varing pop-up hood design parameters 35

Introduction

Pedestrian Injuries and Pop-Up Hood Design

Pedestrian injuries in road traffic are an increasing public-health problem worldwide. Every year over 1.2 million people die and 20 to 50 million people are injured in motor vehicle crashes around the world, and pedestrians account for more than a third of them (WHO, 2009). In the United States, the percentage of pedestrian fatalities among total fatalities from traffic crashes was 17 percent in 2020 and has been on the rise steadily for the past decade (NHTSA, 2022).

Prior research has shown that head injuries are the most common injuries in pedestrian impacts along with lower-extremity injuries, and vehicle hood/bonnet contacts account for a significant portion of pedestrian head injuries (Martin et al., 2011; Mizuno, 2005; Yang, 2005). Numerous studies have demonstrated the effectiveness of redesigning the hood structure to achieve a more yielding stiffness profile and better energy-absorbing efficiency (Belingardi et al., 2009; Kerkeling et al., 2005; Liu et al., 2009). However, even with new hood-structure designs and their increased energy-absorbing efficiency, "bottoming out" during a pedestrian head impact is possible due to limited under-hood clearance and hood stiffness. This is especially true for sports cars, in which the hood is typically lower to achieve better aerodynamics, styling, and visibility. Pop-up hoods that deploy upward in the early stages of a pedestrian crash are designed to address this problem. Several previous studies have presented designs and evaluated the effectiveness of a pop-up hood system (Evrard, 2011; Fredriksson et al., 2001; Huang & Yang, 2010; Inomata et al., 2009; Lee et al., 2007; Oh et al., 2008a; Shin et al., 2008). Such a system provides additional space between the hood and the rigid components beneath by raising the rear of the hood before a pedestrian head contact. As a result, a larger hood deformation and hence greater energy absorption can be accommodated without bottoming out while reducing the head impacting force, acceleration, and head injury risk in pedestrian crashes.

Regulated or Consumer Information Testing Protocols on Pop-Up Hood Designs

Current test procedures do not have an objective means to assess active systems, such as pop-up hoods, that deploy upon striking a pedestrian. In Global Technical Regulation (GTR) No. 9, Pedestrian Safety, a safety assessment is specified for non-deployable hoods that involves launching a hemispherical headform instrumented at 35 km/h with a triaxial accelerometer into the hood of a vehicle sitting at rest. The requirement is Head Injury Criterion (HIC), determined over a 15 ms window, must be less than 1000 or 1700 depending on the targeted area. However, these procedures do not provide an appropriate means to account for pop-up hood deployment, including the timing of the activation.

The United Nations Economic Commission for Europe (UNECE) World Forum for Harmonization of Vehicle Regulations (WP.29) and a new Informal Working Group (IWG) have been working on testing protocols for performing headform tests on vehicles with pop-up hoods. Specifically, a testing protocol draft amendment was developed to include the triggering and sensing capabilities of the pop-up hood system. The draft amendment also stipulates that the head impact time (HIT) is to be determined by the manufacturer using computer modeling. The HIT is determined using crash simulations between the manufacturer's own vehicle model and prescribed human body models of a 6-year-old (YO), a 5th percentile female (F05), a 50th percentile male (M50), and a 95th percentile male (M95). HIT values are to be reported to (and confirmed with) the test authority. For each pedestrian size, a HIT is determined by modeling a

pedestrian walking perpendicular to the vehicle with an impact at the hood centerline at a speed of 40 km/h.

Similar to UNECE, the European New Car Assessment Program (Euro NCAP) assessment of pop-up hoods for pedestrian protection has adopted a hybrid approach including both physical testing and human modeling (Euro NCAP, 2018a). The simulations with the pedestrian models are used to derive inputs for the subsequent physical assessment using conventional headform impactors. The head impact locations and HITs for several pedestrian sizes are determined to assess whether the system is fully deployed at the time of the head impact for the most critical pedestrian size. Based on that result, the hood is impacted with the headform impactors in deployed, undeployed, or dynamic deploying state (location dependent) in the physical test. The hood deflection due to the loading can be simulated to prove that the head protection is not compromised by a collapse of the hood. These simulations must be carried out at varying impact speeds with several sizes of the pedestrian models (6YO, F05, M50, and M95).

Currently, Euro NCAP accepts the results generated by various pedestrian models, as listed in the Technical Bulletin (TB) 024 (Euro NCAP, 2019). However, pedestrian models must be certified through a standardized set of boundary conditions. The certification process involves simulating the pedestrians through a series of impacts with four previously published generic vehicle (GV) geometries at three impact speeds (30, 40, and 50 km/h) (Klug et al., 2017). Three kinematic trajectories from designated anatomical locations on the pedestrian models and total contact force between the pedestrian and vehicle are then compared to a standardized set of corridors to determine whether the model passes certification. Additionally, HIT must fall within a specified range for each simulation. Numerous guidelines regarding posture and pre-simulation checks are also specified.

Although the current pedestrian headform impact tests only consider static hood states (deployed or undeployed), future regulations or consumer information tests could include dynamic pop-up hood deployment into the headform impact testing protocols. In this case, the timing of the pop-up hood deployment and the time that the head hits the hood will become critical, which could potentially affect the headform impact response and safety evaluation. Therefore, understanding variables that could affect HIT values and prediction models that can estimate HIT based on pedestrian, vehicle, and crash conditions are necessary.

Research Gap

The computational human modeling approach proposed by IWG to predict HIT would be challenging to implement in a U.S. Federal regulation. NHTSA safety standards are enforced through NHTSA independently performing compliance testing without need from input vehicle manufacturers. The use of computer simulation as part of vehicle development is well established. However, their use within the context of a Federal Motor Vehicle Safety Standard (FMVSS) would be unprecedented and would raise many novel enforcement issues. Therefore, an alternative approach that can objectively determine HITs based on well-defined and measurable vehicle front-end characteristics is needed for U.S. vehicles. Thus far, all the pedestrian testing protocols were initiated in Europe. As a result, the generic vehicle models used to certify human body models were developed based on European vehicles. The distribution of vehicle sizes and shapes in the United States is significantly different from that of European vehicles. Larger SUVs and pickup trucks are much more popular in the United States than in Europe yet are not represented by the four generic vehicle categories. Moreover, there is a lack

of data and knowledge on how vehicle front-end geometries (particularly for a wide range of U.S. vehicles) may affect HITs in pedestrian crashes and how pop-up hood design parameters may affect pedestrian injury risks.

Research Objectives

The objectives of this NHTSA-funded research were to 1) use finite element (FE) pedestrian models and a large set of vehicle models to generate a virtual database of HITs, which were used to develop prediction models using objective, well-defined, and measurable vehicle front-end characteristics, pedestrian size, and impact speed to predict HITs, and 2) investigate effects from pop-up hood design parameters on pedestrian injury risks. The following specific tasks were conducted:

- Task 1: Fleet survey and literature summary
- Task 2: Simulations and prediction model to determine HIT
- Task 3: Simulations for hood edge impact with a pop-up hood
- Task 4: Simulations in a hood collapse scenario

Specifically, Task 1 identified any variables (crash characteristics, vehicle properties, and pedestrian demographics) that may affect HIT in vehicle-to-pedestrian impacts and identified modeling and testing data available for predicting HITs in vehicle-to-pedestrian impacts. Task 2 focused on developing a virtual database of HITs using FE simulations and developing a prediction function using objective, well-defined, and measurable vehicle front-end geometry, pedestrian size, and impact speed to predict HITs. Task 3 focused on simulations of a single pedestrian-to-vehicle impact on the edge of the hood with and without pop-up hood. Task 4 focused on a parametric study for investigating the effects of design parameters on pop-up hood design performance.

Task 1: Literature Review

The goals of this literature review are to 1) identify any variables (crash characteristics, vehicle properties, and pedestrian demographics) that may affect HIT in vehicle-to-pedestrian impacts, and 2) identify modeling and testing data available for predicting HITs in vehicle-to-pedestrian impacts. The literature databases included Medline (biomedical literature), Scopus (covering most engineering and biomedical literature), and papers published at the conference on the Enhanced Safety of Vehicles (not covered by Medline and Scopus).

Potential Variables That May Affect HIT

UMTRI conducted a comprehensive literature review in 2015 on "designing pedestrian-friendly vehicles" (Hu and Klinich, 2015). Although HIT was not the focus in that review, there are specific sections covering the sources of pedestrian head injuries, risk factors associated with pedestrian head injuries, and vehicle designs for reducing pedestrian head injuries. Many findings there can be applied to define variables that may affect HIT. Moreover, the PhD dissertation from Klug (2018) presented a comprehensive study on many parameters that may affect HIT through computational simulations with the GV models and two human body models (i.e., THUMS and GHBMC). Two tables (Appendix Table A-1 and Table A-2) were also provided for summarizing prior post-mortrem human subject (PMHS) testing (n=24) and human modeling (n=10) studies related to vulnerable road users (bicyclists and pedestrians), which served as a good resource for this literature review.

Based on the studies, the variables investigated in this literature review are below. These variables are important for predicting pedestrian head injury risks in general and are expected to affect HIT values.

- Vehicle-to-pedestrian impact speed
- Vehicle type / front-end geometry
- Vehicle impact location
- Vehicle-to-pedestrian friction
- Pedestrian size
- Pedestrian age
- Pedestrian posture (gait and arm)
- Pedestrian impact angle
- Wrap around distance (WAD)

Vehicle-to-pedestrian impact speed: Impact speed is the most significant crash factor affecting injury risk in vehicle-to-pedestrian crashes. Although the strong correlation between the impact speed and pedestrian injury risk has been well established based on pedestrian crash data (Anderson et al., 1997; Ashton & Mackay, 1979; Cuerden et al., 2007; Davis, 2001; Kong & Yang, 2010; Oh et al., 2008b; Pasanen & Salmivaara, 1993; Rosen & Sander, 2009; Yaksich, 1964), the absolute pedestrian injury risk as a function of impact speed still needs further investigation. Specifically, a literature review (Rosen et al., 2011) found that studies conducted before 2000 were all based on direct analyses of data with oversampling of severe and fatal injuries, resulting in overestimation of pedestrian fatality risks. On the other hand, more recent studies based on less biased data provided substantially lower risk estimates than those previously reported. Figure 1 shows the variations associated with fatality risk functions among different studies. Regardless of the absolute values of fatality risks, there is a consensus that

pedestrian fatality risk increases monotonically with vehicle impact speed. Considering head injuries are one of the main causes of fatalities in pedestrian impacts, impact speed should be considered in any studies related to pedestrian head injury mitigation, including HIT prediction. Intuitively, a higher impact speed will lead to an earlier HIT after controlling other confounding factors.

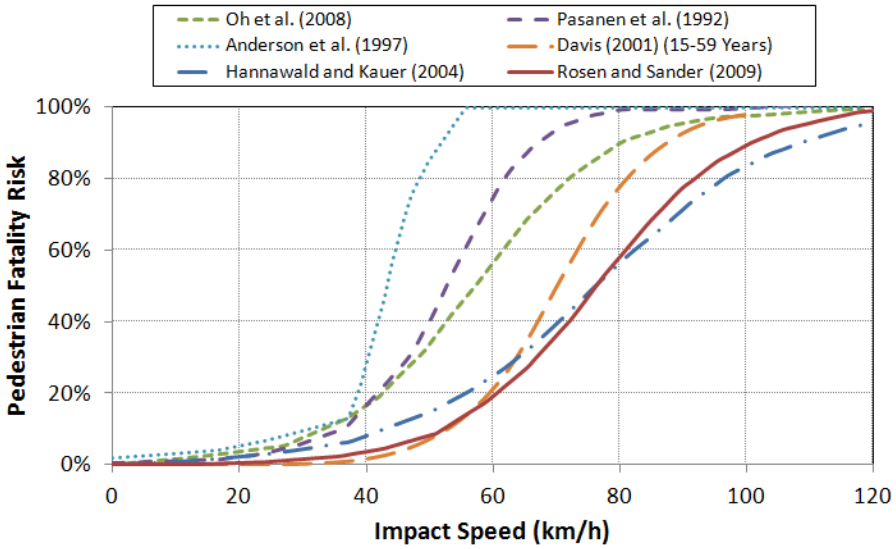

Figure 1. Fatality risk as a function of impact speed in vehicle-to-pedestrian crashes (Rosen et al., 2011)

Vehicle type: Many previous studies have shown that vehicle type has a strong effect on pedestrian-injury and fatality risk (Desapriya et al., 2010; Hu et al., 2023; Lefler & Gabler, 2004; Longhitano et al., 2005; Paulozzi, 2005; Roudsari et al., 2004). Light truck vehicles (LTVs), including pickup trucks, vans, and SUVs, were reported to be associated with higher risk of serious pedestrian injuries and fatality risk than sedans (Hu et al., 2023; Roudsari et al., 2004). Furthermore, LTVs result in different pedestrian-injury patterns and injury sources than those from sedans. Although the head is the most injured body region for both LTVs and sedans, the lower-extremity region is the second for sedans, whereas the torso is the second for LTVs. The most frequent injury sources for sedans are the windshield and the bumper, not the hood, while it is the hood and hood leading edge for LTVs. Desapriya et al. (2010) performed a literature review to quantify the vehicle type on fatal pedestrian injuries based on 11 previous studies. The overall pooled data led to an odds ratio of 1.54 for fatal pedestrian injuries with LTVs compared with cars. Figure 2 provides a more detailed view of the injury-pattern and injury-source differences between LTVs and sedans. Overall, LTVs cause more injuries throughout the whole body of a pedestrian than sedans, but LTVs showed disproportionally higher head injury risks associated with the hood than sedans. Compared with sedans, LTVs are generally stiffer, higher, and with a more vertical front profile. These variables are likely the major reasons for the difference in pedestrian-injury risk, and it was expected that HIT values are lower for LTVs than sedans after controlling other confounding factors. Hoods account for a higher proportion of pedestrian head injuries for LTVs than for sedans, and thus, all other things equal, pop-up hood designs may be more useful for LTVs than sedans. However, the relative need for pop-up hoods as a head impact countermeasure on sedans versus LTVs may be affected by other factors, such as hood clearance from under-hood hard structures.

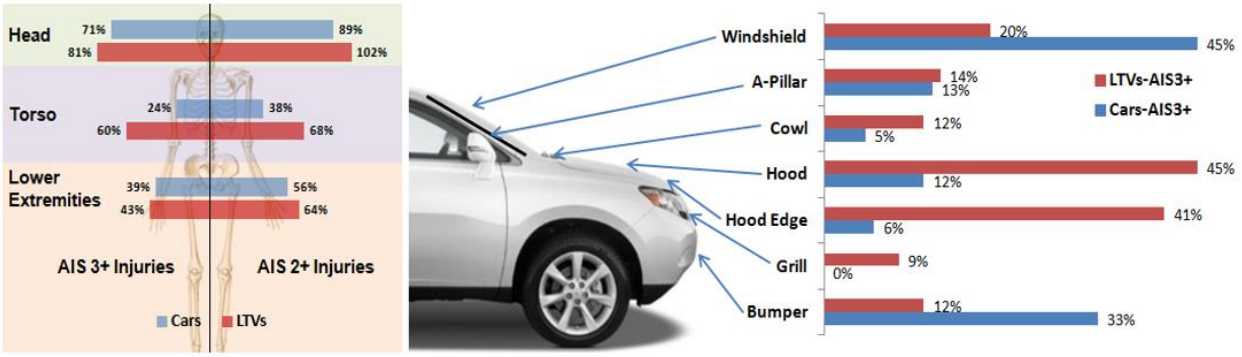

Figure 2. Distributions of pedestrian injuries and injury sources by vehicle type (data from Longhitano et al., 2005)

Pedestrian size: Pedestrian size is an important factor affecting the injury sources and risks in pedestrian impacts. Tables 1 and 2 summarize the sources of pedestrian AIS 2+ injuries for adults and children, respectively, based on data from International Harmonized Research Activities (IHRA) (Mizuno, 2005). Children and adults show different injury sources mainly because of differences in their stature and the associated WAD. For example, head injuries for children are more commonly induced by the hood rather than the windshield and A-pillar, the latter two being the most common injury sources for adult head injuries. As a result, pop-up hood designs may be more effective for children and shorter adults. When estimating HIT values, pedestrian stature is clearly a significant variable: shorter pedestrians will experience lower HIT than taller pedestrians.

Table 1. Sources of IHRA pedestrian AIS 2+ injuries by body region, adults (age>15) (Mizuno, 2005)

Body Region		Head	Face	Neck	Chest	Abdomen	Pelvis	Arms	Legs	Unknown	Total
Part of the Vehicle	Bumper	20	2	0	2	3	3	3	572	0	605
	Hood	140	9	1	122	39	35	73	28	1	448
	Hood leading edge	7	2	1	36	65	80	28	109	0	328
	Windshield	303	52	11	28	3	10	22	3	0	432
	A-pillar	159	28	5	34	7	14	29	6	2	284
	Front Panel	0	1	0	8	13	6	5	63	0	96
	Others	33	7	0	29	9	12	11	54	0	155
	Sub-Total	662	101	18	259	139	160	171	835	3	2348
Indirect		12	0	16	1	0	7	0	6	0	42
Road		125	18	2	21	2	8	32	32	1	241
Unknown		19	6	3	18	9	16	20	45	6	142
Total		818	125	39	299	150	191	223	918	10	2773

Table 2. Sources of IHRA pedestrian AIS 2+ injuries by body region, children (age≤15) (Mizuno, 2005)

Body Region		Head	Face	Neck	Chest	Abdomen	Pelvis	Arms	Legs	Unknown	Total
Part of the Vehicle	Bumper	4	0	0	1	2	0	3	89	1	100
	Hood	83	6	1	17	5	8	13	2	0	135
	Hood leading edge	8	0	3	7	13	5	7	18	0	61
	Windshield	41	4	1	2	2	2	1	1	1	55
	A-pillar	9	0	0	1	0	0	2	0	0	12
	Front Panel	5	0	0	1	0	1	1	9	0	17
	Others	12	0	1	9	3	1	4	32	0	62
	Sub-Total	162	10	6	38	25	17	31	151	2	442
Indirect		1	0	1	0	1	0	1	3	0	4
Road		46	4	0	1	0	1	10	1	0	63
Unknown		8	0	0	1	1	0	5	7	1	23
Total		217	14	7	40	27	18	47	162	3	532

Pedestrian age: Pediatric and elderly pedestrians are overrepresented in vehicle-to-pedestrian crashes (Martin et al., 2011). IHRA data showed that children younger than 15 accounted for over 31 percent of all vehicle-to-pedestrian crashes in the United States, Germany, Japan, and Australia, although they only accounted for 18 percent of the overall population in those countries. Although older individuals did not show a high incidence rate in the IHRA data, they are more likely to suffer severe injuries in pedestrian crashes (Mizuno, 2005). U.S. studies have also reported similar trends with children sustaining the highest incidence rate (Lee & Abdel-Aty, 2005), and the elderly sustaining the highest severe-injury and fatality rate in pedestrian crashes (Demetriades et al., 2004; Henary et al., 2006; Kim et al., 2008). The high involvement of children in pedestrian crashes is largely a consequence of their lack of experience and safety awareness, as well as their small body size, which can make them more difficult for drivers to see; the high injury and fatality rate of the older population is mostly due to their age-related morphological and physiological changes. Figure 3 shows estimated fatal-injury probabilities per crash as a function of pedestrian age (Kim et al., 2008). Age plays a significant role in determining the injury risk in pedestrian crashes, which is consistent with other types of vehicular crashes (Hu et al., 2007; Kent et al., 2005a; Morris et al., 2002). Injury biomechanics literature has shown that older people are more fragile than younger adults, meaning they tend to sustain more severe injuries at a given level of impact loading (Kent et al., 2005b; Laituri et al., 2005; Zhou et al., 1996). This also means older people tend to sustain worse outcomes from a given injury than younger adults (Kent et al., 2009; Li et al., 2003). Although literature has clearly shown significant age effects on pedestrian injury risks, it is not clear how age could affect HIT.

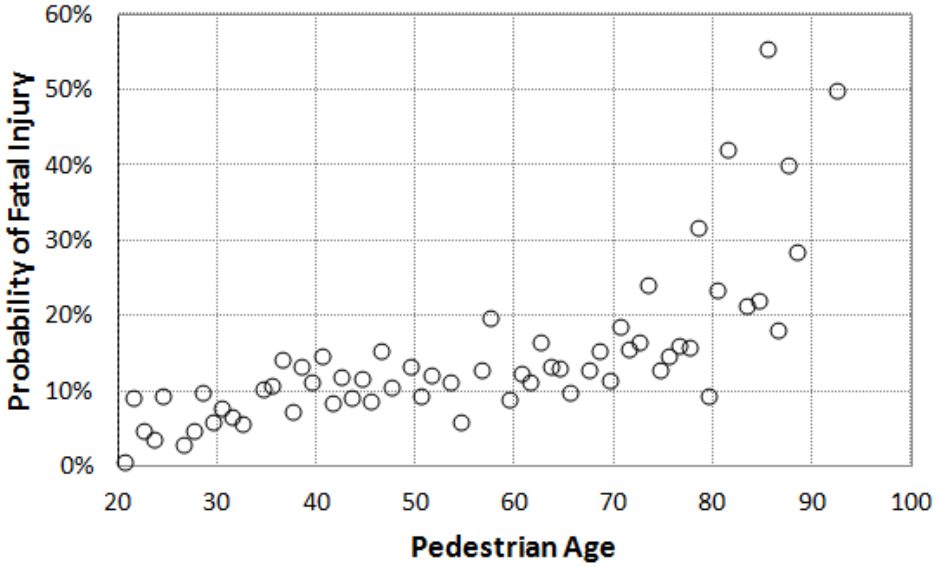

Figure 3. Fatality risk per crash as a function of pedestrian age (Kim et al., 2008)

WAD: WAD is often used to define pedestrian-to-vehicle impact locations. For example, Euro NCAP pedestrian tests include legform-to-bumper tests, upper-legform-to-hood-leading-edge tests, and child/adult-headform-to-hood/windshield tests. The headform test area is defined based on the pedestrian WAD as shown in Figure 4, in which child and adult headform test zones are separated. The test zones cover almost the full width of the vehicle, so that the overall pedestrian protection can be evaluated throughout the vehicle front-end structures. Since the WAD is highly

correlated to the traveling distance of the head of a pedestrian in a vehicle-to-pedestrian impact, it should also be highly correlated to the HIT value after controlling confounding factors.

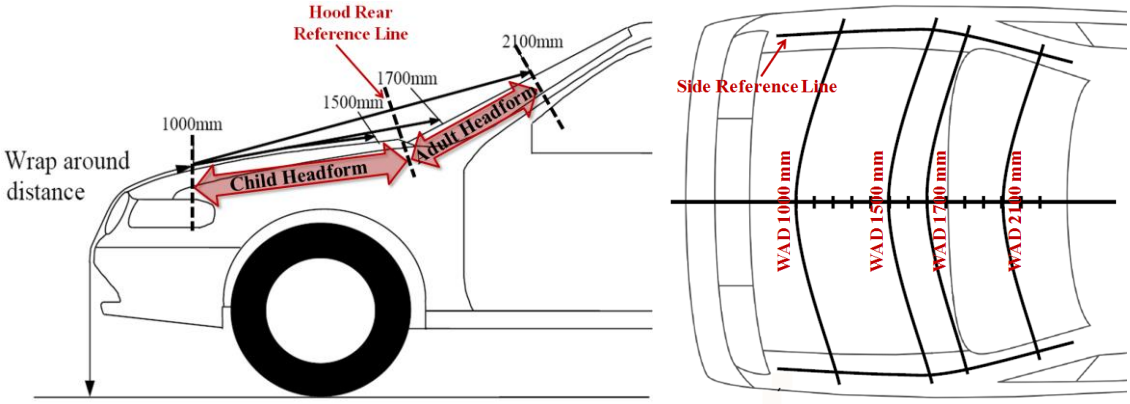

Figure 4. Headform test zones based on wrap around distance (Euro NCAP 2012b)

Other impact condition factors: Impact condition factors, including vehicle impact location, vehicle-to-pedestrian friction, pedestrian posture, and pedestrian angle should affect HIT to some extent. However, such factors may not be as significant as the variables in affecting HIT.

Recent Testing and Modeling Studies on HIT and Associated Variables in Pedestrian Impacts

Since the pop-up hood testing protocol was introduced not long ago, most studies addressing HIT and variables affecting HIT are recent work using physical testing or computational modeling.

Kerrigan et al. (2012) conducted a total of 15 full-scale PMHS and anthropomorphic test device (ATD) pedestrian to vehicle impact tests with small sedan (n=8) and large SUV (n=7) at 40 km/h. Although the study focused on PMHS and ATD kinematics and injury risks for the whole-body, HIT values were reported, indicating a significant difference between the sedan and SUV. In particular, the HITs are significantly higher with the small sedan than the large SUV (Figure 5). The results also showed a strong correlation between HIT and WAD.

Test	WAD (mm)	Impact Velocity (m/s)	HIC15	t1-HIC15 (ms)	t2-HIC15 (ms)	HC1 (ms)	HC2 (ms)
Sed D1	1930	14.69	1437	123.6	138.6	124	125
Sed D2	1940	13.30	1447	122.3	137.3	123	124
Sed D3	1970	13.88	1321	125.4	140.4	127	128
Sed DA1	1970	15.89	1749	122.6	137.6	122	123
Sed DA2	2130	15.31	1091	131.4	146.4	133	134
Sed P1	2410	13.56	824	147.3	162.3	151	152
Sed P2	2200	14.48	3647	135.3	139.4	134	135
Sed P3	2320	11.80	511	138.8	153.8	141	142
SUV D1	1685	9.29	577	92.4	107.4	98	99
SUV D2	1660	10.45	826	85.2	100.2	93	94
SUV D3	1665	9.29	752	84.7	99.7	93	94
SUV DA1	1700	11.39	1704	87	102	93	94
SUV DA2	1850	12.03	1642	94.8	109.8	99	100
SUV P1	1860	12.11	3694	96.8	101.8	95	96
SUV P2	1845	10.64	745	85.9	100.9	91	92

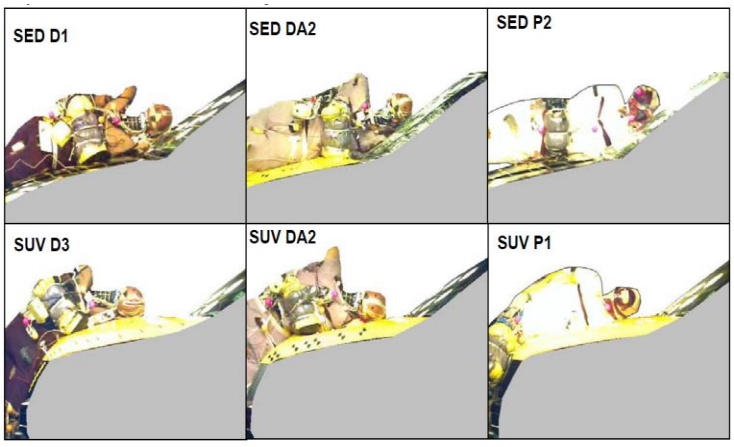

Figure 5. Head contact time (HC1 and HC2) and contact locations in (Kerrigan et al., 2012)

Peng et al. (2012) presented 280 Mathematical Dynamic Model (MADYMO) simulations with two pedestrian sizes (adult and child), seven pedestrian postures/angles, five vehicle front-end geometries, and four impact speeds (30 to 60 km/h). Although HIT values were not reported, WAD values were analyzed. It was found that child and SUV are associated with lower WAD than adult and other vehicle geometries (Figure 6). Because HIT and WAD are highly correlated, it is reasonable to believe that such effects will stay the same in HIT prediction.

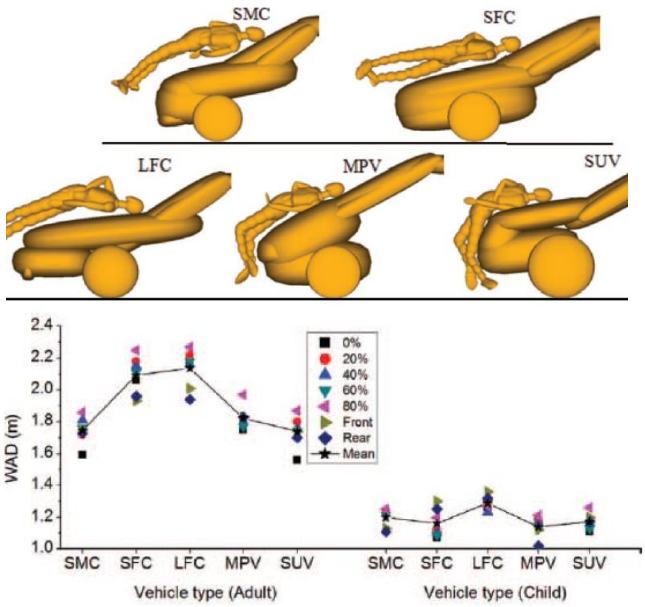

Figure 6. Exemplar impact locations and WAD values under 40 km/h pedestrian impact (Peng et al., 2012)

Watanabe et al. (2012) conducted 72 FE simulations of pedestrian impacts using three vehicle models (sedan, SUV, minivan), three pedestrian FE model sizes (F05, M50, and M95), at two different impact locations (center and the corner of the bumper) and four impact speeds (20, 30, 40 and 50 km/h). Although HITs were not reported numerically, some of the HIT values can be estimated from Figures as shown in Figure 7. Their results demonstrated that impact speed, vehicle model, pedestrian size, and impact location all affected the HIT values.

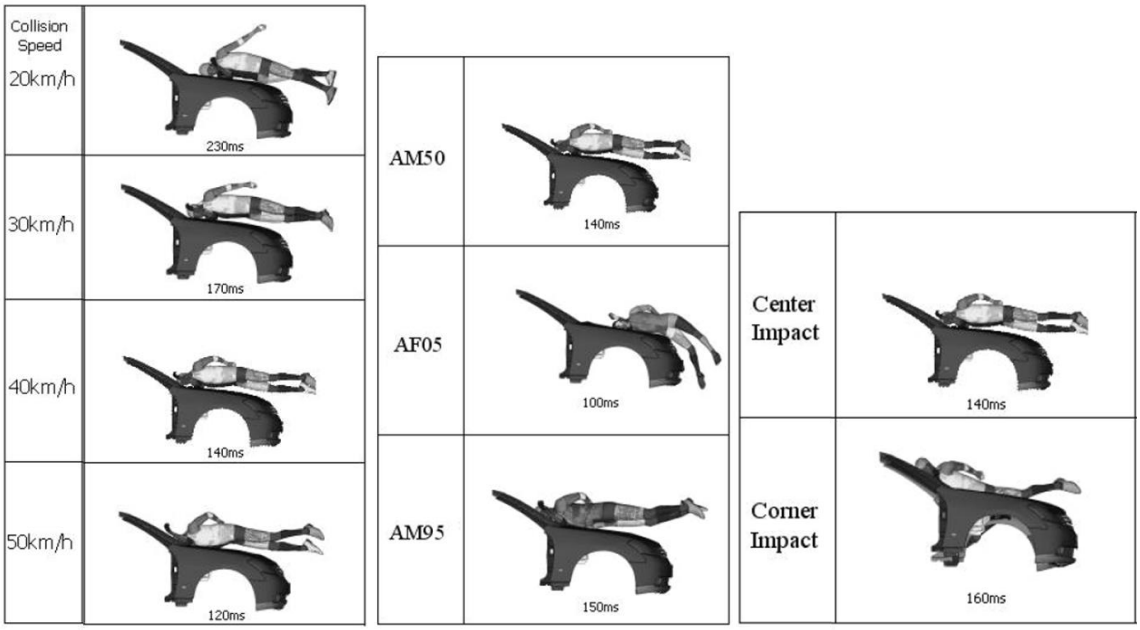

Figure 7. Exemplar impact locations and HIT values under various impact conditions (Watanabe et al., 2012)

Elliott et al. (2012) used MADYMO simulations to reconstruct PMHS and ATD pedestrian impact tests. Model-predicted HIT values were compared to the test results as shown in Figure 8. It was reported that pedestrian posture and height of the hood leading edge are significant factors affecting HIT, while vehicle stiffness and vehicle-to-pedestrian friction are not significant.

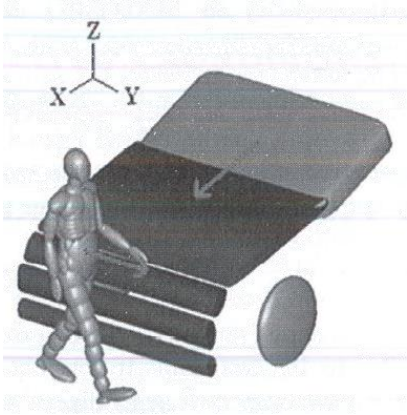

Test	Head impact time (ms) PMHS	Head impact time (ms) MADYMO model	Head impact time difference (ms) MADYMO – PMHS
MSS-S	100	103.0	3.0
MSS-T	140	126.0	−14.0
SCC-S	80	78.0	−2.0
SCC-T	88	81.0	−7.0
S1	112.5	119.5	7.0
S2	114.3	121.1	6.8
S3	115.1	122.5	7.4
M4	120.9	133.2	12.3
M5	121.9	135.4	13.5
T6	129.0	134.5	5.5
T7	135.2	136.2	1.0
P1	151.5	128.5	−23.0
P2	134.4	118.6	−15.8
P3	141.5	124.1	−17.4
D1	124.5	120.3	−4.2
D2	123.5	120.3	−3.2
D3	127.5	120.3	−7.2
DA1	122.5	118.0	−4.5
DA2	133.5	122.5	−11.0

Note: MSS-S–SCC-T: PMHS,[21] S1–T7: PMHS,[23] P1–P3: PMHS[24] and D1–DA2: dummy.[24]

Figure 8. HIT values reported in (Elliott et al., 2012)

Peng et al. (2013) used MADYMO to reconstruct 43 real-world sedan-to-pedestrian crashes in China and Germany. Second order polynomial curves were developed to use impact speed to predict HIT depending on impact location (Figure 9). Although impact speed is negatively correlated with HIT, there is no clear difference of HIT between different vehicle impact locations.

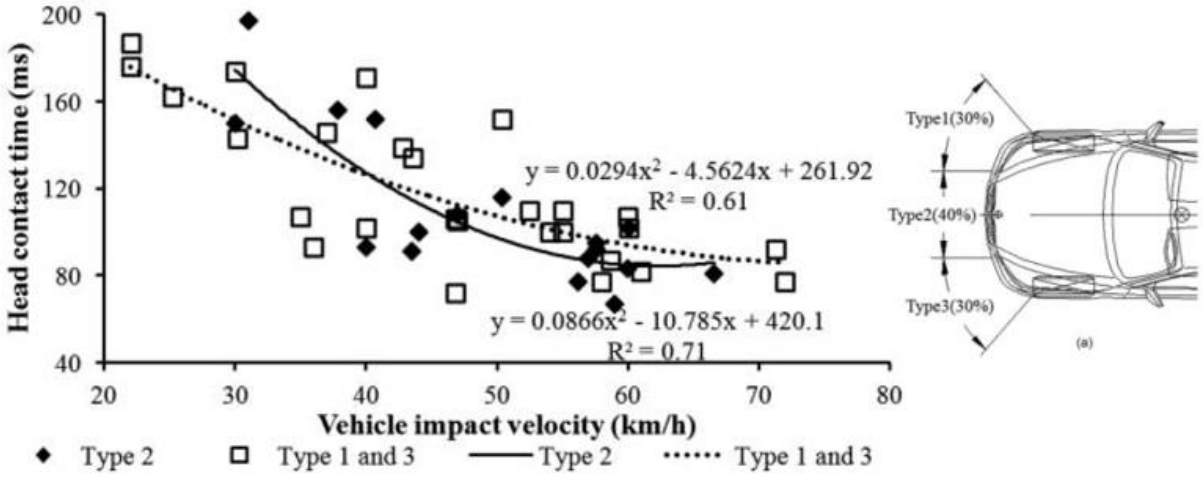

Figure 9. Relationship between impact speed and HIT (Peng et al., 2013)

Pal et al. (2014) conducted FE simulations with three Japan Automobile Manufacturers Association (JAMA) pedestrian models (AC06, AF05, and AM50) and two vehicle models (PV and SUV) at 45 km/h impact speed. HIT was reported as the percentage to the pop-up hood deploying time as shown in Table 3. SUV had much shorter HIT compared to the passenger car, and the 6-year-old pedestrian sustained the shortest HIT among all three pedestrians. The 6-year-old pedestrian-to-SUV impact is the only condition where HIT is shorter than the pop-up hood deploying time. Interestingly, it was also reported that human models with pelvis fracture option showed a longer HIT than without fracture. This is somewhat counterintuitive, because a fractured pelvis will provide less support to the torso, causing the torso/head to hit the vehicle quicker than those without a pelvis fracture.

Table 3. HIT/pop-up hood deploying time (Pal et al., 2014)

	PV: HIT/Deploying time %	SUV: HIT/Deploying time %
AC06	114	**60**
AF05	194	148
AM50	240	196

Chen et al. (2015) conducted FE simulations with the midsize male THUMS pedestrian model under nine orientations and three gaits at 40 km/h with a sedan model. Model-predicted HIT values are shown in Figure 10. They found that posture and impact direction are not statistically significant for predicting HIT.

Cases	Head impact time (ms)	Head impact site	Head impact location	V_h (m/s)	Torso impact angle (°)	Torso rotation (°)	Upper extremity impact
S0	139	lateral	C	11.6	15	15	both
S15	139	occipital	C,D	10.8	72.6	57.6	elbow
SN15	135	frontal	C	10.8	-83.9	-68.9	elbow
S30	134	occipital	C	11.8	84.0	54.0	elbow
SN30	125	frontal	C	12	-89.0	-59.0	elbow
S60	123	occipital	C	14.6	77.6	17.6	-
SN60	117	frontal	B,C	13.4	-88.3	-28.3	-
S90	117	occipital	C	15.3	87.9	-2.1	-
SN90	111	frontal	B	14.0	-88.6	1.4	-
RF0	128	occipital	C	12.2	29.5	29.5	shoulder
RF15	124	occipital	C	12.7	47.6	32.6	shoulder
RFN15	129	lateral	B,C	13.6	8.5	23.5	shoulder
RF30	125	occipital	B,C	12.7	75.5	45.5	elbow
RFN30	129	lateral	B	14.9	-27.0	3.0	shoulder
RF60	123	occipital	B,C	13.5	77.5	17.5	elbow
RFN60	130	frontal	B,C	12.5	-86.5	-26.5	-
RF90	130	occipital	B	15	87.0	-3.0	-
RFN90	129	frontal	B,C	13.3	-75.0	15.0	-
LF0	132	frontal	C	11.7	-40.0	-40.0	both
LF15	132	lateral	C	12.5	11.8	-3.2	both
LFN15	131	frontal	C	11.2	-76.0	-61.0	elbow
LF30	130	lateral	B,C	13.9	23.9	-6.1	both
LFN30	118	frontal	B,C	10.7	-77.6	-47.6	elbow
LF60	134	occipital	B,C	13.3	90.0	30.0	-
LFN60	124	frontal	B	12.1	-52.2	7.8	elbow
LF90	132	occipital	B, C	15.4	88.2	-0.8	-
LFN90	129	frontal	B	13.2	-106.0	-16.0	elbow

*A: WAD < 1800 mm (hood), B: 1800 ≤ WAD<1950 (cowl), C: 1950 ≤ WAD< 2100 (windshield frame), D: WAD ≥ 2100 mm (windshield).

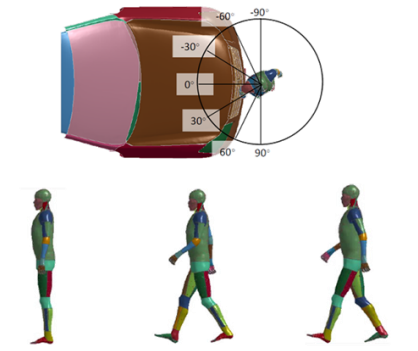

Figure 10. Model-predicted HIT values and simulation conditions (Chen et al., 2015)

Bhattacharjee et al. (2017) conducted 12 FE vehicle-to-pedestrian impact simulations with three in-production vehicles (a sedan, a midsize SUV, and a pickup truck) and four GHMBC pedestrian models (6YO, F05, M50, and M95). A regression model was also developed for using bonnet leading edge (BLE) height and WAD to predict HIT (Figure 11). While this is a relatively small sample size (n=12), this is the only HIT prediction model with U.S. vehicles. However, one of the limitations of this study is that HIT was predicted by WAD, which is not a measurement that can be determined easily for various combinations of vehicle, pedestrian, and impact conditions. Moreover, impact speed was not varied. This study also reported a high correlation between WAD and HIT, which is consistent with other studies.

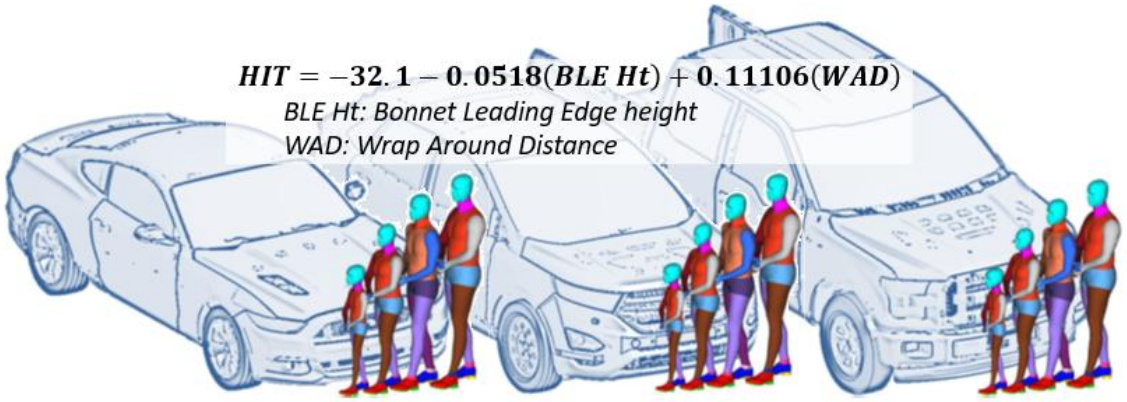

Figure 11. Pedestrian impact simulations and prediction model of HIT by (Bhattacharjee et al., 2017)

Klug et al. (2017) conducted pedestrian FE simulations for estimating HIT with four GV models, two pedestrian models (THUMS and GHBMC M50), and three impact speeds (30, 40, and 50km/h). Pedestrian postures were also varied in the simulations. It was found that boundary condition variations induced higher HIT variations than the HIT differences from using different pedestrian models. Therefore, the boundary conditions of the pedestrian impact simulations,

including the posture of the arm, friction between the pedestrian and the vehicle, and contact definitions need to be defined properly and consistently to achieve reliable HIT predictions. One of the major contributions of this study is the development of GV models. The geometries of the four GV models (Sport Utility Vehicle [SUV], Family Car [FCR], Roadster [RDS], and Multi-Purpose Vehicle [MPV]) were based on the front-end geometries of 11 European vehicles provided by five car manufacturers or pictures with vehicle dimensions.

Song et al. (2017) conducted 11 PMHS pedestrian impact tests at 40 km/h with an adjustable generic buck representing different types of vehicles. As providing a set of reference PMHS tests for model validation is the main purpose of the study, HIT was not the focus but was reported. Nevertheless, the van impacts resulted in much shorter HIT than those impacts with the SUV and sedan (Figure 12).

Test #	TIR 01	TIR 02	TIR 03	TIR 04	TIR 05	TIR 06	TIR 07	TIR 08	TIR 09	TIR 10	TIR 11
Subject #	MS 697	MS 698	MS 699	MS 700	MS 701	MS 712	MS 708	MS 707	MS 711	MS 710	MS 709
Right lower extremity contact time (ms)	0	0	0	0	0	0	0	0	0	0	0
Left lower extremity contact time (ms)	17	15	17	15	22	18	21	20	19	17	18
Pelvis contact time (ms)	10	10	10	10	10	5	5	5	50	50	50
Right elbow contact time (ms)	75	75	65	70	70	30	30	30	70	70	65
Shoulder contact time (ms)	105	100	85	100	100	45	45	45	100	100	95
Head contact time (ms)	115	115	105	115	110	70	60	65	115	115	115

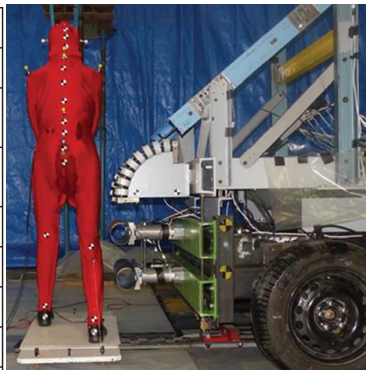

Figure 12. HIT values reported in (Song et al., 2017), TIR 01-05: SUV, TIR 06-08: Van, TIR 09-11: Sedan

More recently, Decker et al. (2019) conducted pedestrian FE simulations with four GV models, four sizes of pedestrian models (GHBMC 6YO, F05, M50, and M95), and three impact speeds (30, 40, and 50km/h). Pedestrian size, vehicle type, and impact speed all affected HIT values. As shown in Figure 13, impact speed and pedestrian size dominated the results, with lower impact speed and taller pedestrians consistently associated with longer HIT. The SUV and MPV models had shorter HITs than those from FCRs and RDSs.

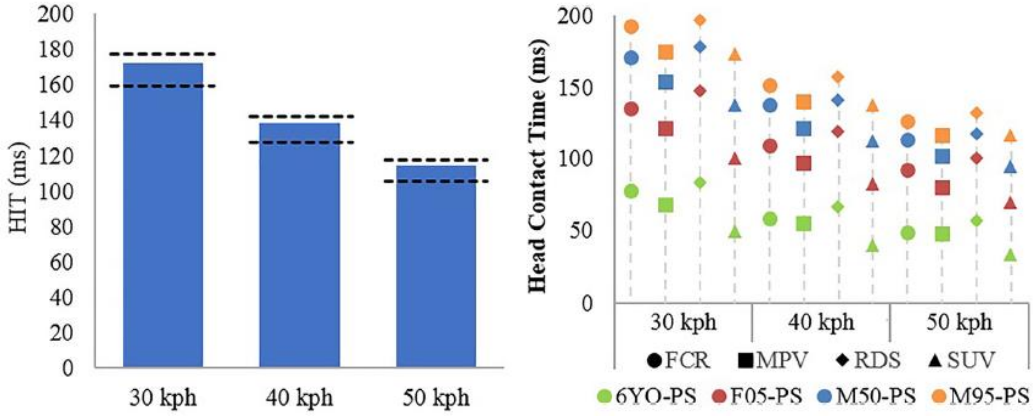

Figure 13. Effects from impact speed, vehicle type, and pedestrian size on HIT values (Decker et al., 2019)

Discussion and Summary

HIT is the time difference between the vehicle first hitting the pedestrian, and the pedestrian's head contacting the vehicle (likely the hood or windshield). Figure 14 shows a simplistic view of how HIT could be affected by vehicle impact speed, pedestrian size, and vehicle front-end geometry.

A) If the vehicle hood leading edge is taller than the pedestrian, the pedestrian's head will be hit by the vehicle quickly after the vehicle hits the pedestrian's limbs and torso. As a result, HIT will be very short in this condition.
B) If the vehicle hood leading edge is shorter than the pedestrian, the pedestrian will rotate around the hood leading edge and wrap around the hood. In this condition, HIT is determined by the speed of the vehicle and the travel distance between the head and the hood impact point.
C) Similar to condition B, if the hood is flatter, the travel distance between the head and the hood impact point will be greater. Consequently, HIT will be longer.
D) If the hood leading edge is lower or the pedestrian is taller, the upper portion of the pedestrian's body that rotates around the hood leading edge will be longer, which will result in longer HIT.

Based on this simple analysis, vehicle-to-pedestrian impact speed, vehicle type or front-end geometry, and pedestrian size should be the three dominating variables affecting HIT. Other factors may affect HIT to some extent but are not as significantly.

Table 4 shows the summary of the effects from all discussed variables on HIT based on the reviewed literature. Higher impact speed will lead to shorter HIT, LTVs have shorter HIT than passenger cars, and shorter pedestrians are associated with shorter HIT. WAD has also been reported to be highly correlated to HIT. On the other hand, vehicle impact location, friction, pedestrian age, pedestrian posture, and angle show limited and complex effects on HIT.

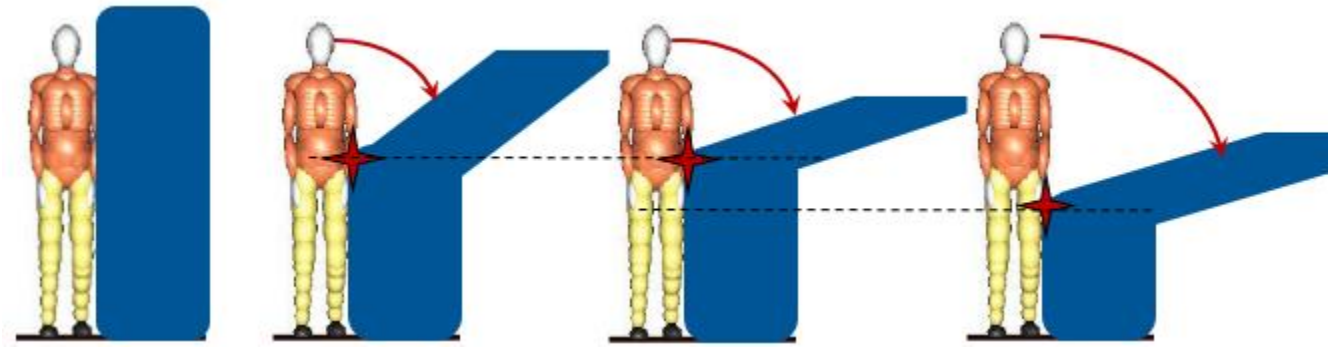

Figure 14. Simplistic view of HIT and associated variables

Table 4. Variables and their effects on HIT prediction

Variables	Effects on HIT	References
Vehicle-to-pedestrian impact speed	Strong, negatively correlated	(Decker et al., 2019; Peng et al., 2013; Peng et al., 2012; Watanabe et al., 2012)
Vehicle type / front-end geometry	Strong, shorter in LTVs	(Bhattacharjee et al., 2017; Decker et al., 2019; Elliott et al., 2012; Kerrigan et al., 2012; Kerrigan et al., 2009; Klug et al., 2017; Pal et al., 2014; Peng et al., 2012; Song et al., 2017; Watanabe et al., 2012)
Pedestrian size	Strong, positively correlated	(Bhattacharjee et al., 2017; Decker et al., 2019; Pal et al., 2014; Watanabe et al., 2012)
Wrap around distance (WAD)	Strong, positively correlated	(Bhattacharjee et al., 2017; Kerrigan et al., 2012)
Vehicle impact location	Weak, mixed trends	(Peng et al., 2013; Watanabe et al., 2012)
Vehicle-to-pedestrian friction	Weak, mixed trends	(Elliott et al., 2012; Klug et al., 2017)
Pedestrian posture (gait and arm)	Weak, mixed trends	(Chen et al., 2015; Elliott et al., 2012; Klug et al., 2017; Peng et al., 2012)
Pedestrian age	Weak, no trends	(Pal et al., 2014)
Pedestrian impact angle	Weak, no trends	(Chen et al., 2015)

In summary, this literature review suggested that variables that affect HIT in pedestrian impacts have been well documented, and their general trends are clear. PMHS test data are generally limited for HIT prediction, but more simulation data using MADYMO and FE ATD or human models are available for HIT prediction. However, simulations using a large set of vehicle models are not available and HIT prediction models are very limited in the current literature. This literature review provides a solid foundation for developing a HIT prediction model based on a large set of simulation data.

Task 2: Simulations and Prediction Model to Determine HIT

The goal of this task was to generate a virtual database and develop a surrogate prediction model to determine HIT through pedestrian impact simulations with various impact speeds, vehicle geometries, and pedestrian characteristics. Head impact velocity and impact angle were also collected in the simulation process, and associated prediction models were developed as well.

Generic Vehicle (GV) and Pedestrian Models

As mentioned in the previous sections, Euro NCAP TB 024 requires pedestrian models to be certified by simulating a series of impacts with 4 previously published GV models at 3 impact speeds (30, 40, and 50 km/h) with a series of kinematics criteria. As described in Klug et al. (2017), the geometries of the four GV models (SUV, MPV, FCR, and RDS) were based on the front-end geometries of 11 European vehicles provided by five car manufacturers or pictures with vehicle dimensions. These publicly available FE models are shown in Figure 15.

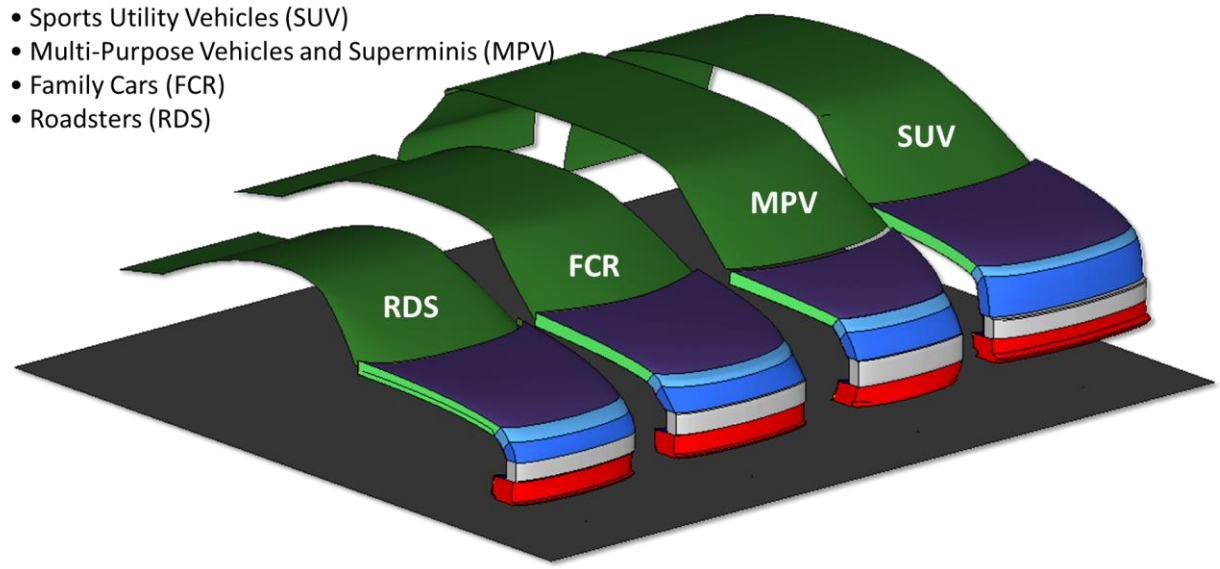

Figure 15. GV models from https://cloud.tugraz.at/index.php/s/ehzfzo3CIoZLy0c

In this study, four GHBMC simplified pedestrian models (-PS) were used, including 6YO-PS, F05-PS, M50-PS, and M95-PS (Figure 16). All of these models were specifically developed for the Euro NCAP pedestrian simulation protocol, validated extensively against PMHS tests (Meng et al., 2017; Pak et al., 2019; Untaroiu et al., 2018), and certified through Euro NCAP TB 024 procedures (Decker et al., 2019). Figure 16 shows the GHBMC pedestrian models and associated versions used in this study.

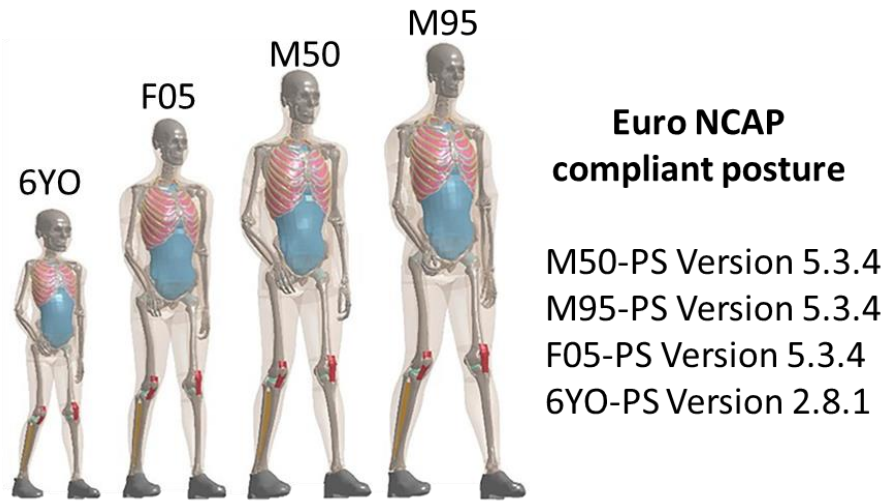

Figure 16. GHBMC simplified pedestrian models and latest versions

U.S. Vehicle Front-End Geometries

The size classes of GVs used in TB024 include SUV, MPV, FCR, and RDS, which are only representative of European vehicles and are not necessarily aligned with the traditional vehicle classes used in the United States (e.g., sedan, minivan, SUV, pickup truck). However, based on the geometries of the GVs, we proposed a mapping between the GV categories and U.S. vehicle categories as shown in Table 5. In particular, the SUV category in GVs is close to small to midsize SUVs in the United States; MPV category in GVs is close to minivans in the United States; FCR category in GVs is close to larger sedans in the United States; and RDS category in GVs is close to smaller sedans and coupes, especially those with two seats. However, none of the GV categories is representative of large SUVs and pickup trucks that are common in the U.S. market. As mentioned in previous sections, one of the main differences between the U.S. and European vehicles is that U.S. has more large vehicles than the Europe. Unfortunately, based on the field data mentioned earlier, large SUVs and pickup trucks tend to cause more pedestrian injuries in terms of both frequency and severity. Therefore, it is beneficial to include a fifth vehicle class (i.e., large SUV and pickup) specifically to account for U.S. larger vehicles as shown in Table 5.

Table 5 also shows a list of the 20 vehicles used in this study. This list included the vehicle FE models that are already available and additional vehicles that are popular in the U.S. market, for which 3D scans were used to collect their front-end geometries. The set of FE vehicle models have been validated against vehicle frontal crash tests, although not the pedestrian impact tests. These models are publicly available through either the NHTSA website (www.nhtsa.gov/crash-simulation-vehicle-models) or the George Mason University website (www.ccsa.gmu.edu/models/). We have used many of these vehicle models and simulations for various applications (Hu et al., 2017). In this study, 13 FE vehicle models were used as the basis for U.S. vehicle front-end geometries. In addition, 3D front-end geometries of seven U.S. vehicle models across different GV model classes were also acquired, which resulted in vehicle front-end geometries from a total of 20 U.S. vehicles.

A vehicle scanning procedure was developed using Microsoft Azure depth cameras to obtain high-resolution 3D point cloud data. Shapes of the vehicles from the B-pillar forward were

recorded. After manual processing, cleanup, and smoothing, the front-end geometry of a vehicle can be reconstructed virtually as shown in Figure 17.

Table 5. Category mapping between GV models and U.S. vehicles

GV Category	U.S. Vehicle Category	FE Models Available	Scanned Vehicles
-	Large SUV, Pickup, or Van	F-250 (2006), Silverado (2014), Econoline (1999)	
SUV	Small to Midsize SUV	**Explorer (2003),** RAV4 (1997), Rogue (2020)	CR-V (2017), Highlander (2019)
MPV	Mini-van	**Caravan (1997)**	Odyssey (2018), Sienna (2016), Pacifica (2019)
Family Car	Midsize to Full-size Sedan	Camry (2012), Accord (2014), Taurus (2001), **CT4 (2022)**	
Roadster	Smaller Sedan	**Neon (1996)**, Yaris (2010)	Focus (2013), Civic (2009)

Note: Four vehicle models in **bold** were used to compare the HIT predictions between the morphed GV models and the FE vehicle models.

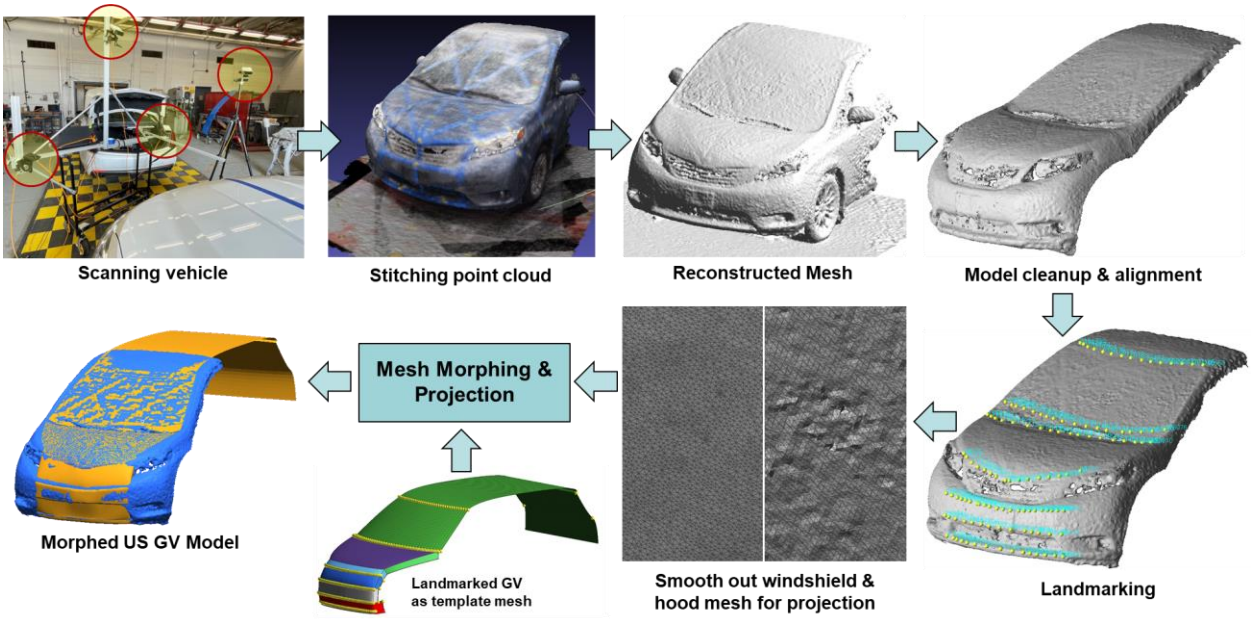

Figure 17. Process to scan a vehicle front-end geometry and reconfigure/morph a GV model to the scanned vehicle geometry

GV Models Morphed Into Different U.S. Vehicle Geometries

The FE GV model's geometry was morphed to each selected U.S. vehicle's geometry for pedestrian simulations. As shown in Figure 17, the mesh morphing process involved four steps. First, a set of landmarks at the boundaries of the bumper, grille, hood, windshield, and other major components were identified on the vehicle geometry either from the FE vehicle model or the reconstructed vehicle geometry model from the 3D scans. Second, the same set of landmarks identified on the vehicles were identified in the FE GV model. A cubic-spline method was then used to re-sample the landmarks on each boundary line, which ensured the same number of

landmarks on each vehicle and the GV model. As a result, the two corresponding sets of landmarks (same number and corresponding locations) could be defined on the U.S. vehicle model and the GV model. Third, a landmark-based mesh morphing method based on radial basis functions (RBF) was used to morph the FE GV model into the U.S. vehicle geometry based on the landmark locations. After the mesh morphing, the geometry of the morphed GV models were very close to the target geometry with only minor differences, especially in the regions that were far away from the landmarks. Last, the surface mesh of the GV model was further projected to the target geometry to ensure 100-percent geometry accuracy, and then another mesh morphing was performed to the solid elements of the GV model based on the projected surface meshes.

The RBF mesh morphing has been used extensively in a variety of our previous research, particularly for morphing a midsize male FE human body model into a wide range of sizes, shapes, and postures (Hu et al., 2019; Hwang et al., 2016; Zhang et al., 2017). In this study, because of the similarity of U.S. vehicle geometry and GV model geometry, it was easy for RBF mesh morphing to reconfigure the GV models to the target geometry with high mesh quality. It should be noted that the thickness of the GV models were kept intact in the reconfiguration process. That is, the clearance between the hood and the rigid component underneath it was not changed for any of the GV model, although it is well known that the Roadster model has lower clearance than the other GV models. The weight of the morphed GV models were adjusted to the vehicle curb weight + 150 kg for accounting two occupants at the driver and front passenger locations. The 20 morphed GV models are shown in Figure 18.

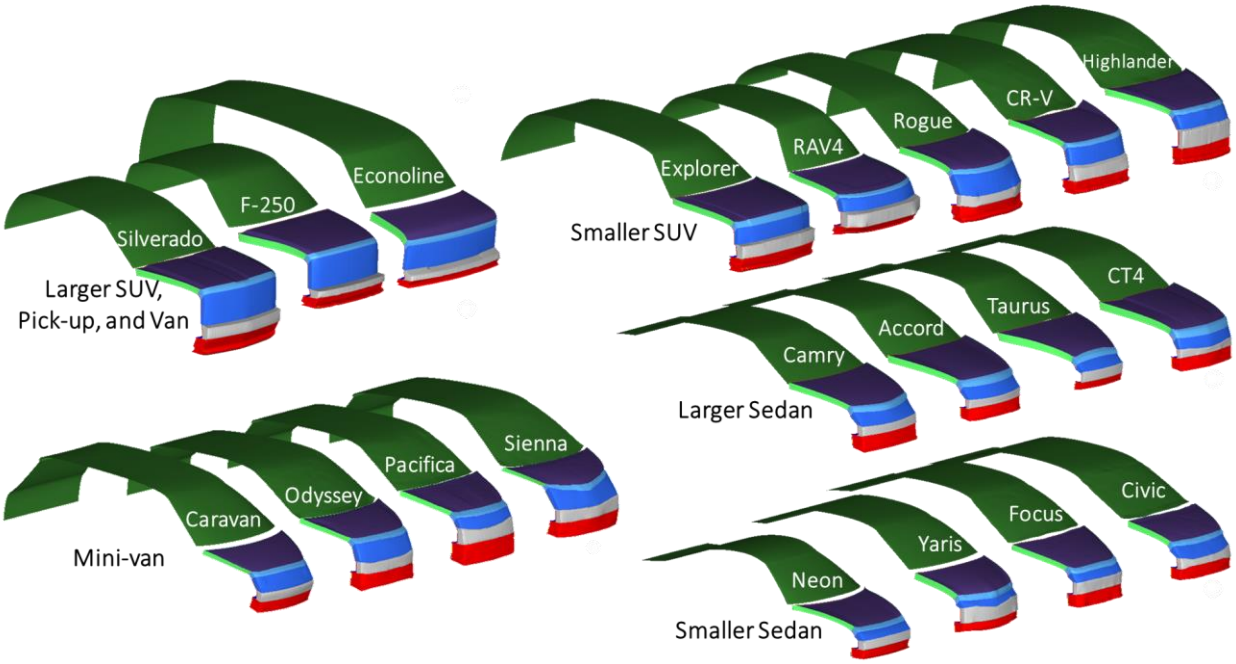

Figure 18. Morphed GV models representing the U.S. vehicle front-end geometries

The morphed GV model front centerlines were further analyzed using Principal Component Analysis (PCA) to better understand the variations of the front-end geometries for U.S. vehicles. In PCA, the first PC presents the direction in the space of the data with the highest geometric variance, the second PC represents in the direction orthogonal to the first PC with the second highest variance, and so on. As shown in Figure 19, the first PC accounts for 68.5 percent of the geometry variations, the second PC accounts for 27.6 percent of the geometry variations, and all

other PCs account for negligible amounts of geometry variation. More specifically, the first PC represents the hood height variations, while the second PC represents a combination of hood angle and length variations. This result confirms that using hood height, angle, and length as the design variables should be able to account for most of the geometric variations in the vehicle front-end geometries close to the centerline.

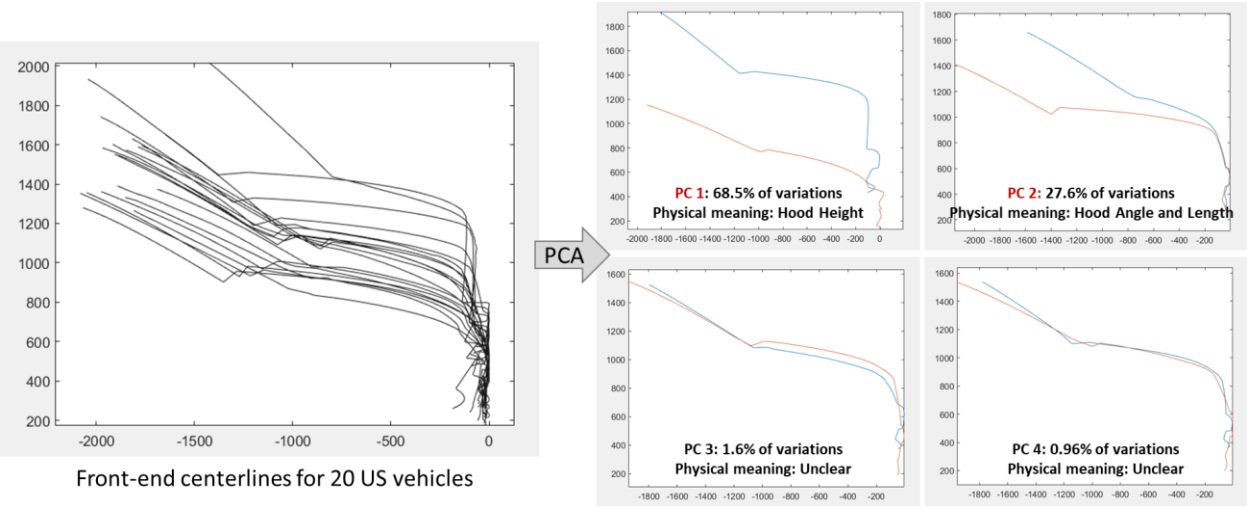

Figure 19. PCA results for the U.S. vehicle front-end geometries
(Bounds of the figures on the right represent geometries with PC scores of mean ± 2 standard deviations.)

HIT Comparison Between the Morphed GV Models and Vehicle Models

Simulation Matrix and Setup

In this study, the four vehicle models in **bold** in Table 5 were used to compare the HIT predictions between the morphed GV models and the FE vehicle models. Specifically, we used a 2003 Ford Explorer as an SUV, a 1997 Dodge Caravan as an MPV, a 2022 Cadillac CT4 as a Family Car, and a 1996 Chrysler Neon as a Roadster.

Vehicle-to-pedestrian simulations were conducted as described in TB024 with four pedestrian models (GHBMC 6YO-PS, F05-PS, M50-PS, and M95-PS), eight vehicle models (four U.S. vehicle models and four morphed GV models corresponding to the four U.S. vehicles), and three impact speeds (30, 40, and 50 km/h). A full factorial design of experiment (DOE) was conducted, which resulted in a total of 96 (4×8×3) simulations. All simulations were conducted along the vehicle centerline.

The simulation conditions closely followed the TB024 requirements, including:

- The initial posture of the pedestrian model follows the target natural posture defined in TB024. It is especially important to have accurate arm locations, because arm locations tend to affect the HIT significantly.
- A segment-based contact was defined between the vehicle and the skin of the pedestrian model with both dynamic and static coefficients of friction at 0.3.
- The mass scaling and time step settings were closely monitored.

Assessment of Simulation Results

Figure 20 shows the HIT comparison between the FE vehicle models and the morphed GV models. Overall, the HIT values predicted by the morphed GV models matched those predicted by the FE vehicle models well. Specifically, a R^2 value of 0.997 was achieved between the two sets of HIT values, and the mean difference between the two sets of HIT values is 0.59 ms, indicating a great match. However, there are a few cases, in which the HIT difference is over 10 ms. Figure 21 shows two examples of the pedestrian kinematic comparisons between the morphed GV model and the vehicle model, in which the example on the left (Explorer/M50 pedestrian/30 kph) represents a case with minimal HIT difference, and the example on the right (Caravan/F50 pedestrian/30 kph) represents a case with relatively large HIT differences. The relatively large HIT difference was mainly caused by the stiffness differences between the morphed GV and vehicle model. In the specific Caravan case in Figure 21, the hood is less stiff in the vehicle model than in the morphed GV model, causing the pedestrian torso to move more rapidly toward the vehicle and shorter HIT in the vehicle model than the morphed GV model. Nevertheless, the HIT values predicted by the morphed GV models are highly correlated to those predicted by the vehicle models.

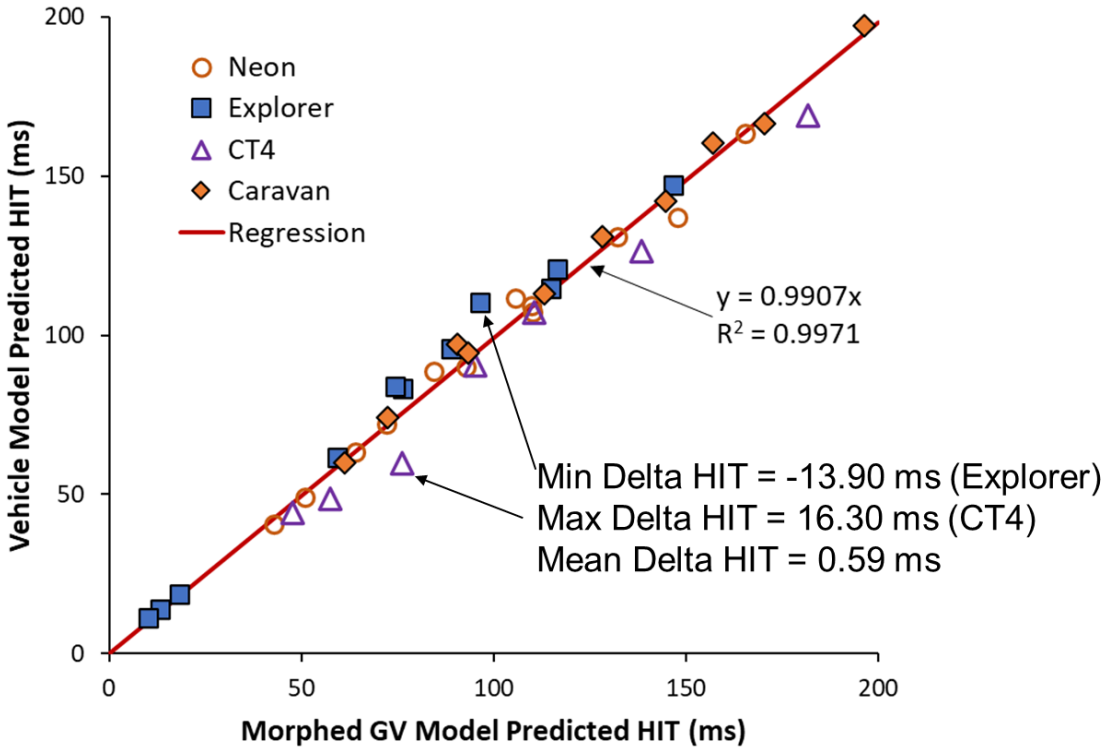

Figure 20. HIT comparison between the morphed GV models and FE vehicle models (Delta HIT = $HIT_{morphed\text{-}GV} - HIT_{vehicle\text{-}model}$)

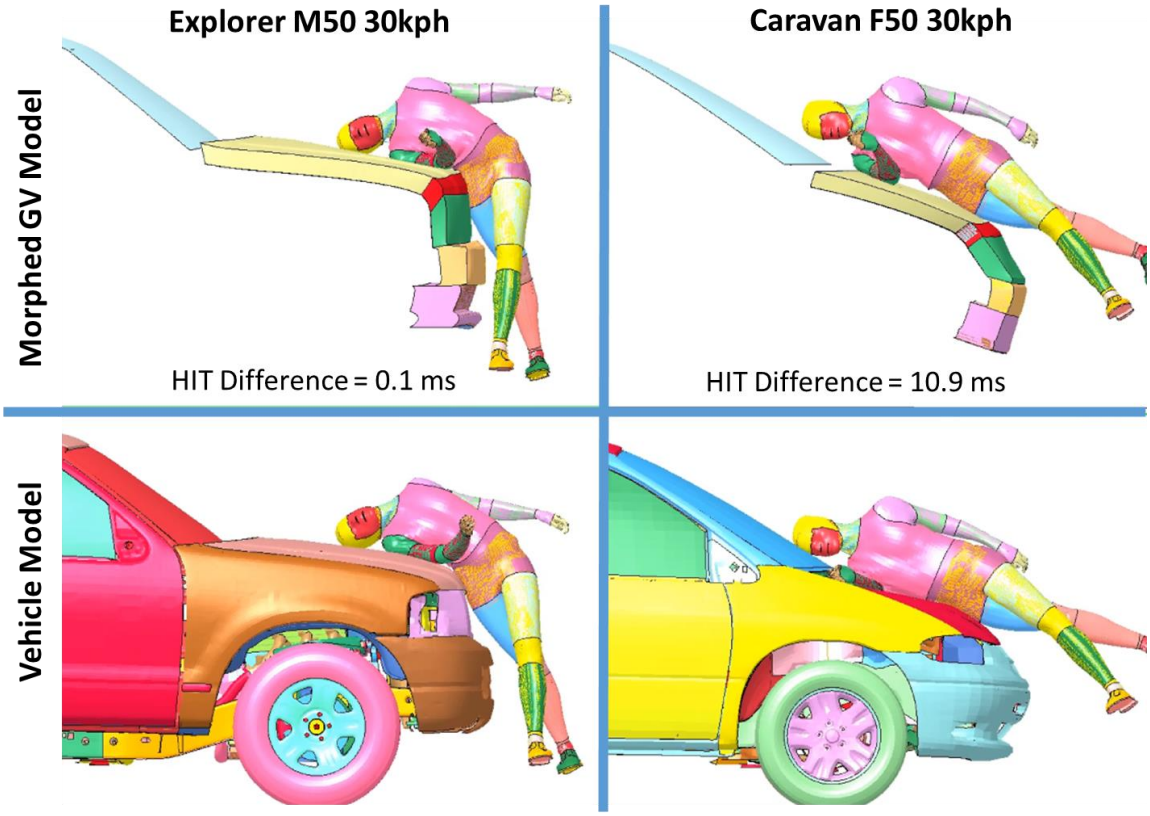

Figure 21. Exemplar pedestrian kinematic comparisons between morphed GV models and vehicle models

Virtual Database of Pedestrian Impacts

Simulation Matrix

In this study, all 20 morphed GV models shown in Figure 18 along with four (4) pedestrian models (GHBMC 6YO-PS, F05-PS, M50-PS, and M95-PS) and three (3) impact speeds (30, 40, and 50 km/h) were used to generate the virtual data for HIT prediction. Based on a full factorial design, a total of 240 pedestrian simulations were conducted for the virtual database.

Simulation Results

For each simulation, the pedestrian kinematics were output along with pedestrian HIT, WAD, resultant head contact velocity relative to the vehicle (HeadV), and head velocity angle relative to the horizontal line (HVAng). Due to the large number of simulations, the process for collecting output measures was automated using a combination of MetaPost and Matlab, so that the results can be recorded automatically and accurately. Figure 22 shows a few examples of the simulated vehicle-to-pedestrian crashes with varied vehicle front-end geometry, pedestrian size, and impact speed. Figure 23 shows the result for one of the pedestrian simulations using the automated procedure.

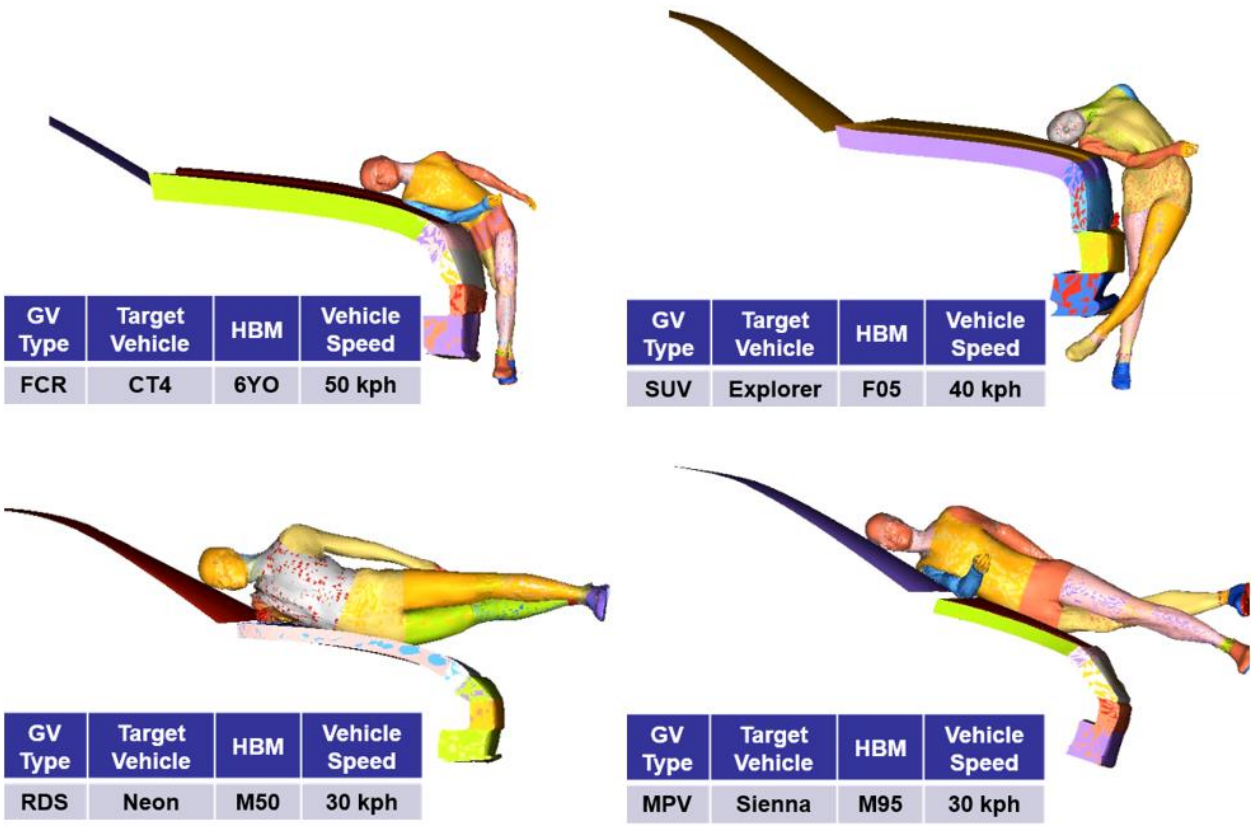

Figure 22. Examples of pedestrian simulation results with varied vehicle geometry, pedestrian size, and impact speed

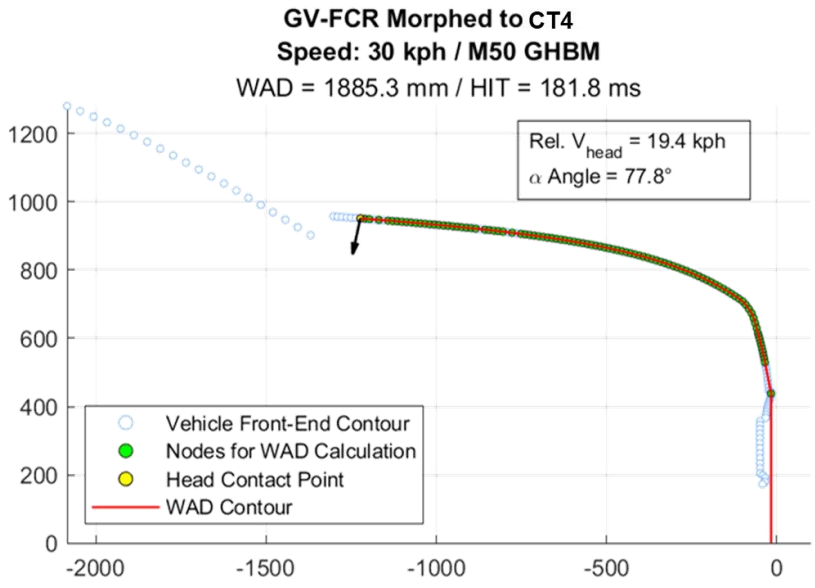

Figure 23. An example of automated simulation results for pedestrian simulations

Among the 240 simulations, initially about 15 percent of the simulations ended with error terminations. The errors included out-of-range force or negative volume at the knee area, lower leg flesh, or foot. All these errors were fixed by disabling bone failure, adding internal contact, and/or reducing the simulation time step. As a result, 234 out of 240 simulations were finished

with proper head contact and HIT values. There were two simulations still with error terminations and four simulations terminated normally but without any head contact. The four simulations without head contact were all with the pickup truck or van at lower impact speed, in which the vehicle knocked down the pedestrian without any head contact. The full set of simulation results are provided in Appendix A.

Data Trends on HIT, HeadV, and HVAng

Figure 24 shows factor effects on HIT as well as WAD ranges based on each pedestrian. It is clear that hood height, WAD, pedestrian size, vehicle type and vehicle impact speed all have substantial effects on HIT, which are consistent with the findings from the literature review. In addition, simulation results showed that pedestrian size had a strong effect on WAD.

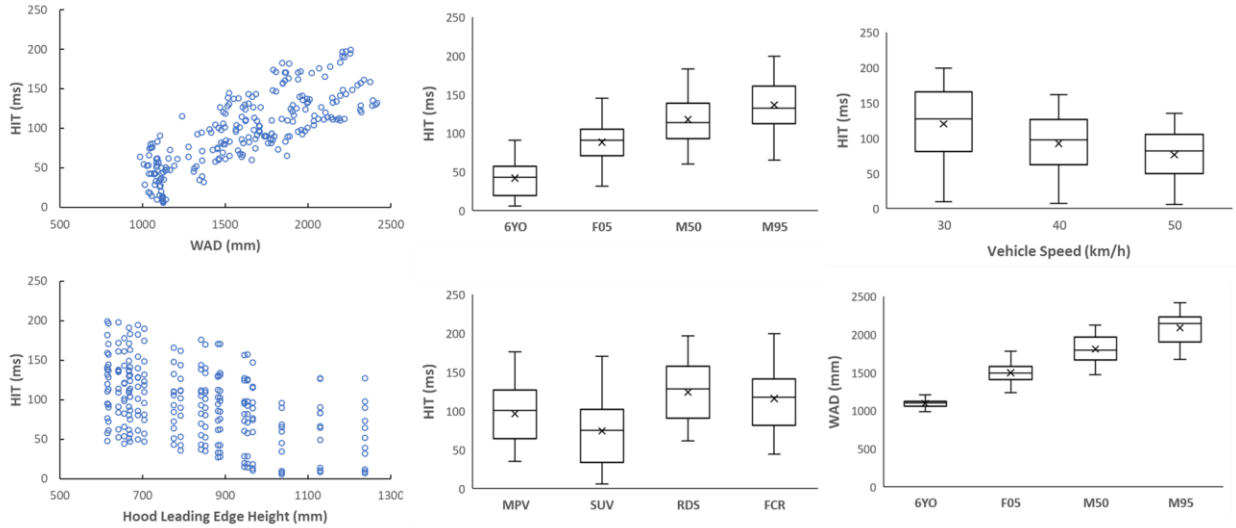

Figure 24. Factor effects on HIT and WAD ranges by pedestrian

Figures 25 and 26 show factor effects on head contact velocity and head contact velocity angle. Compared to HIT, HeadV and HVAng values varied more, and the associated factor effects are not as strong. Nevertheless, there is a clear correlation between the vehicle impact speed and HeadV. The HVAng distributions are more complex, especially for the 6YO and larger vehicles. It should be noted that the SUV category included all SUVs, pickup trucks, and vans in Figures 25 and 26.

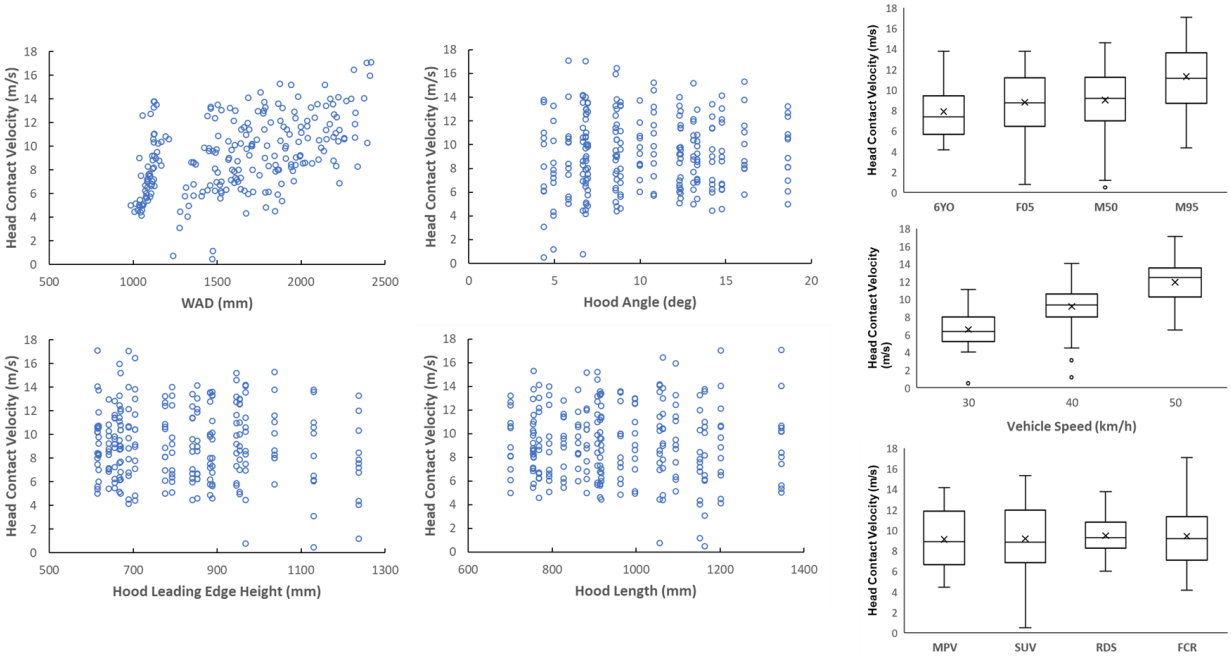

Figure 25. Factor effects on HeadV

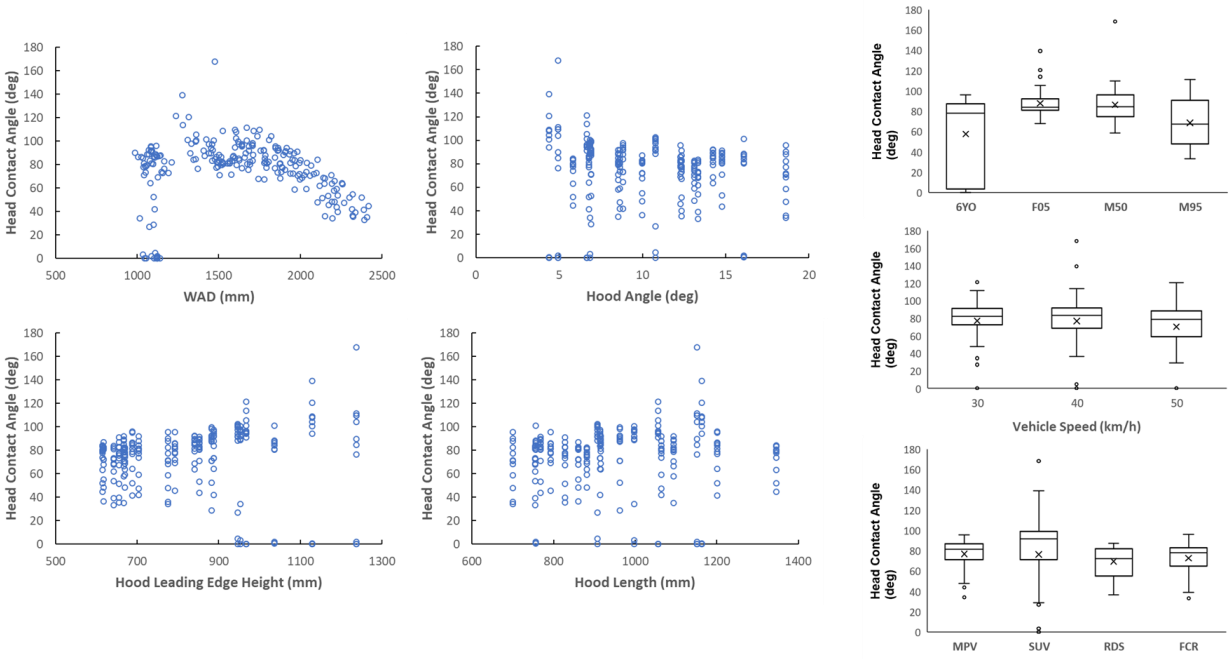

Figure 26. Factor effects on HVAng

Development of HIT Prediction Models

Using the virtual database of the 240 simulations with morphed U.S. GV models, stepwise multiple linear regressions were performed to predict HIT values using the available input variables, including pedestrian size, impact speed, WAD, and a set of vehicle front-end geometry descriptors. As shown in Figure 19, hood height, angle, and length account for more than 96 percent of the vehicle front-end geometry variations, therefore these three design variables were used in the regression model. Figure 27 shows the definitions of the hood height, hood length, and hood angle. Specifically, hood height is defined as the height of the hood leading edge from the ground, hood length is defined as the length of the hood centerline from the trailing edge to the leading edge, and hood angle is defined as the angle between the horizontal line and the line passing the hood trailing edge and hood mid-point.

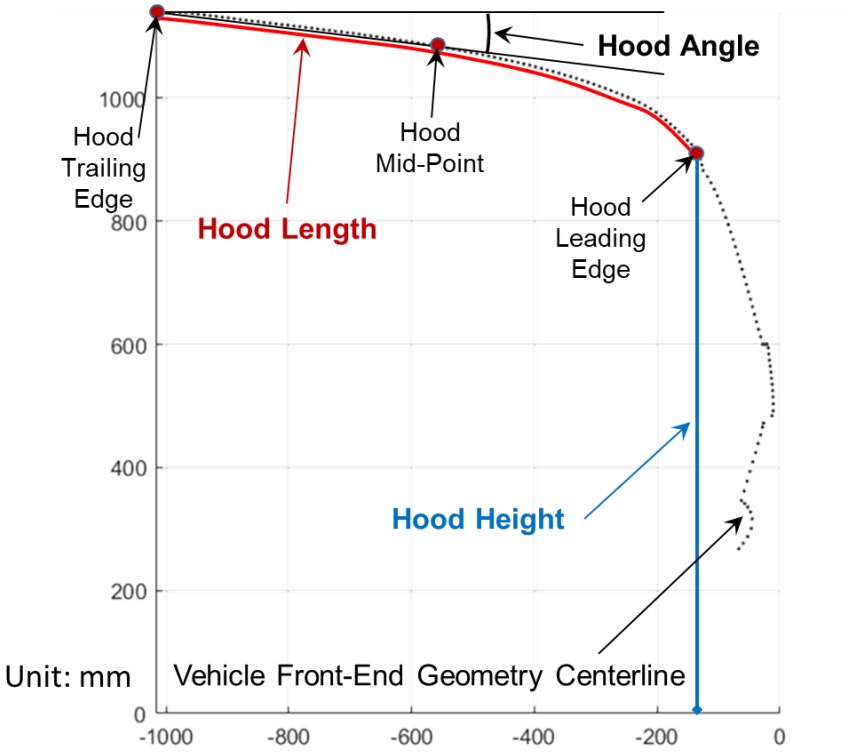

Figure 27. Definitions of hood height, hood length, and hood angle

In this study, the adjusted R^2 value and the root mean square error (RMSE) were considered in the stepwise regression model as the criteria to find the best combinations of input variables for predicting HIT. Two types of models were exercised: a linear model and a quadratic model. The linear model only included the linear terms from each input variable, and quadratic model included the linear, interaction, and quadratic terms between the input variables selected by the linear model.

Figure 28 shows the error analysis for both the linear and quadratic models for predicting HIT. High adjusted R^2 values were achieved by both models with 0.949 for the linear model and 0.979 for the quadratic model. The RMSE is 10.41 ms and 6.61 ms for the linear and quadratic models, respectively. Figure 29 shows the error analysis for two additional regression models for predicting HIT, in which pedestrian stature was removed. Because pop-up hood testing may only use WAD to identify the impact location, pedestrian stature may not always be available.

Removing pedestrian stature slightly reduced the adjusted R^2 values and increase the RMSE for both the linear and quadratic models. The model coefficients and significant levels for all the four regression models for predicting HIT are provided in Table 6.

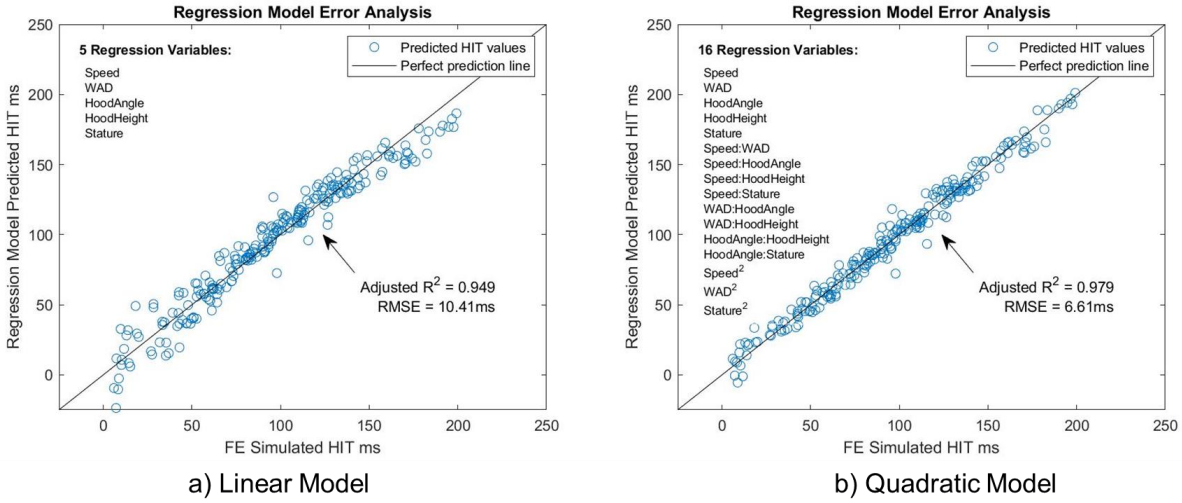

Figure 28. Error analysis for the HIT prediction models

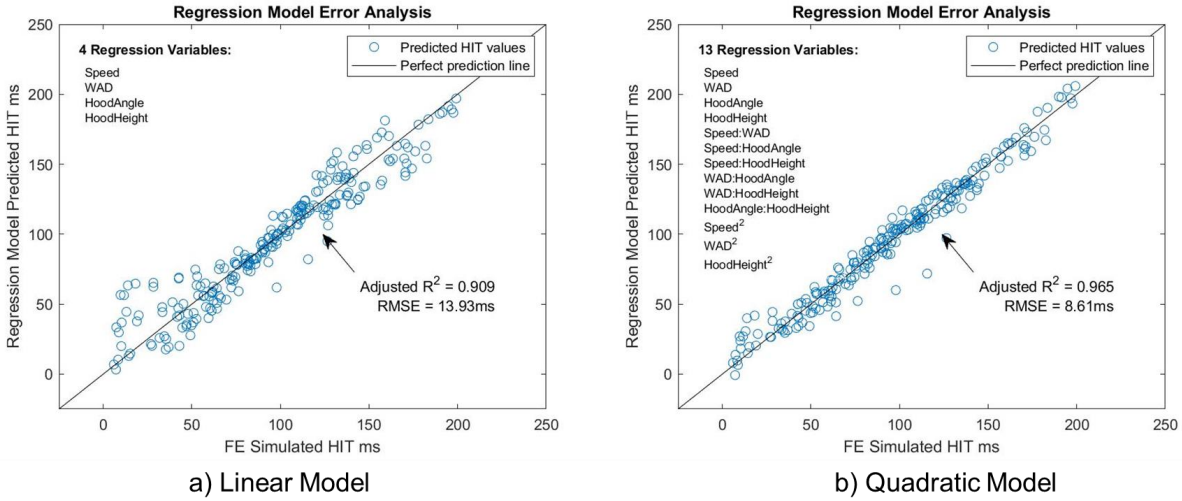

Figure 29. Error analysis for the HIT prediction models (without pedestrian stature)

Table 6. Model coefficients and significant levels for the four HIT prediction models

Linear model with pedestrian stature			**Linear model without pedestrian stature**		
Variables	Estimate	pValue	Variables	Estimate	pValue
(Intercept)	90.75392	<0.001	(Intercept)	113.4387	<0.001
Speed	-2.10913	<0.001	Speed	-2.65451	<0.001
WAD	0.001194	0.8626	WAD	0.09098	<0.001
HoodAngle	-0.86218	<0.001	HoodAngle	-0.78888	0.0014
HoodHeight	-0.11901	<0.001	HoodHeight	-0.06118	<0.001
Stature	0.121307	<0.001			
Quadratic model with pedestrian stature			**Quadratic model without pedestrian stature**		
Variables	Estimate	pValue	Variables	Estimate	pValue
(Intercept)	8.481195	0.7891	(Intercept)	94.87157	0.0213
Speed	-3.2659	<0.001	Speed	-5.80418	<0.001
WAD	-0.10435	0.0042	WAD	0.209354	<0.001
HoodAngle	3.556065	<0.001	HoodAngle	3.383944	0.0140
HoodHeight	-0.24821	<0.001	HoodHeight	-0.14745	0.0039
Stature	0.399259	<0.001	Speed:WAD	-0.00201	<0.001
Speed:WAD	0.000739	0.1879	Speed:HoodAngle	0.033142	0.0813
Speed:HoodAngle	0.019258	0.2227	Speed:HoodHeight	0.001039	0.0214
Speed:HoodHeight	0.002568	<0.001	WAD:HoodAngle	-0.00138	<0.001
Speed:Stature	-0.00395	<0.001	WAD:HoodHeight	7.63E-05	<0.001
WAD:HoodAngle	0.001486	0.1960	HoodAngle:HoodHeight	-0.00416	<0.001
WAD:HoodHeight	4.48E-05	0.0029	$Speed^2$	0.065289	<0.001
HoodAngle:HoodHeight	-0.00266	0.0113	WAD^2	-2.51E-05	<0.001
HoodAngle:Stature	-0.00331	0.0247	$HoodHeight^2$	-2.56E-05	0.2433
$Speed^2$	0.047413	<0.001			
WAD^2	1.66E-05	0.0346			
$Stature^2$	-3.96E-05	0.0143			

Table 7 shows HIT comparisons between those from FE simulations and two prediction models with and without pedestrian stature. Overall, the prediction models provided reasonable HIT values, but prediction models with stature provided more accurate results.

Table 7. HIT comparison of a future BEV between the FE simulations and prediction models

HBM	Stature (mm)	Speed (kph)	WAD (mm)	Hood Height (mm)	Hood Angle* (deg)	**FE HIT (ms)**	**Predicted HIT** (ms)**	**Predicted HIT w/o Stature** (ms)**
6YO	1164	40	1020.1	764	5.82	**46.7**	**45.4**	**37.2**
F05	1548	40	1469.6	764	5.82	**92.2**	**93.7**	**89.8**
M50	1780	40	1899.2	764	5.82	**127.0**	**125.1**	**130.6**

* Hood angle is based on CT4.

** Predictions were based on regression models with interaction and quadratic terms.

Prediction Models for Head Contact Velocity

The method of developing the prediction models for the HeadV is like those used for the HIT prediction model. Figure 30 shows the error analysis results for the linear and quadratic models along with the adjusted R^2 and RMSE. Although the adjusted R^2 values are not as high as those for the HIT prediction models, high correlations (0.699 and 0.799) were achieved between predictors and HeadV.

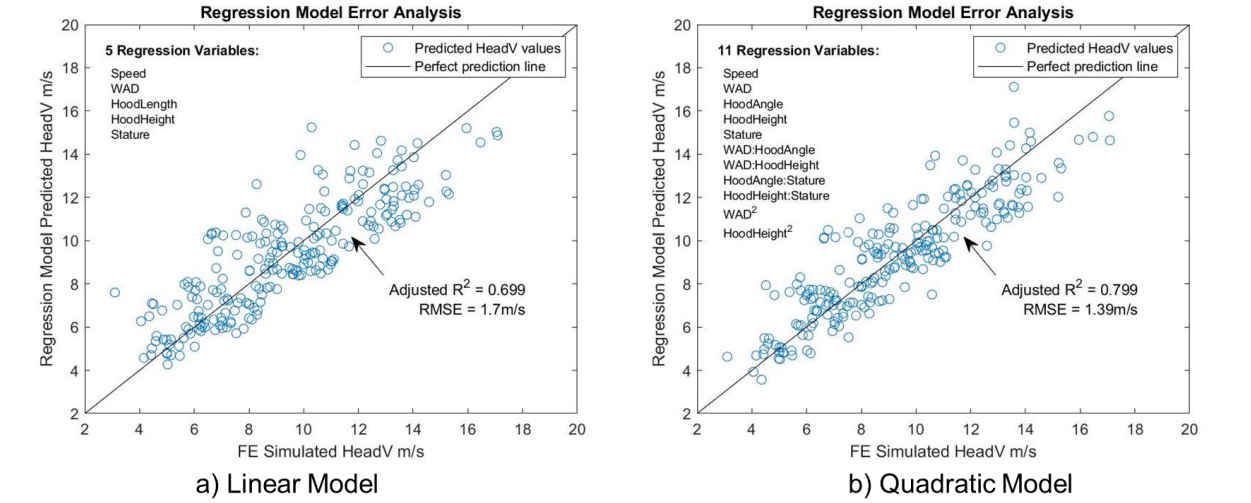

Figure 30. Error analysis for the HeadV prediction models

Prediction Models for Head Velocity Angle

Figure 31 shows the error analysis results, adjusted R^2 and RMSE for the linear and quadratic models with all the simulation results, while Figure 32 shows the results with only the adult pedestrian simulations. Overall, high correlations were achieved. Regression models with only the adult pedestrian results provided higher adjusted R^2 and lower RSME, because many of the 6YO simulations are associated with HeadVAng close to zero, in which the vehicle knocks down the 6YO pedestrian by the grille or front-end components below the hood. In such cases, pop-up hood designs may not provide benefit for pedestrian protection. The model accuracy reduced significantly when HeadVAngle is over 110 deg, which are rare cases with extreme head/neck rotations. An example of such pedestrian kinematics can be found in the SUV case shown in Figure 22.

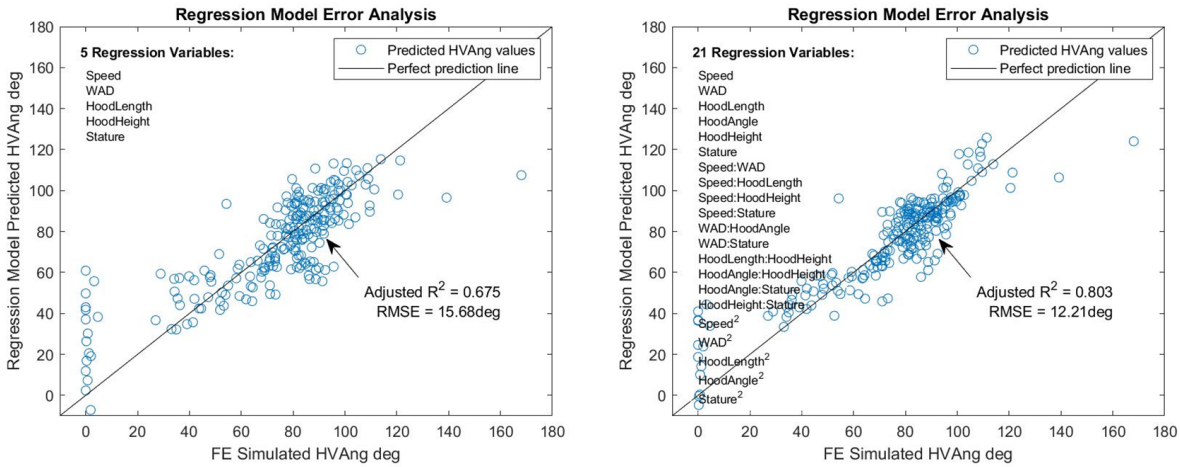

Figure 31. Error analysis for the HeadVAng prediction models

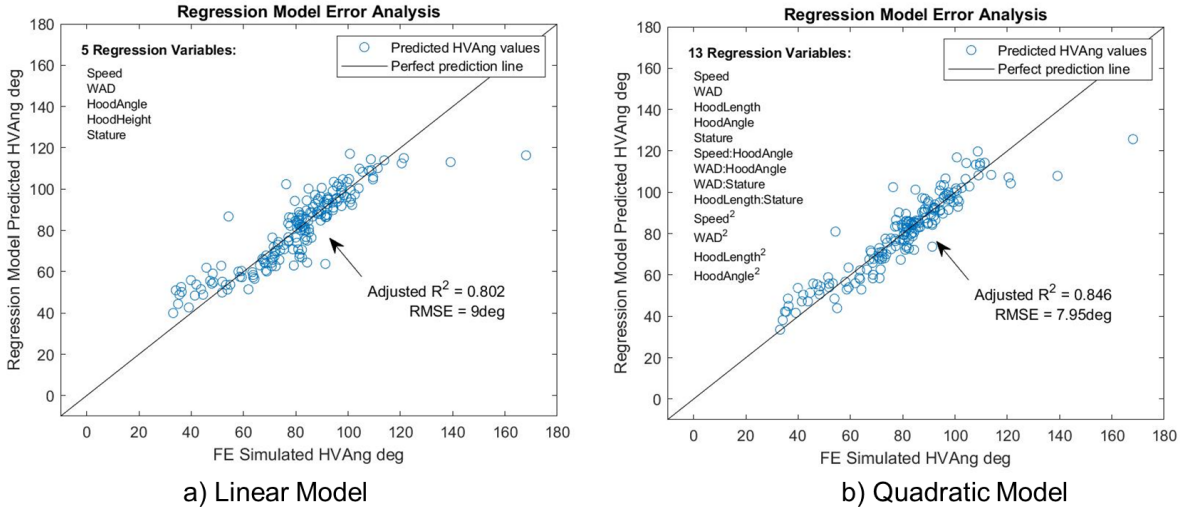

Figure 32. Error analysis for the HeadVAng prediction models with only the adult pedestrians

Task 3: Simulations for Hood Edge Impact With a Pop-Up Hood

The goal of this task was to produce an impact scenario where the pedestrian body strikes the edge of a deployed pop-up hood. Based on our experience, the benefit of a pop-up hood in pedestrian protection may be the most when the pedestrian head contact is around the side edge(s) of the hood. Therefore, our simulations focused on the cases where the pedestrian's head may contact the side edge of the hood and the contact edge may create a safety hazard to the head.

Pop-Up Hood Model

A GM vehicle (2022 Cadillac CT4) model with a pop-up hood design was previously developed and validated against physical tests. Figure 33 shows exemplar model validation results against the Euro NCAP headform impact tests. Figure 34 shows headform acceleration time history comparisons between tests and simulations of the vehicle pop-up hood design. Overall, the model provided good correlations to the test data.

Description (Target Location/Zone)	Measured Velocity (kph)	Impact Angle (deg)	Peak Accel (G's)	HIC	Deploy Time (ms)
Live NCAP (A,10,-7) 30ms	40.2	65	169	590	27
Live NCAP (A,10,7) 30ms	40.2	65	160	540	26
Live NCAP (A,10,7) 100ms	40.5	65	161	400	99
Live NCAP (A,10,-7) 100ms	40.0	65	161	420	98
Live NCAP (C,9,-7) 30ms	40.1	50	191	680	28
Live NCAP (C,9,7) 30ms	40.1	50	234	940	29
Live GTR (C, WAD1700,y=667) 30ms	34.9	50	160	650	25
Live GTR (A, WAD1700,y=667) 30ms	35.1	65	156	600	27
Live GTR (A, WAD1700,y=-667) 30ms	34.9	65	134	530	27
Live GTR (C, WAD1700,y=-667) 30ms	34.9	50	149	710	29

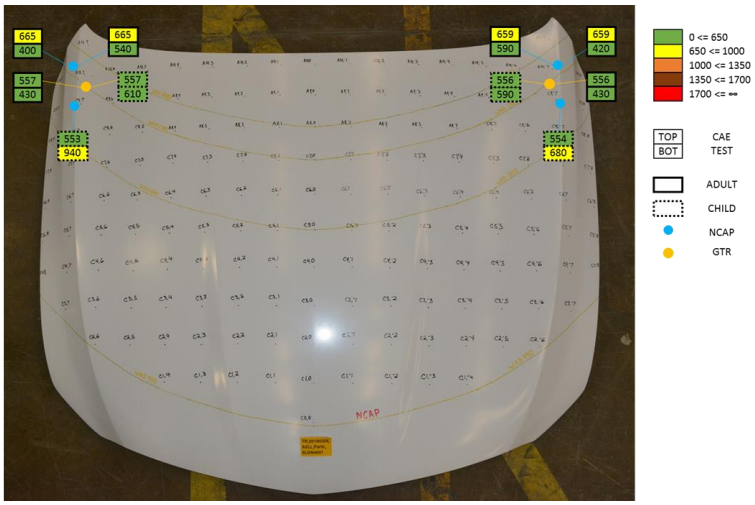

Figure 33. Pop-up hood model validation results against headform impact tests at different hood locations

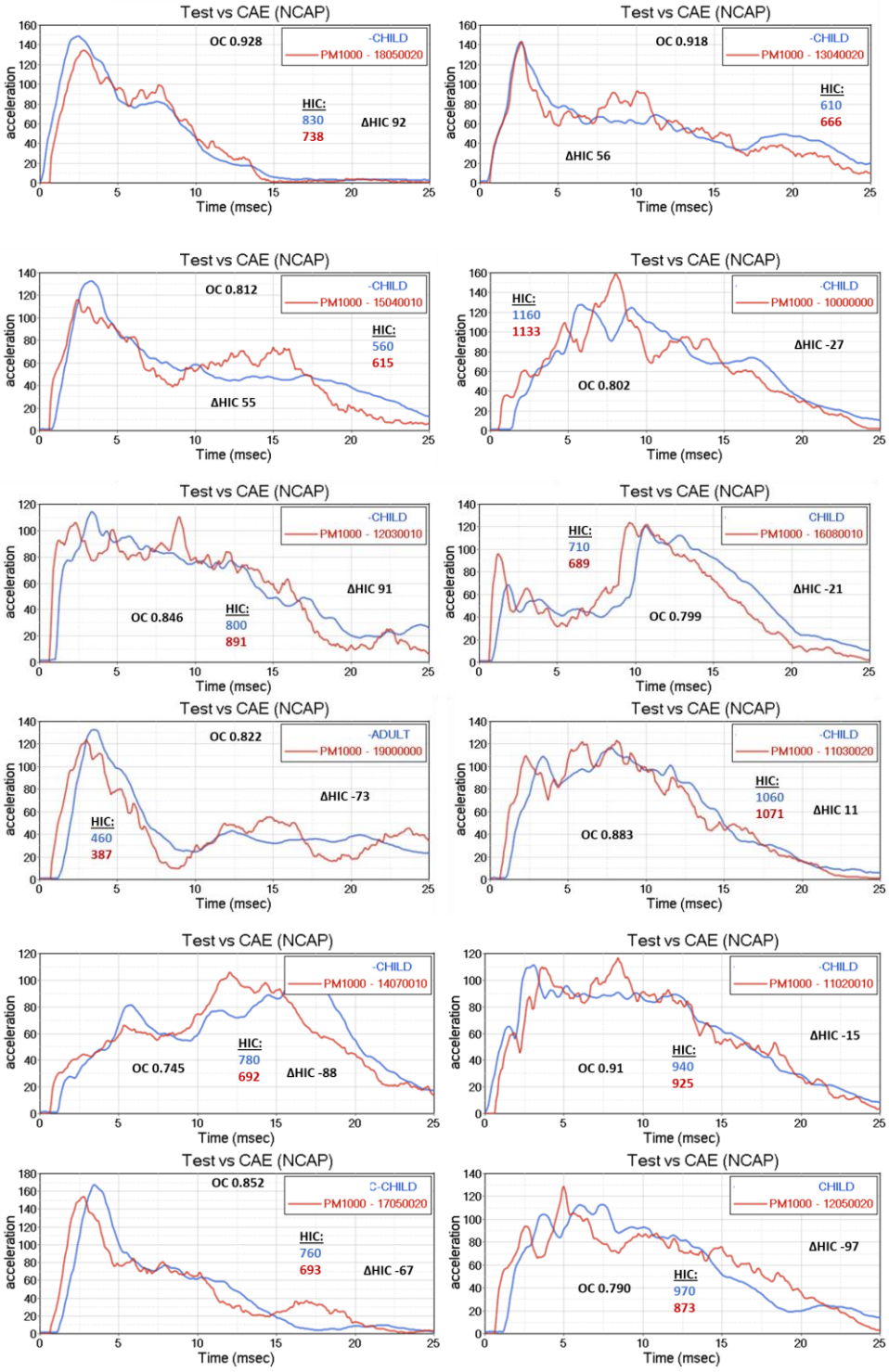

Figure 34. Headform acceleration comparison between tests and simulations of the GM pop-up hood design

Figure 35 shows the GM CAE modeling for the pop-up hood actuator system as well as an exemplar simulation with the GHBMC-F05-PS model. The actuator system in the model is represented by two Actuators (Dynamic and Static) and a tether wire to achieve the intended deployment.

- **Dynamic Actuator** activates and pushes the bonnet in deployed condition and returns.
- **Tether wire** helps limit the bonnet actuation to the intended deployment.
- **Static Actuator** remains out of contact until bonnet pops out completely and provides the resting face for the deployed bonnet to come back afterwards.

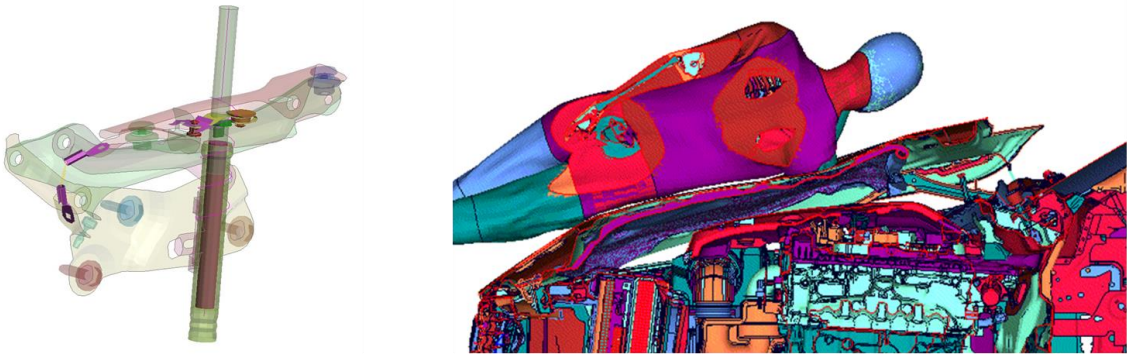

Pop-up Hood Actuator System

Vehicle-to-Pedestrian simulation
with GHBMC-F05-PS model and a pop-up hood

Figure 35. CT4 pop-up hood model actuator system and exemplar simulation with GHBMC pedestrian model

Simulation in a Hood Edge Impact Scenario

Simulations were initially conducted with the pop-up hood design and four GHBMC pedestrian models (6YO, F05, M50, and M95) at three speeds (30, 40, and 50 kph). All simulations were conducted at the centerline (Y=0 mm) of the vehicle front-end. None of the simulations with the M95 pedestrian model had a head-to-hood contact, and all head contacts occurred at the windshield. For the M50 model, head-to-hood contact only occurred at 30 kph. Because a higher body weight of pedestrian and higher vehicle speed could cause a pop-up hood to collapse, the M50th and M95th were simulated by increasing the vehicle height to ensure a head impact on the hood. It should be noted that the full body weight is not applied to the hood because of this adjustment.

Figure 36 shows two hood edge impact scenarios, both with the GHBMC M50 pedestrian model at 40 kph, the location of the pedestrian was varied along the lateral direction of the vehicle from the centerline (Y=500 mm and Y=400 mm). In both simulations, the pop-up hood was pushed down by the pedestrian, and the HIC values are relatively high. Since the Y=400 mm condition at 40 kph resulted in higher HIC, this condition was used as the hood edge impact scenario for further analysis in Task 4.

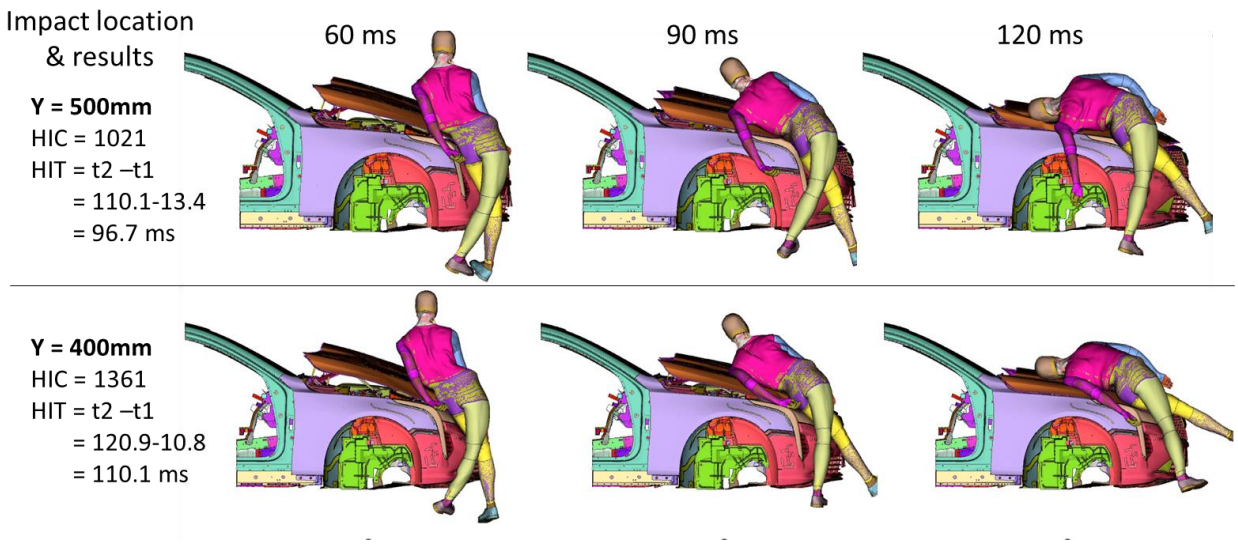

Figure 36. Two hood edge impact scenarios with M50 GHBM at 40 kph

Task 4: Simulations in a Hood Collapse Scenario

Selection of a Hood Collapse Case

In this task, the hood edge impact scenario identified in Task 3 was further used to study effects from pop-up hood design parameters on pedestrian head injury responses. As shown in Task 3, the hood edge impact scenario was conducted with M50 GHBMC pedestrian model under 40 kph at the Y=400mm impact location. In this scenario, the pedestrian's body force is high enough to "bottom out" the hood before a head strike occurs, which resulted in a relatively high HIC value.

Parametric Simulations in the Hood Collapse Scenario

A total of eight simulations were conducted with the pop-up hood design with two levels of actuator stiffness (0.3 and 1.5 kN), two levels of actuator bracket thickness (1.5 and 3 mm), and two levels of hinge reinforcement thickness (0.8 and 1.5 mm). Table 8 shows the simulation matrix and results, in which design #1 is the original/baseline design. Actuator stiffness dominated the pedestrian HIC values, while effects from actuator bracket thickness and hinge reinforcement thickness are not as significant. The higher level of actuator stiffness reduced HIC significantly. HIT and WAD are insensitive to any pop-up hood design parameters.

Table 8. Pedestrian simulation results by varing pop-up hood design parameters

Design No.	Actuator Stiffness (kN)	Actuator Bracket Thickness (mm)	Hinge Reinf. Thickness (mm)	HIC	HIT (ms)	WAD (mm)
1	0.3	1.5	0.8	845.6	110.4	1854.9
2	0.3	1.5	1.5	973.5	110.4	1854.8
3	0.3	3	0.8	941.8	110.7	1854.8
4	0.3	3	1.5	872.5	109.9	1865.7
5	1.5	1.5	0.8	503.7	107.1	1864.3
6	1.5	1.5	1.5	532.7	107.3	1873.6
7	1.5	3	0.8	527.2	107.4	1877.3
8	1.5	3	1.5	533.8	107.2	1876.4

Based on the results from Table 8, design #8 (Actuator stiffness of 1.5 kN, Actuator bracket thickness of 3 mm, and hinge reinforcement thickness of 1.5 mm) was selected as a good pop-up hood design for further simulations. Three additional simulations under 40 kph at the Y=400 location were conducted to further evaluate the pop-up hood design #8, in which F05, M50, and M95 GHBMC pedestrian models were used. In each of the additional simulations, the height of the vehicle was adjusted, so that the head of the pedestrian always hit the pop-up hood in an area close to the actuator. The pedestrian kinematics as well as the HIC and HIT values are shown in Figure 37. The pop-up hood design #8 provided good pedestrian protection in terms of the HIC values. Hood collapse did not occur in any of the additional simulations. With deployment system design as per hood design #8, HIC for the smaller pedestrian slightly increased (HIC of 425 compared to original HIC value of 350), but it is still much lower than threshold value of HIC 1000.

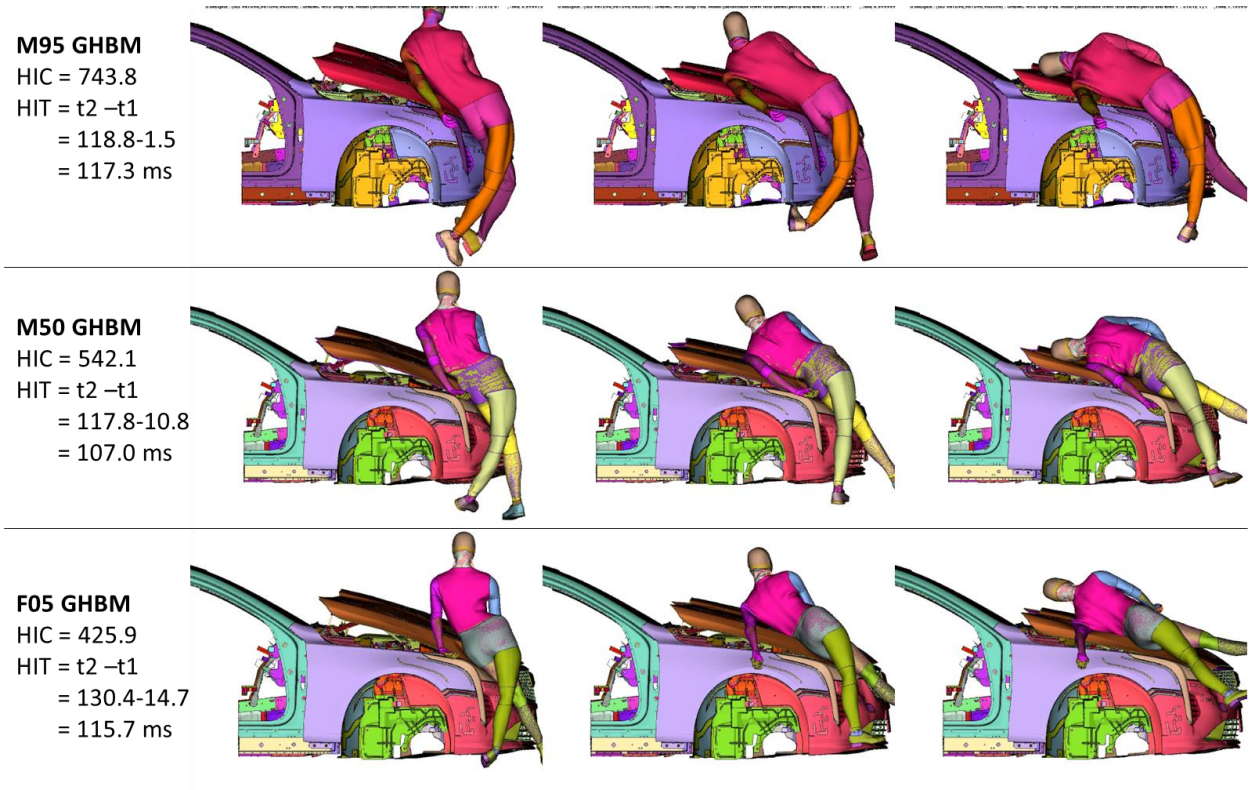

Figure 37. Pop-up hood design #8 evaluation results with varied HBM size

Summary

This study generated a virtual database of pedestrian impacts with a wide range of vehicle front-end geometries; developed prediction models to use vehicle front-end geometry, pedestrian size, impact speed, and WAD to predict pedestrian HIT, head contact velocity, and head contact angle; and investigated effects from pop-up hood design parameters on pedestrian head injury responses.

The GV models originally developed based on European vehicle geometries were morphed into 20 U.S. vehicle front-end geometries across a wide range of vehicle types and characteristics. A total of 240 pedestrian impact simulations were conducted using the 20 morphed GV models with four sizes of pedestrian human body models at three impact speeds. A set of predictors were selected based on the literature to predict HIT, head contact velocity, and head contact angle. High correlations and good accuracies were achieved in the prediction models.

Simulations with the pop-up hood design found that deployed hoods could potentially collapse due to body weight of a pedestrian under certain situations – based on impact location and pedestrian stature. The actuator stiffness during impact duration is the biggest contributor for the pop-up hood design to avoid hood collapse. Due to the variations of kinetic energy provided by different sizes of the pedestrian, the deployment system of a pop-up hood needs to be designed for highest pedestrian stature for avoiding hood collapse. With deployment system design as per the highest pedestrian stature, HIC for smaller pedestrian may slightly increase, but it is still lower compared to an undeployed hood for this vehicle design. It should be noted that this study is not intended to suggest that a pop-up hood is the only way for every vehicle to meet pedestrian safety requirement. A passive hood can also be designed to meet pedestrian safety requirements.

References

Anderson, R. W., McLean, A. J., Farmer, M. J., Lee, B. H., & Brooks, C. G. (1997). Vehicle travel speeds and the incidence of fatal pedestrian crashes. *Accident Analysis & Prevention, 29*, 667-674.

Ashton, S. J., & Mackay, G. M. (1979). Some characteristics of the population who suffer trauma as pedestrians when hit by cars and some resulting implications. IRCOBI Conference, Gothenburg, Sweden.

Belingardi, G., Scattina, A., & Gobetto, E. (2009). *Development of a hybrid hood to improve pedestrian safety in case of vehicle impact.* The 21st International Technical Conference on the Enhanced Safety of Vehicles, Stuttgart, Germany.

Bhattacharjee, S. S., Mane, S., Kusnoorkar, H., Hwang, S., & Niesluchowski, M. (2017). *Pedestrian head impact time estimate based on vehicle geometric parameters* (SAE Technical Paper 2017-01-1453). WCX 17: SAE World Congress Experience, Detroit, MI. www.sae.org/publications/technical-papers/content/2017-01-1453/

Chen, H., Poulard, D., Crandall, J. R., & Panzer, M. B. (2015). *Pedestrian response with different initial positions during impact with a mid-sized sedan* (15-0391). The 24th International Technical Conference on the Enhanced Safety of Vehicles, Gothenburg, Sweden.

Cuerden, R., Richards, D., & Hill, J. (2007). *Pedestrians and their survivability at different impact speeds*. The 20th International Technical Conference on the Enhanced Safety of Vehicles, Lyon, France.

Davis, G. A. (2001). Relating severity of pedestrian injury to impact speed in vehicle-pedestrian crashes: Simple threshold model. *Transport Research Record, 1773*(1), 108-113.

Decker, W., Koya, B., Pak, W., Untaroiu, C. D., & Gayzik, F. S. (2019). Evaluation of finite element human body models for use in a standardized protocol for pedestrian safety assessment. *Traffic Injury Prevention, 20*, S32-S36.

Demetriades, D., Murray, J., Martin, M., Velmahos, G., Salim, A., Alo, K., & Rhee, P. (2004). Pedestrians injured by automobiles: relationship of age to injury type and severity. *Journal of the American College of Surgeons, 199*, 382-387.

Desapriya, E., Subzwari, S., Sasges, D., Basic, A., Alidina, A., Turcotte, K., & Pike, I. (2010). Do light truck vehicles impose greater risk of pedestrian injury than passenger aars? A meta-analysis and systematic review. *Traffic Injury Prevention, 11*, 48-56.

Elliott, J. R., Lyons, M., Kerrigan, J., Wood, D. P., & Simms, C. K. (2012). Predictive capabilities of the MADYMO multibody pedestrian model: Three-dimensional head translation and rotation, head impact time and head impact velocity. *Proceedings of the Institution of Mechanical Engineers Part K-Journal of Multi-Body Dynamics, 226*, 266-277.

European New Car Assessment Programme. (2018a). Pedestrian testing protocol. (Version 8.5). https://cdn.euroncap.com/media/41769/euro-ncap-pedestrian-testing-protocol-v85.201811091256001913.pdf

Euro NCAP. (2019). Pedestrian human model certification (Version 2.0). *Techical Bulletin 024*. https://cdn.euroncap.com/media/56949/tb-024-pedestrian-human-model-certification-v20.pdf

Evrard, B. (2011). *Innovative bonnet active actuator (B2A) for pedestrian protection.* The 21st International Technical Conference on the Enhanced Safety of Vehicles, Stuttgart, Germany.

Fredriksson, R., Yngve Håland, & Yang, J. (2001). *Evaluation of a new pedestrian head injury protection system with a sensor in the bumper and lifting of the bonnet's rear part* (SAE Technical Paper 2001-06-0089). The 17th International Technical Conference on the Enhanced Safety of Vehicles, Amsterdam, The Netherlands. www.sae.org/publications/technical-papers/content/2001-06-0089/

Henary, B. Y., Ivarsson, J., & Crandall, J. R. (2006). The influence of age on the morbidity and mortality of pedestrian victims. *Traffic Injury Prevention, 7,* 182-190.

Hu, J., Chou, C. C., Yang, K. H., & King, A. I. (2007). A weighted logistic regression analysis for predicting the odds of head/face and neck injuries during rollover crashes. *Annual Proceedings of the Association for the Advancement of Automotive Medicine, 51,* 363-379.

Hu, J., & Klinich, K. D. (2015). Toward designing pedestrian-friendly vehicles. *International Journal of Vehicle Safety 8,* 22-53.

Hu, J., Klinich, K. D., Manary, M. A., Flannagan, C. A. C., Narayanaswamy, P., Reed, M. P., Andreen, M., Neal, M., & Lin, C. H. (2017). Does unbelted safety requirement affect protection for belted occupants? *Traffic Injury Prevention, 18,* S85-S95.

Hu, J., Zhang, K., Reed, M. P., Wang, J. T., Neal, M., & Lin, C. H. (2019). Frontal crash simulations using parametric human models representing a diverse population. *Traffic Injury Prevention, 20,* S97-S105.

Hu, J. W., Flannagan, C., Ganesan, S., Bowman, P., Sun, W. B., Farooq, I., Kalra, A., & Rupp, J. (2023). Understanding the new trends in pedestrian injury distribution and mechanism through data linkage and modeling. *Accident Analysis & Prevention, 188.*

Huang, S., & Yang, J. (2010). Optimization of a reversible hood for protecting a pedestrian's head during car collisions. *Accident Analysis & Prevention, 42,* 1136-1143.

Hwang, E., Hu, J., Chen, C., Klein, K. F., Miller, C. S., Reed, M. P., Rupp, J. D., & Hallman, J. J. (2016). Development, Evaluation, and Sensitivity Analysis of Parametric Finite Element Whole-Body Human Models in Side Impacts. *Stapp Car Crash Journal, 60,* 473-508.

Inomata, Y., Iwai, N., Maeda, Y., Kobayashi, S., Okuyama, H., & Takahashi, N. (2009). *Development of the pop-up engine hood for pedestrian head protection.* The 21st International Technical Conference on the Enhanced Safety of Vehicles, Stuttgart, Germany.

Kent, R., Henary, B., & Matsuoka, F. (2005a). On the fatal crash experience of older drivers. *Annual Proceedings of the Association for the Advancement of Automotive Medicine, 49,* 371-391.

Kent, R., Lee, S. H., Darvish, K., Wang, S., Poster, C. S., Lange, A. W., Brede, C., Lange, D., & Matsuoka, F. (2005b). Structural and material changes in the aging thorax and their role in crash protection for older occupants. *Stapp Car Crash Journal, 49,* 231-249.

Kent, R., Trowbridge, M., Lopez-Valdes, F. J., Ordoyo, R. H., & Segui-Gomez, M. (2009). How many people are injured and killed as a result of aging? Frailty, fragility, and the elderly risk-exposure tradeoff assessed via a risk saturation model. *Annals of Advances in Automotive Medicine, 53*, 41-50.

Kerkeling, C., Schäfer, J., & Thompson, D. G.-M. (2005). *Year structural hood and hinge concepts for pedestrian protection.* The 19th International Technical Conference on the Enhanced Safety of Vehicles, Washington, DC.

Kerrigan, J., Arregui-Dalmases, C., & Crandall, J. (2012). Assessment of pedestrian head impact dynamics in small sedan and large SUV collisions. *International Journal of Crashworthiness, 17*, 243-258.

Kerrigan, J., Arregui, C., & Crandall, J. (2009). *Pedestrian head impact dynamics: Comparison of dummy and PMHS in small sedan and large suv impacts.* The 21st International Technical Conference on the Enhanced Safety of Vehicles, Stuttgart, Germany.Kim, J. K., Ulfarsson, G. F., Shankar, V. N., Kim, S. (2008). Age and pedestrian injury severity in motor-vehicle crashes: A heteroskedastic logit analysis. *Accident Analysis & Prevention, 40*, 1695-1702.

Klug, C. (2018). Assessment of passive vulnerable road user protection With human body models. Graz University of Technology.

Klug, C., Feist, F., Raffler, M., Sinz, W., Petit, P., James Ellway, & Ratingen, M.v. (2017). Development of a procedure to compare kinematics of human body models for pedestrian simulations. IRCOBI Conference, Gothenburg, Sweden.

Kong, C., & Yang, J. (2010). Logistic regression analysis of pedestrian casualty risk in passenger vehicle collisions in China. *Accident Analysis & Prevention, 42*, 987-993.

Laituri, T. R., Prasad, P., Sullivan, K., Frankstein, M., & Thomas, R. S. (2005). *Derivation and evaluation of a provisional, age-dependent, AIS3+ thoracic risk curve for belted adults in frontal impacts* (SAE Technical Paper 2005-01-0297). SAE World Congress & Exhibition, Detroit, MI. www.sae.org/publications/technical-papers/content/2005-01-0297/

Lee, C., & Abdel-Aty, M. (2005). Comprehensive analysis of vehicle-pedestrian crashes at intersections in Florida. *Accident Analysis & Prevention 37*, 775-786.

Lee, K. B., Jung, H. J., & Bae, H. I. (2007). *The study on developing active hood lift system for decreasing pedestrian head injury* The 20th International Technical Conference on the Enhanced Safety of Vehicles,Lyon, France.

Lefler, D. E., & Gabler, H. C. (2004). The fatality and injury risk of light truck impacts with pedestrians in the United States. *Accident Analysis & Prevention, 36*, 295-304.

Li, G., Braver, E. R., & Chen, L. H. (2003). Fragility versus excessive crash involvement as determinants of high death rates per vehicle-mile of travel among older drivers. *Accident Analysis & Prevention, 35*, 227-235.

Liu, Q., Xia, Y., Zhou, Q., & Wang, J.-T. (2009). *Design analysis of a sandwich hood structure for pedestrian protection.* The 21st International Technical Conference on the Enhanced Safety of Vehicles, Stuttgart, Germany.

Longhitano, D., Henary, B., Bhalla, K., Ivarsson, J., & Crandall, J. (2005). *Influence of vehicle body type on pedestrian injury distribution* (SAE Technical Paper 2005-01-1876). SAE World Congress & Exhibition, Detroit, MI. www.sae.org/publications/technical-papers/content/2005-01-1876/

Martin, J. L., Lardy, A., & Laumon, B. (2011). Pedestrian injury patterns according to car and casualty characteristics in france. *Annals of Advances in Automotive Medicine, 55*, 137-146.

Meng, Y., Pak, W., Guleyupoglu, B., Koya, B., Gayzik, F. S., & Untaroiu, C. D. (2017). A finite element model of a six-year-old child for simulating pedestrian accidents. *Accident Analysis & Prevention, 98*, 206-213.

Mizuno, Y. (2005). Summary of IHRA pedestrian safety WG activities: *Proposed test methods to evaluate pedestrian protection afforded by passenger cars*. The 19th International Technical Conference on the Enhanced Safety of Vehicles, Washington, DC.

Morris, A., Welsh, R., Frampton, R., Charlton, J., & Fildes, B. (2002). An overview of requirements for the crash protection of older drivers. *Annual Proceedings of the Association for the Advancement of Automotive Medicine, 46*, 141-156.

NHTSA. (2022). *Traffic safety facts 2020 data: pedestrians.* National Highway Traffic Safety Administration. https://crashstats.nhtsa.dot.gov/Api/Public/ViewPublication/813310

Oh, C., Kang, Y. S., & Kim, W. (2008a). Assessing the safety benefits of an advanced vehicular technology for protecting pedestrians. *Accident Analysis & Prevention, 40*, 935-942.

Oh, C., Kang, Y. S., Youn, Y., & Konosu, A. (2008b). Development of probabilistic pedestrian fatality model for characterizing pedestrian-vehicle collisions. *International Journal of Automotive Technology, 9*, 191-196.

Pak, W., Meng, Y. Z., Schap, J., Koya, B., Gayzik, S. F., & Untaroiu, C. D. (2019). Finite Element Model of a High-Stature Male Pedestrian for Simulating Car-to-Pedestrian Collisions. *International Journal of Automotive Technology, 20,* 445-453.

Pal, C., Okabe, T., Vimalathithan, K., Manoharan, J., Muthanandam, M., & Narayanan, S. (2014). *Estimation of pelvis injuries and head impact time using different pedestrian human FE models* (SAE Technical Paper 2014-01-0522). SAE World Congress & Exhibition, Detroit, MI.

Pasanen, E., & Salmivaara, H. (1993). Driving speeds and pedestrian safety in the city of Helsinki. *Traffic Engineering & Control, 34*, 308-310.

Paulozzi, L. J. (2005). United States pedestrian fatality rates by vehicle type. *Injury Prevention, 11*, 232-236.

Peng, Y., Deck, C., Yang, J. K., Otte, D., & Willinger, R. (2013). A study of adult pedestrian head impact conditions and injury risks in passenger car collisions based on real-world accident data. Traffic Injury Prevention, 14, 639-646.

Peng, Y., Deck, C., Yang, J. K., & Willinger, R. (2012). Effects of pedestrian gait, vehicle-front geometry and impact velocity on kinematics of adult and child pedestrian head. *International Journal of Crashworthiness, 17,* 553-561.

Rosen, E., & Sander, U. (2009). Pedestrian fatality risk as a function of car impact speed. *Accident Analysis & Prevention, 41*, 536-542.

Rosen, E., Stigson, H., & Sander, U. (2011). Literature review of pedestrian fatality risk as a function of car impact speed. *Accident Analysis & Prevention, 43*, 25-33.

Roudsari, B. S., Mock, C. N., Kaufman, R., Grossman, D., Henary, B. Y., & Crandall, J.,(2004). Pedestrian crashes: higher injury severity and mortality rate for light truck vehicles compared with passenger vehicles. *Injury Prevention, 10*, 154-158.

Shin, M. K., Park, K. T., & Park, G. J. (2008). Design of the active hood lift system using orthogonal arrays. *Proceedings of the Institution of Mechanical Engineers Part D-Journal of Automobile Engineering, 222*, 705-717.

Song, E., Petit, P., Trosseille, X., Uriot, J., Potier, P., Dubois, D., & Douard, R. (2017). New reference PMHS tests to assess whole-body pedestrian impact using a simplified generic vehicle front-end. *Stapp Car Crash Journal, 61,* 299-354.

Untaroiu, C. D., Pak, W., Meng, Y. Z., Schap, J., Koya, B., & Gayzik, S. (2018). A finite element model of a midsize male for simulating pedestrian accidents. *Journal of Biomechanical Engineering-Transactions of the American Society of Mechanical Engineers, 140*.

Watanabe, R., Katsuhara, T., Miyazaki, H., Kitagawa, Y., Yasuki, T. (2012). Research of the relationship of pedestrian injury to collision speed, car-type, impact location and pedestrian sizes using human FE model (THUMS Version 4). *Stapp Car Crash Journal, 56*, 269-321.

WHO. (2009). *Global status report on road safety.* World Health Organization.

Yaksich, S. J. (1964). Pedestrians with milage: A study of elderly pedestrian accidents in St. Petersburg, Florida. American Automobile Association..

Yang, J. (2005). Review of injury biomechanics in car-pedestrian collisions. *International Journal of Vehicle Safety, 1*, 100-117.

Zhang, K., Cao, L., Fanta, A., Reed, M. P., Neal, M., Wang, J. T., Lin, C. H., & Hu, J. (2017). An automated method to morph finite element whole-body human models with a wide range of stature and body shape for both men and women. *Journal of Biomechanics, 60*, 253-260.

Zhou, Q., Rouhana, S. W., Melvin, J. W. (1996). *Year age effects on thoracic injury tolerance* (SAE Technical Paper 962421). The 40th Stapp Car Crash Conference.

Appendix A: Simulation Results (HIT, WAD, HeadV, HVAng)

Honda Accord (2014)

	6YO	F05
30 kph	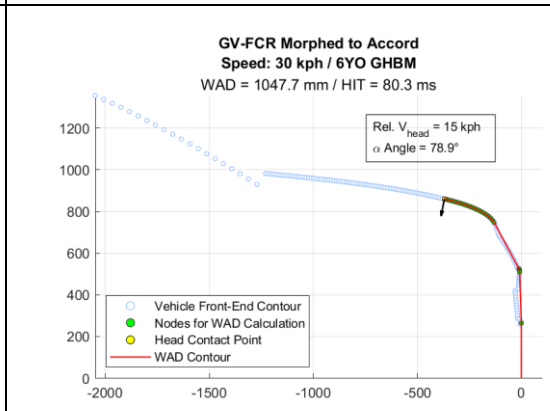	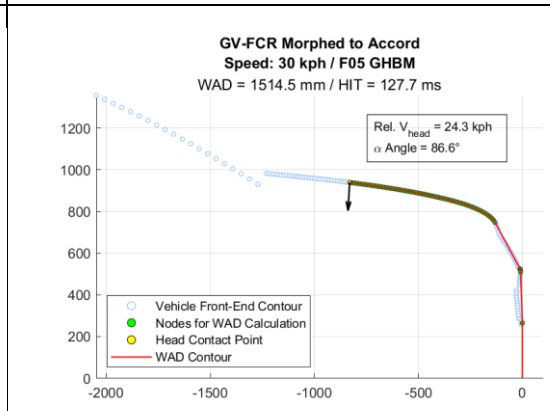
40 kph	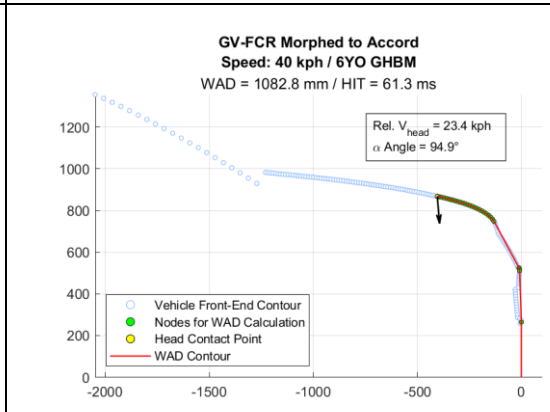	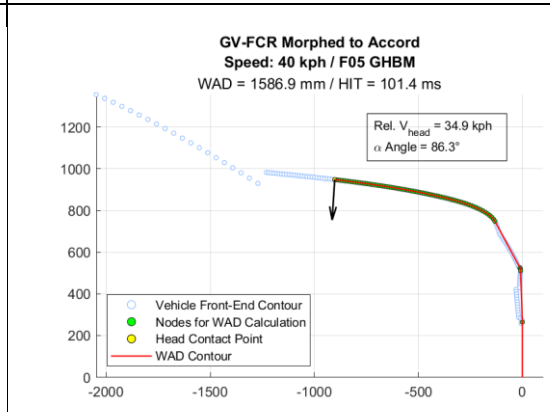
50 kph	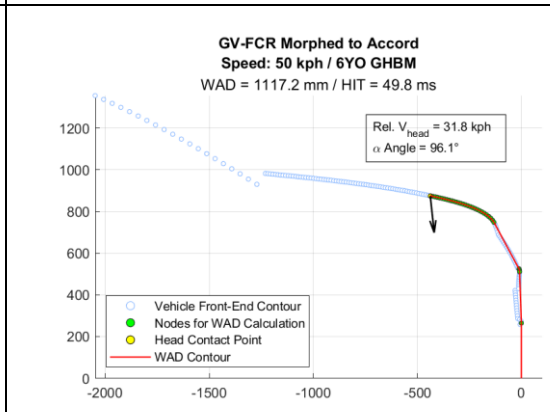	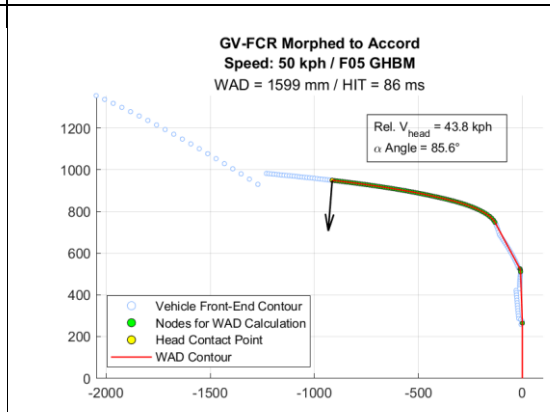

Honda Accord (2014)

	M50	M95
30 kph	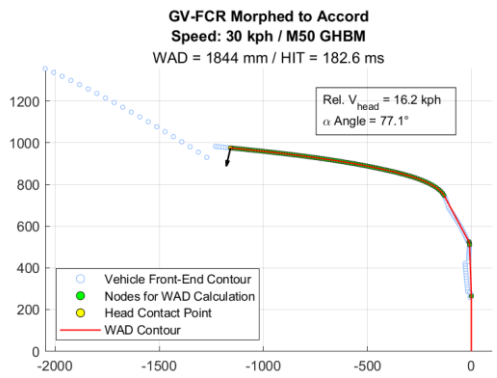	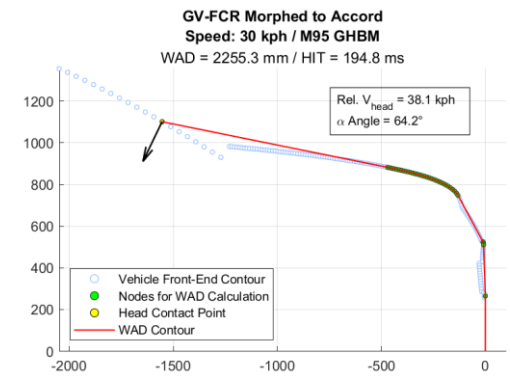
40 kph	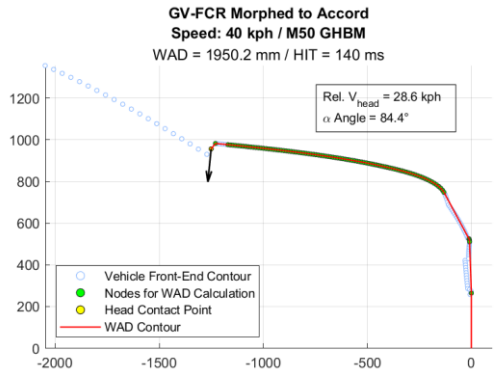	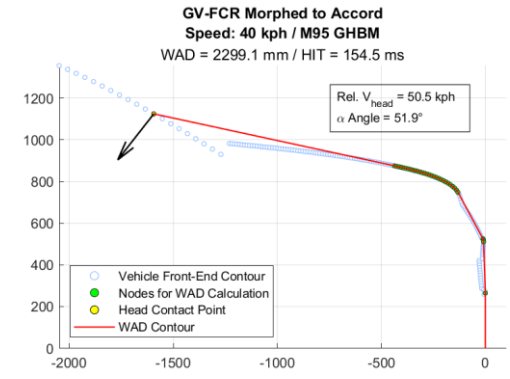
50 kph	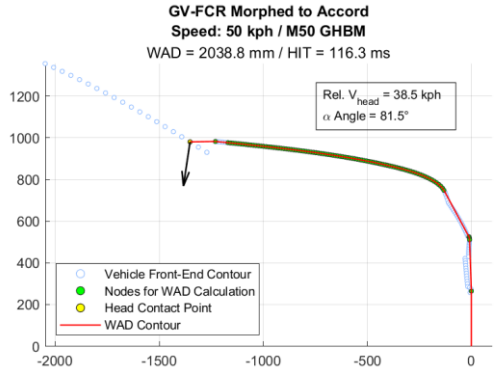	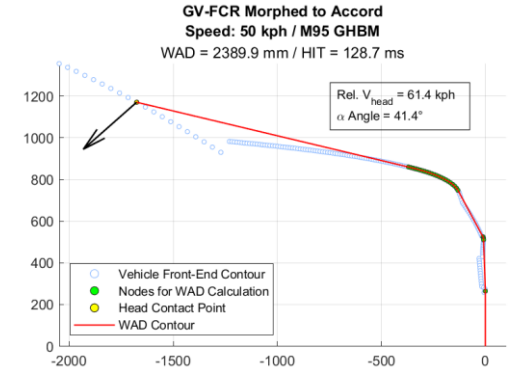

Toyota Camry (2012)

	6YO	F05
30 kph	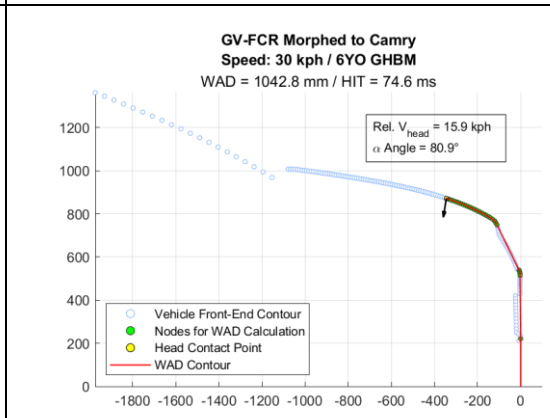	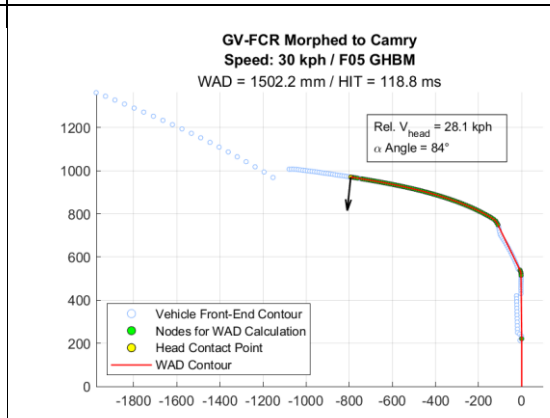
40 kph	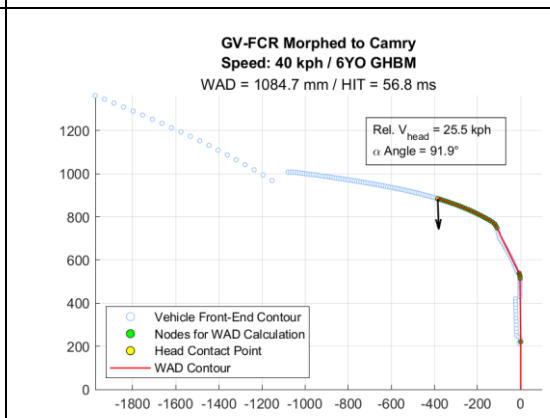	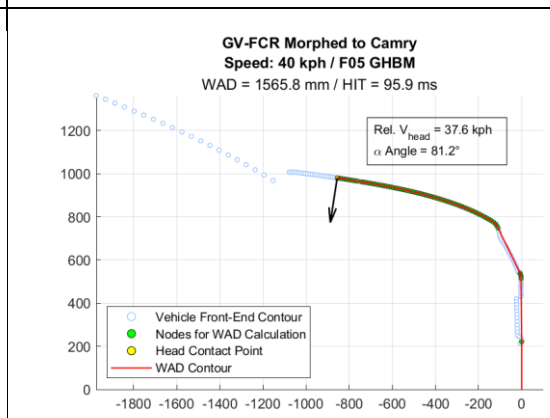
50 kph	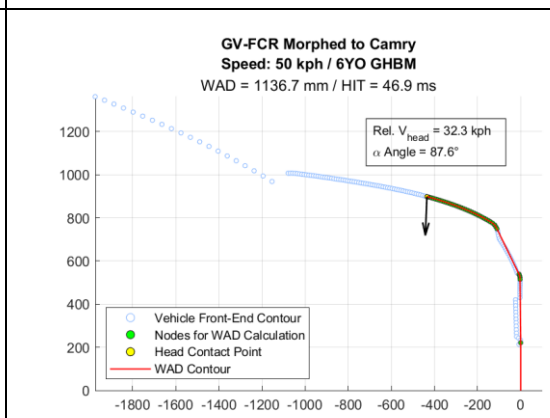	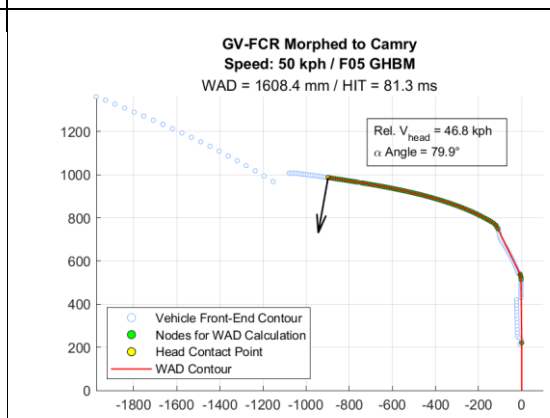

Toyota Camry (2012)

	M50	M95
30 kph	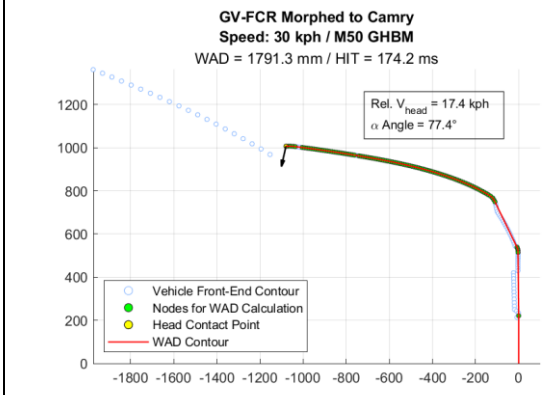	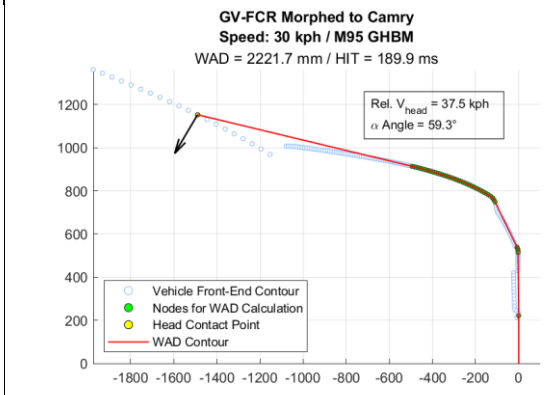
40 kph	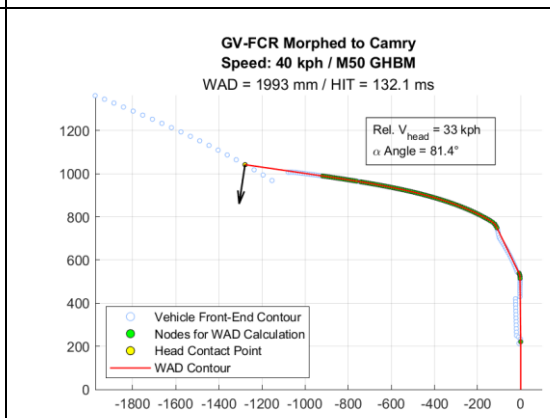	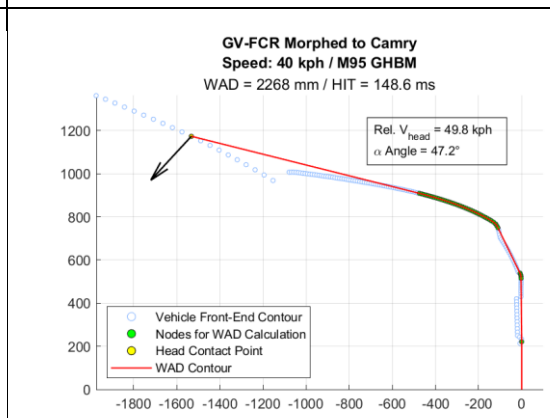
50 kph	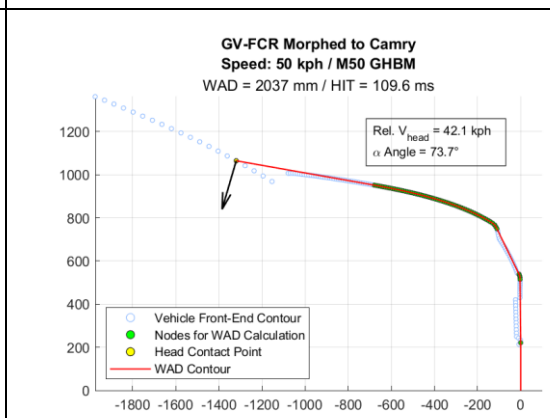	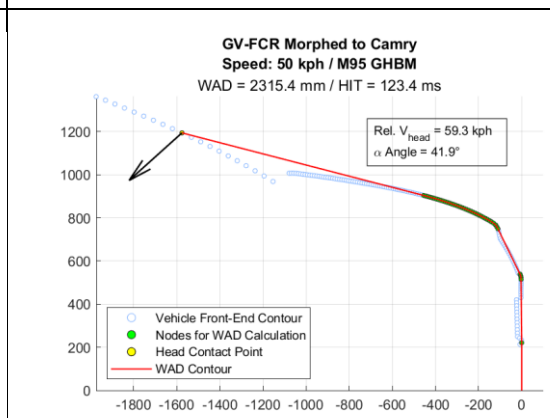

Dodge Caravan (1997)

	6YO	F05
30 kph	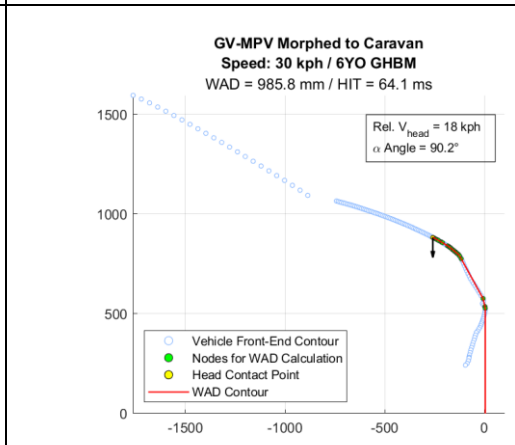	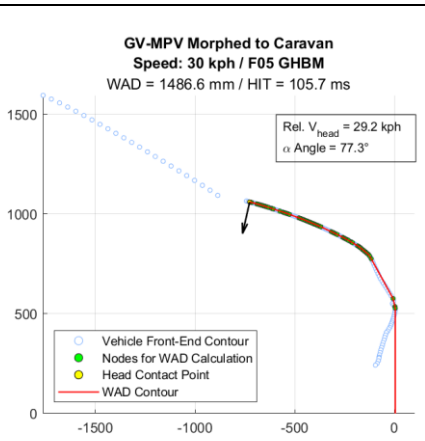
40 kph	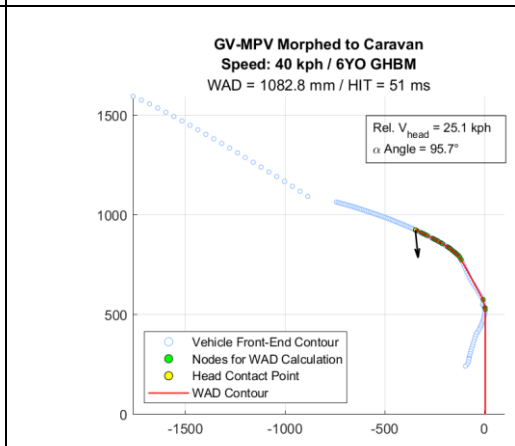	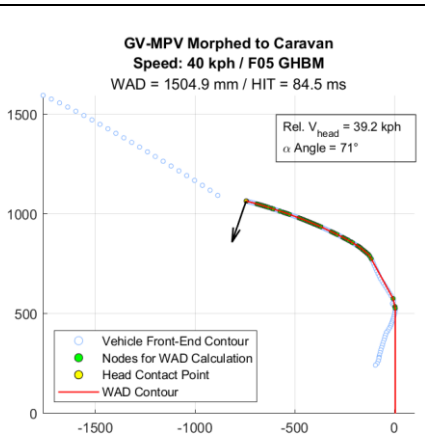
50 kph	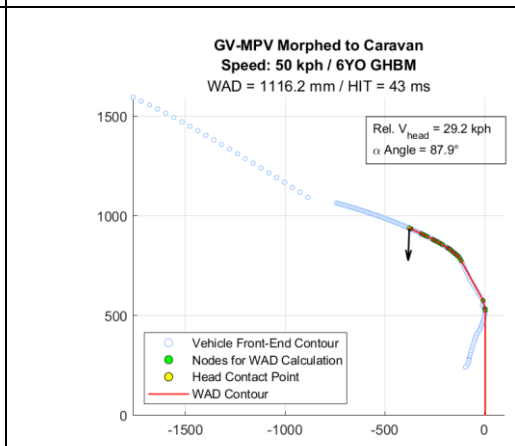	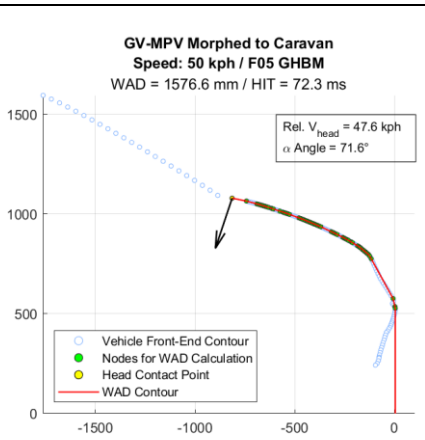

Dodge Caravan (1997)

	M50	M95
30 kph	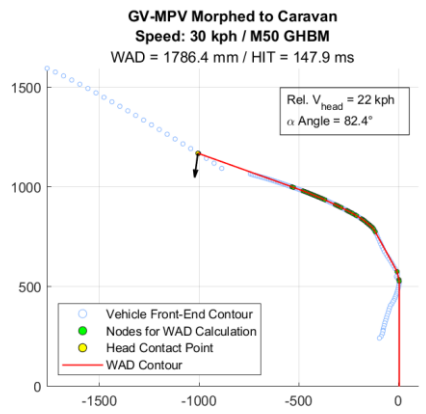	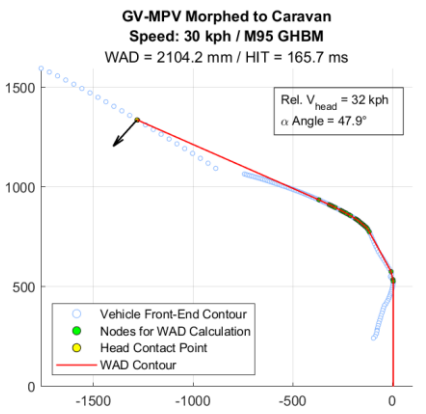
40 kph	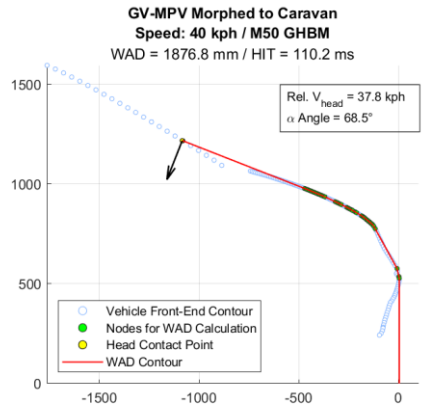	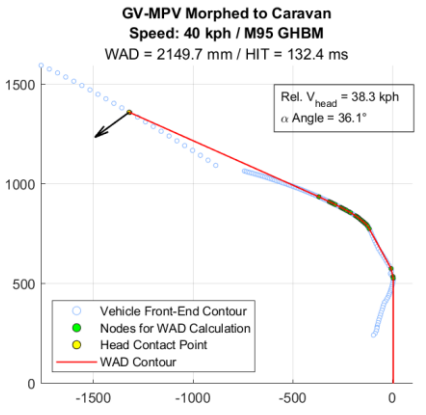
50 kph	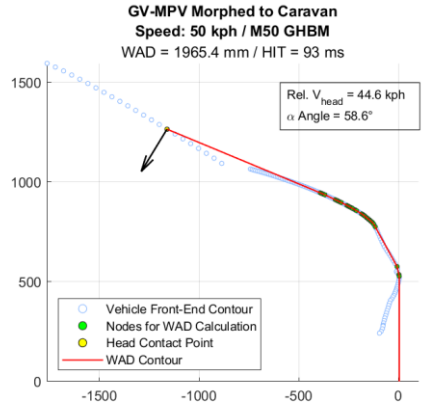	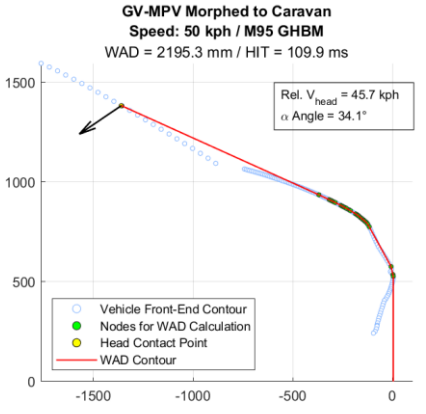

Honda Civic (2009)

	6YO	F05
30 kph	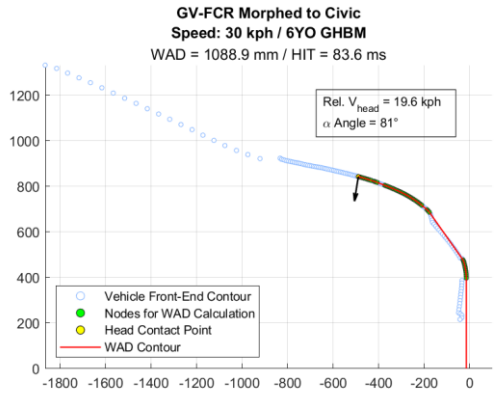	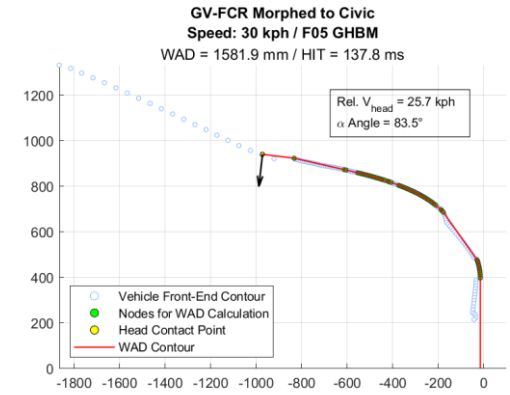
40 kph	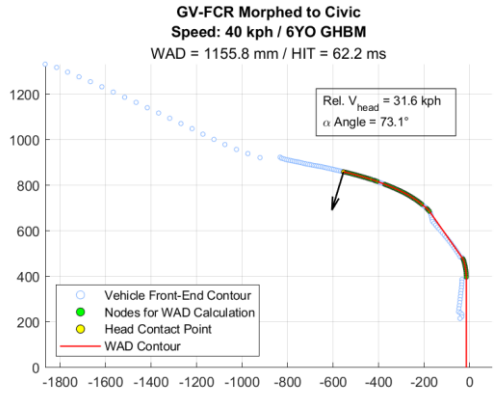	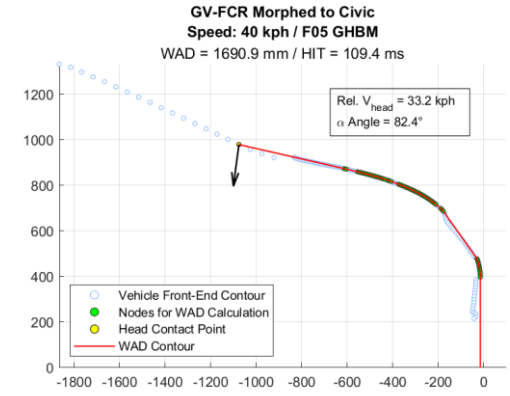
50 kph	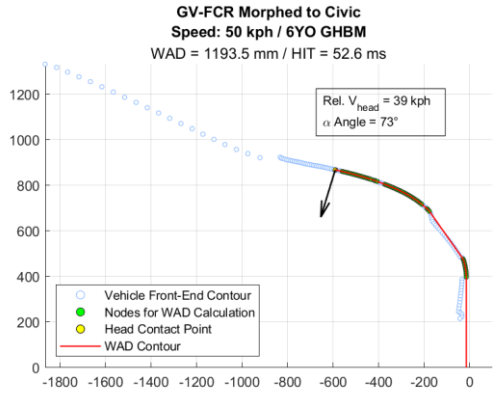	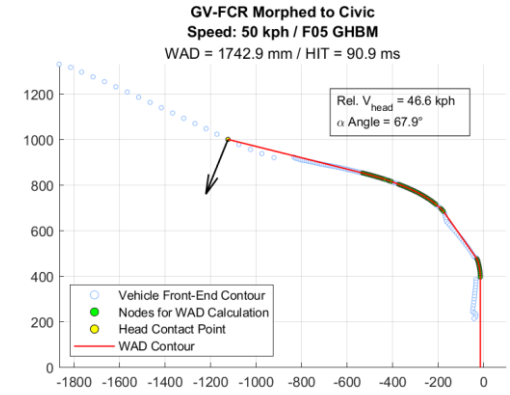

Honda Civic (2009)

	M50	M95
30 kph	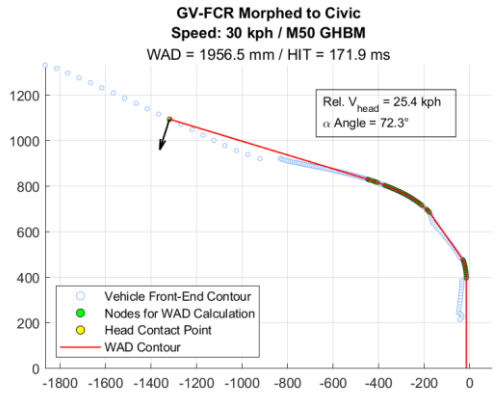	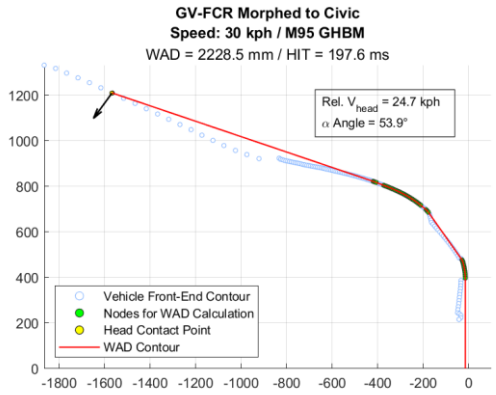
40 kph	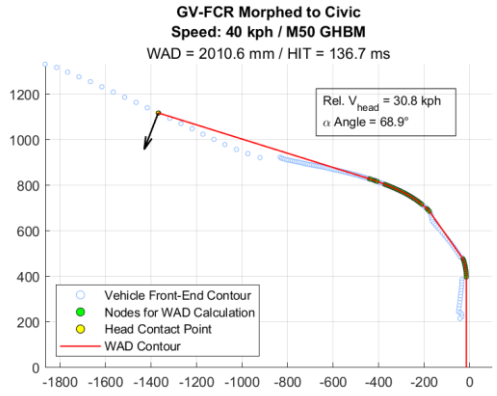	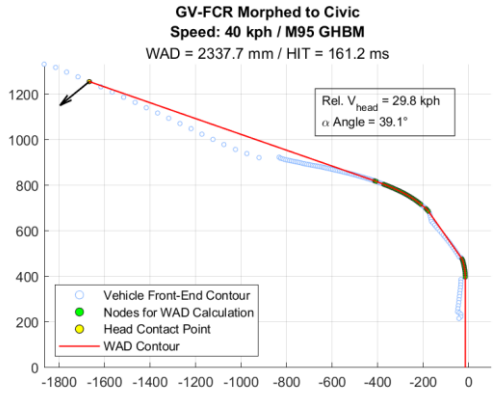
50 kph	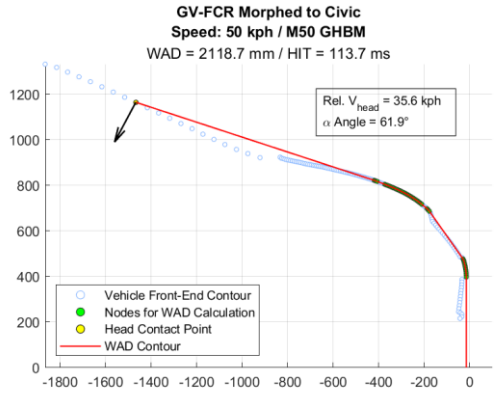	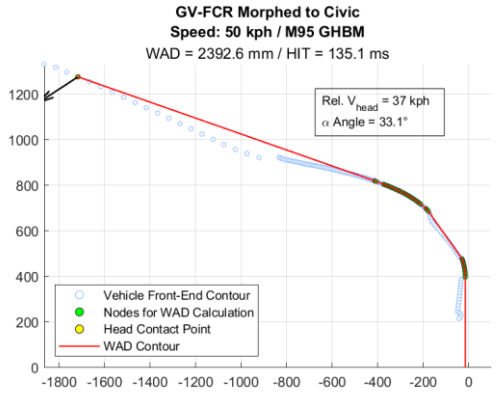

Honda CR-V (2017)

	6YO	F05
30 kph	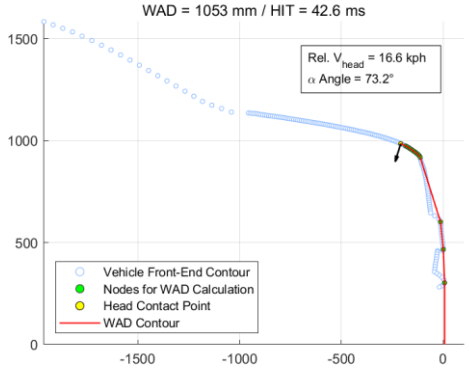	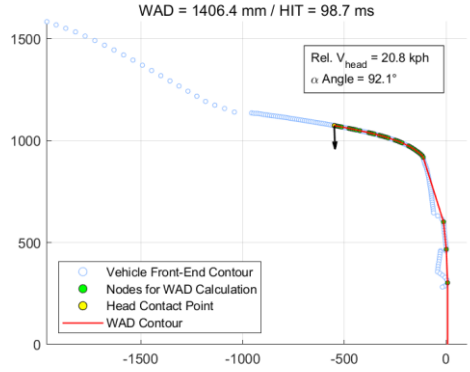
40 kph	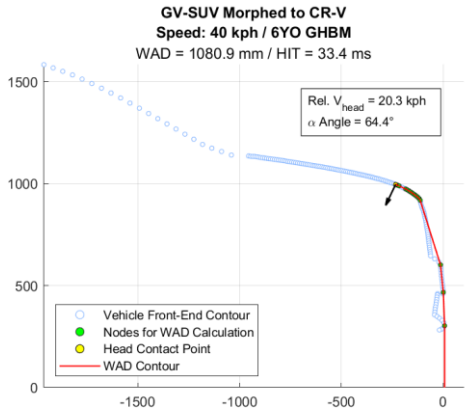	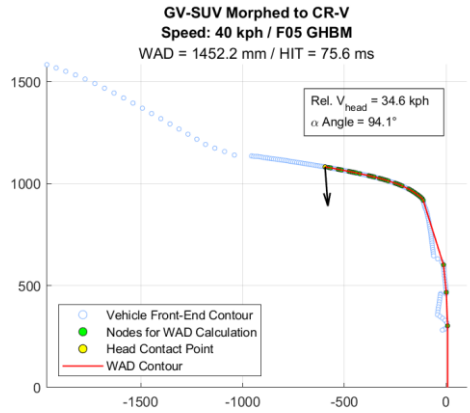
50 kph	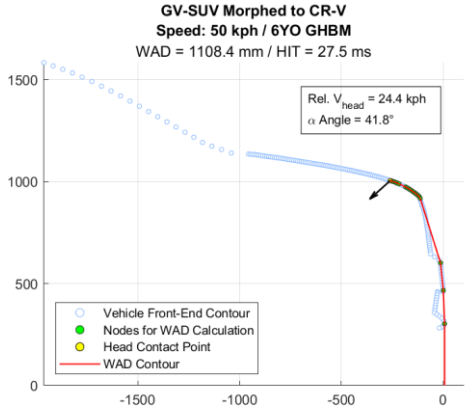	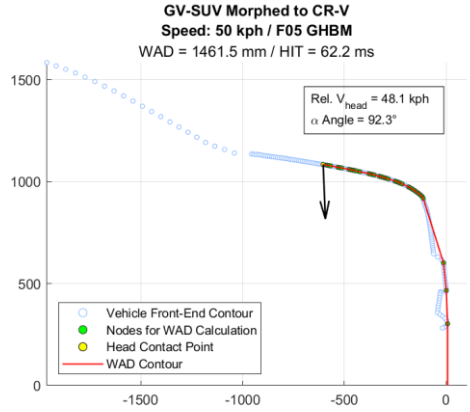

Honda CR-V (2017)

	M50	M95
30 kph	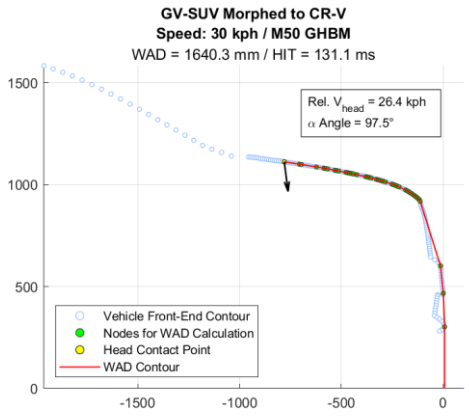	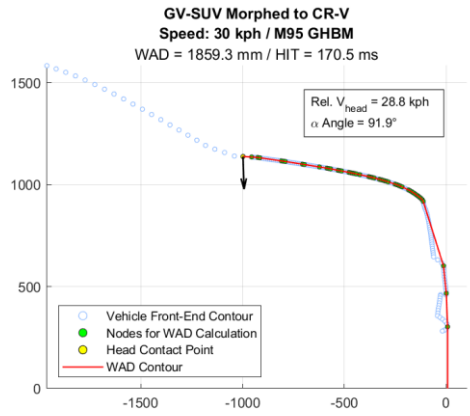
40 kph	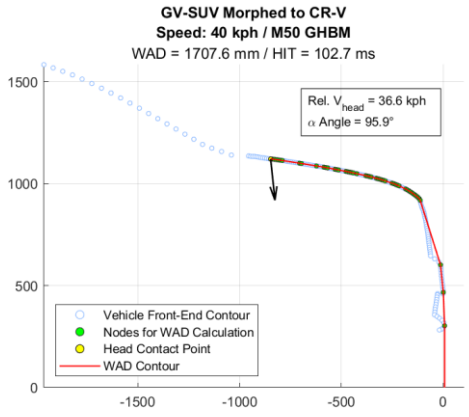	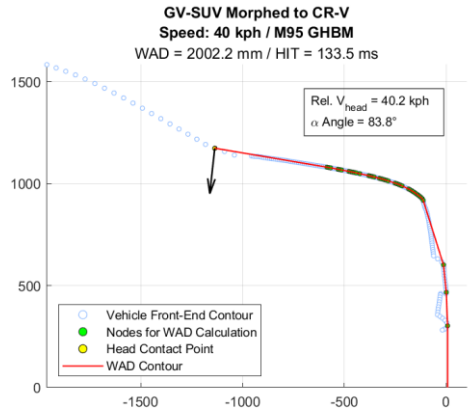
50 kph	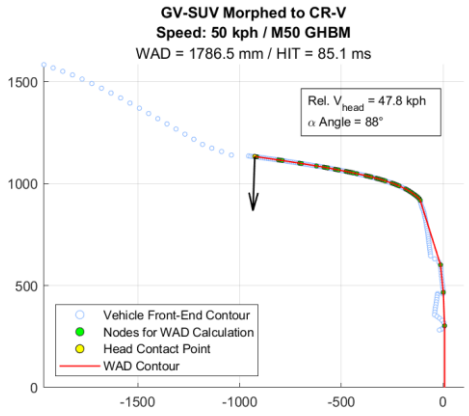	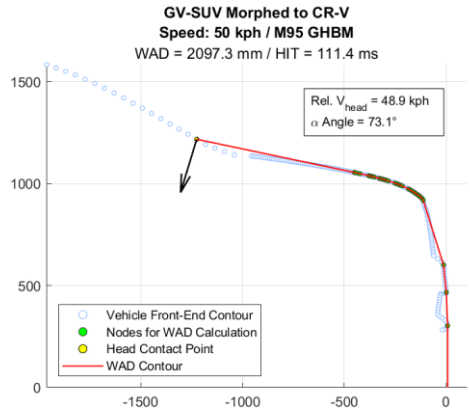

Cadillac CT4 (2022)

	6YO	F05
30 kph	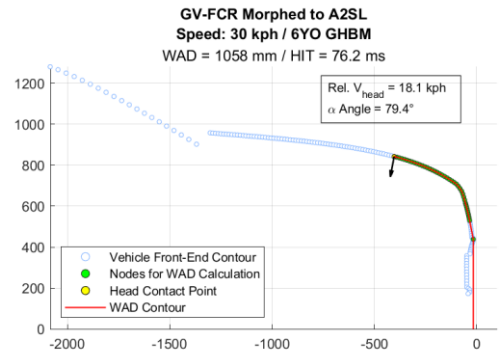	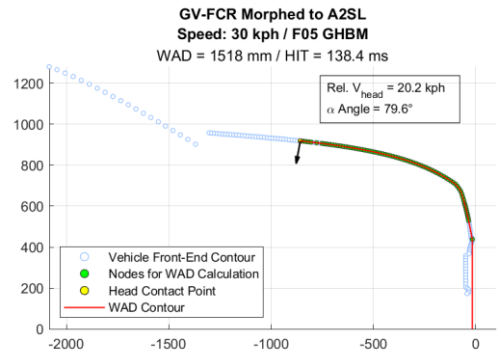
40 kph	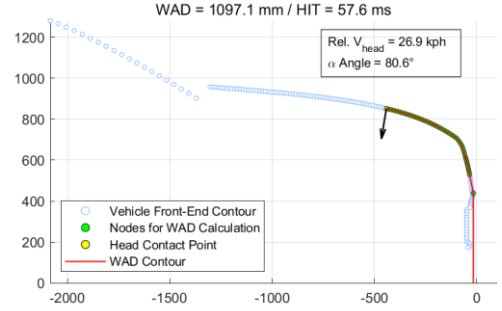	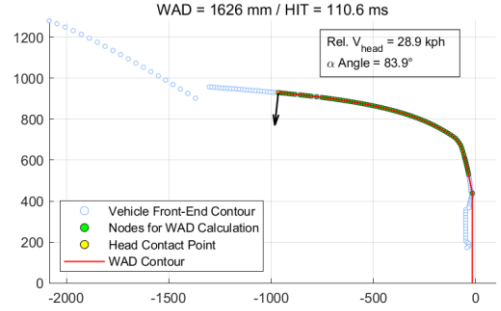
50 kph	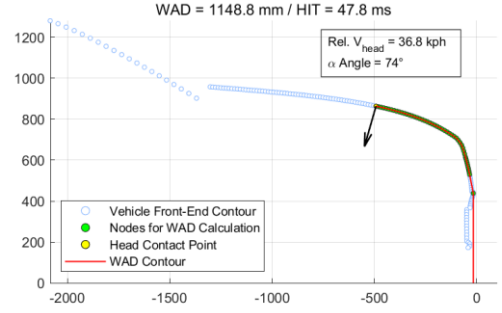	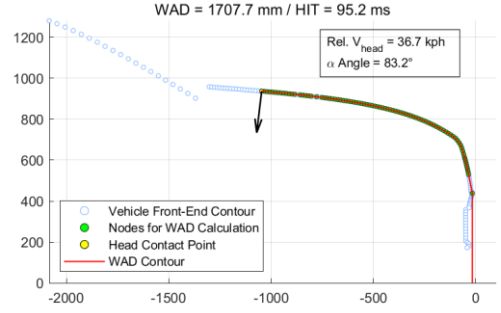

Cadillac CT4 (2022)

	M50	M95
30 kph	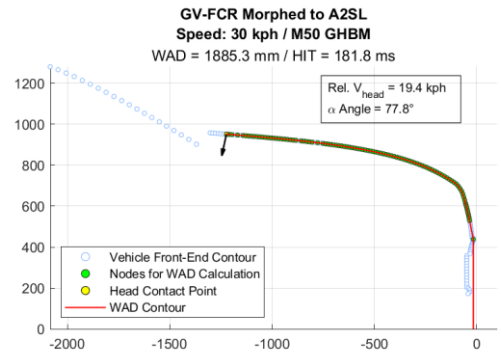	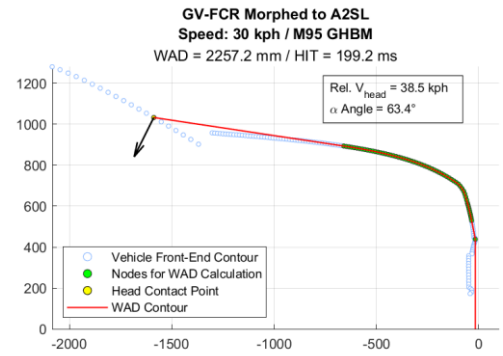
40 kph	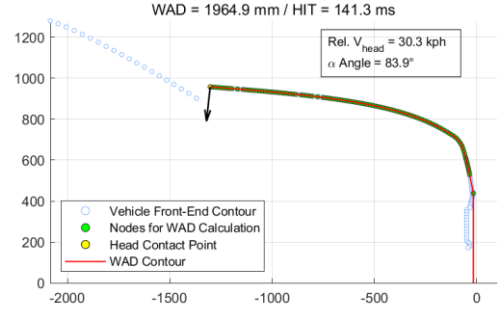	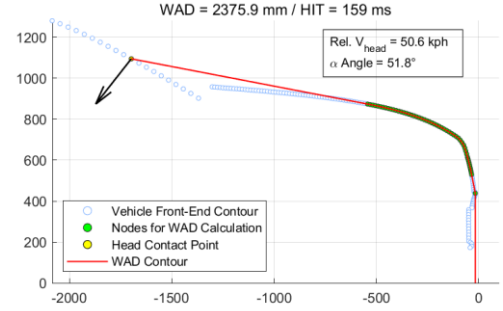
50 kph	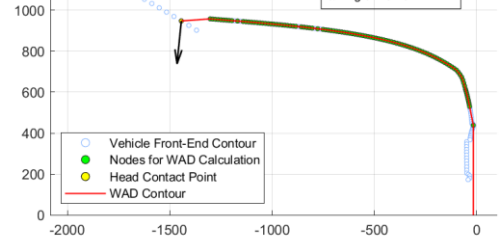	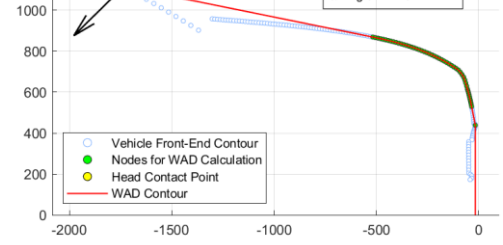

Ford Econoline (1999)

	6YO	F05
30 kph	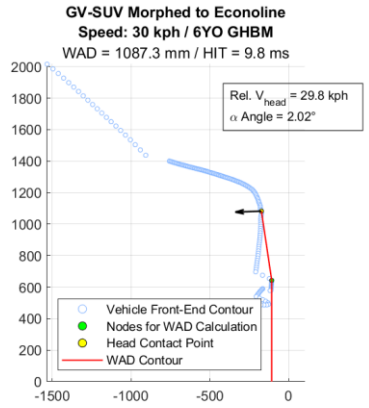	**Normal termination (Pedestrian knocked down without head contact)**
40 kph	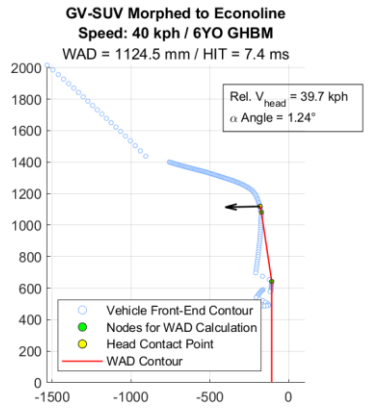	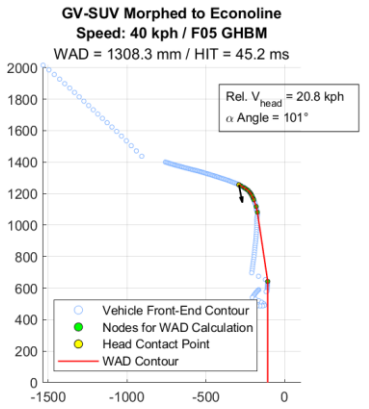
50 kph	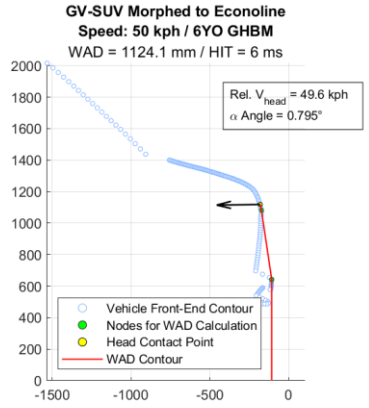	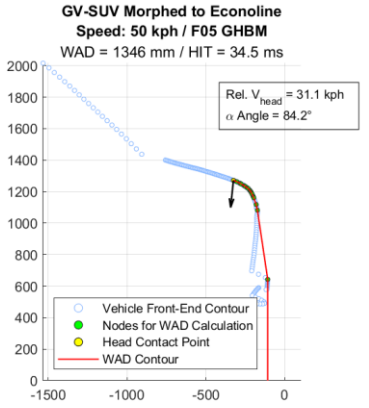

Ford Econoline (1999)

	M50	M95
30 kph	**Normal termination (Pedestrian knocked down without head contact)**	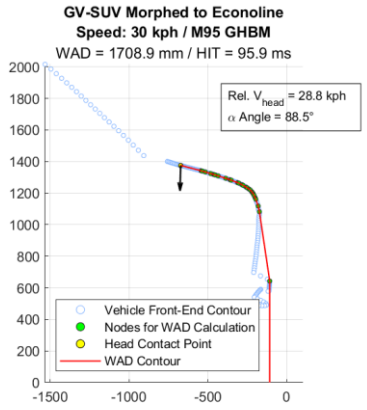
40 kph	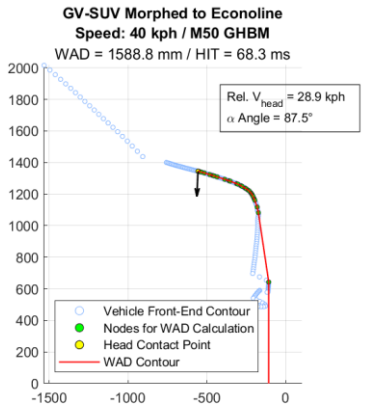	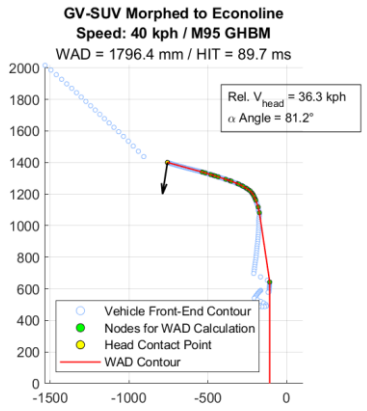
50 kph	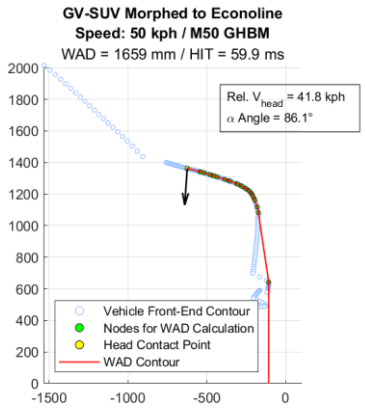	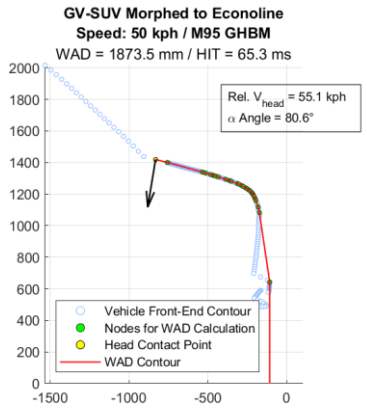

Ford Explorer (2003)

	6YO	F05
30 kph	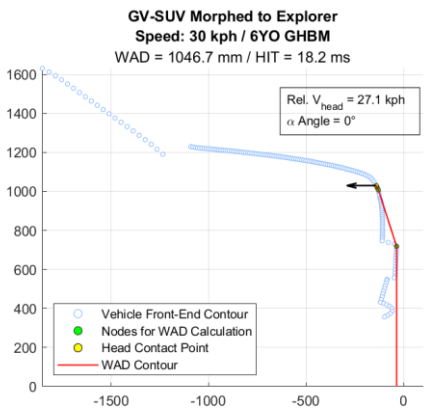	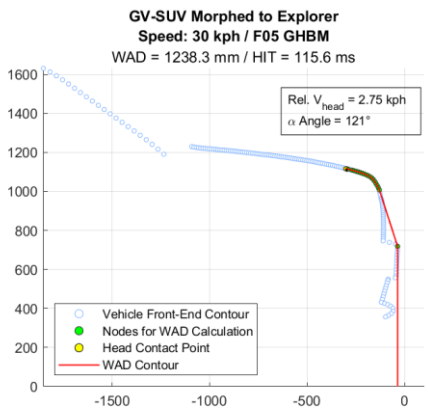
40 kph	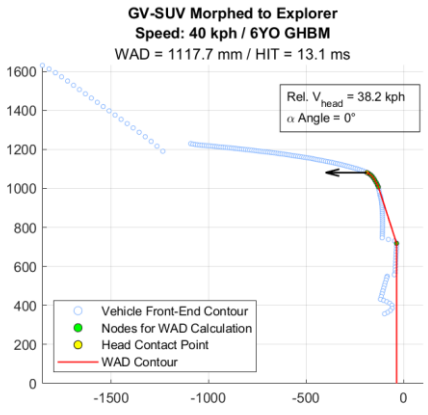	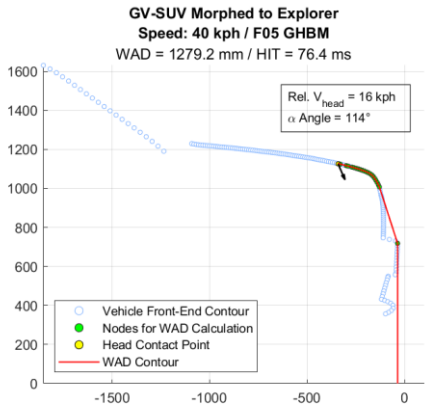
50 kph	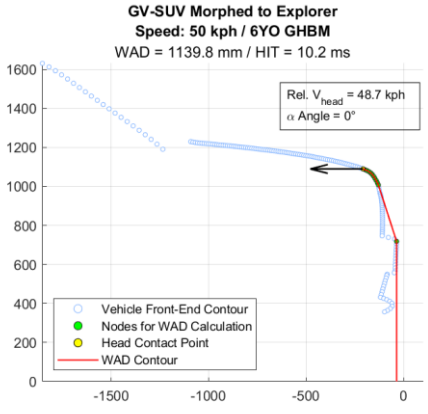	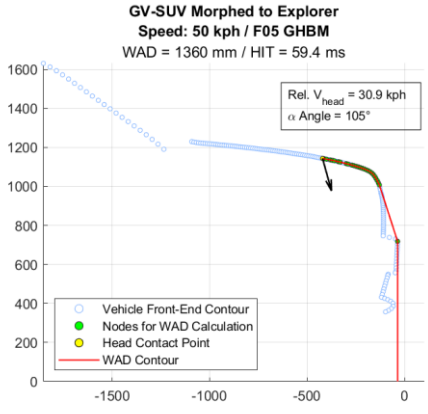

Ford Explorer (2003)

	M50	M95
30 kph	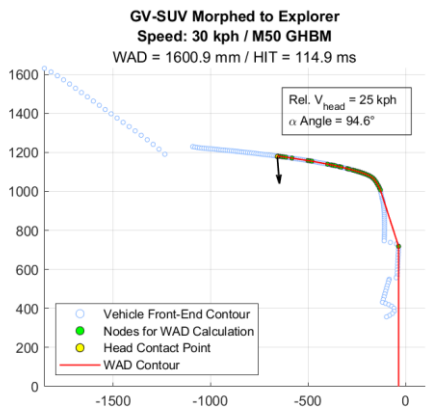	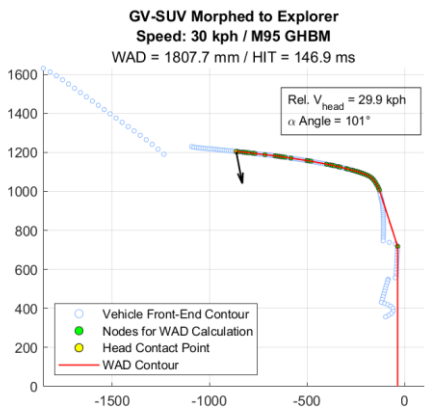
40 kph	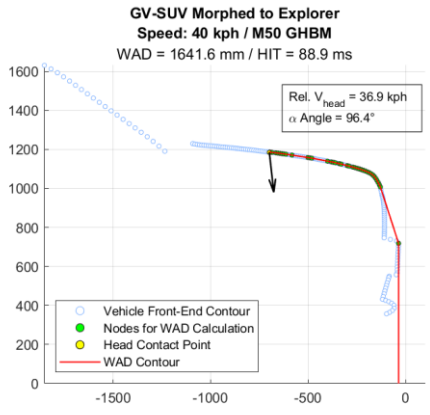	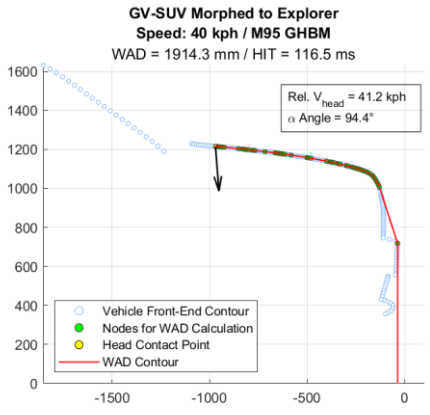
50 kph	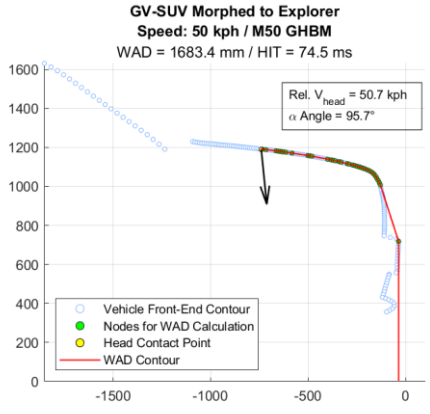	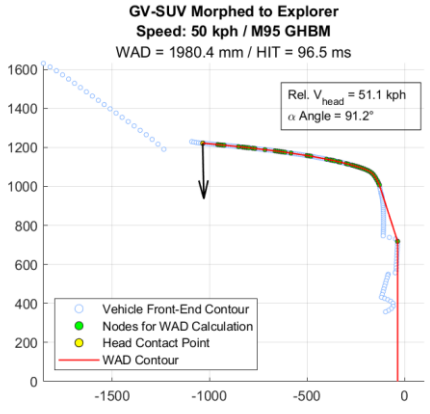

Ford F-250 (2006)

	6YO	F05
30 kph	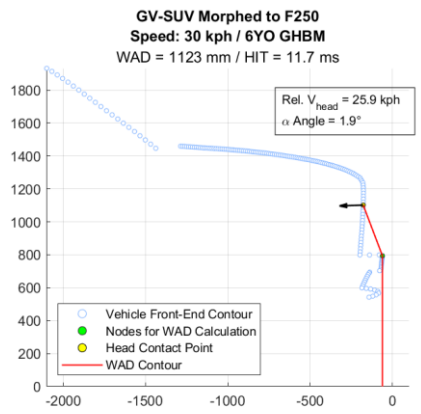	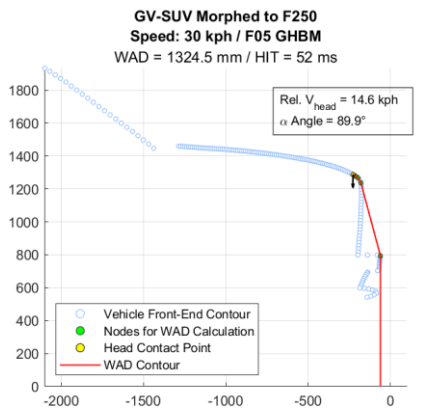
40 kph	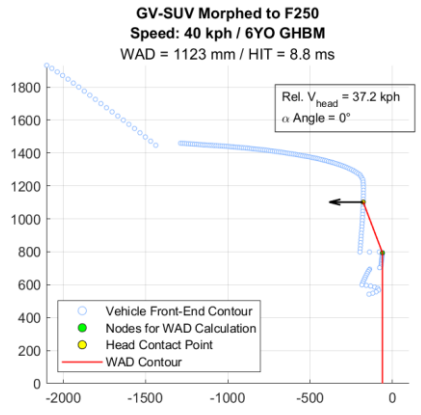	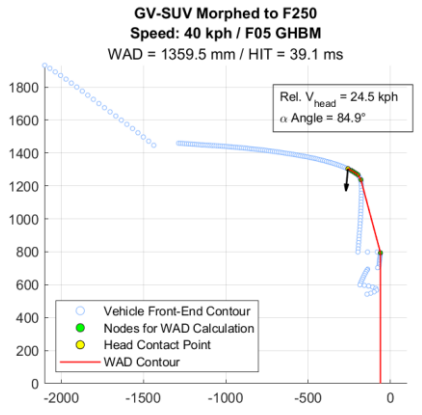
50 kph	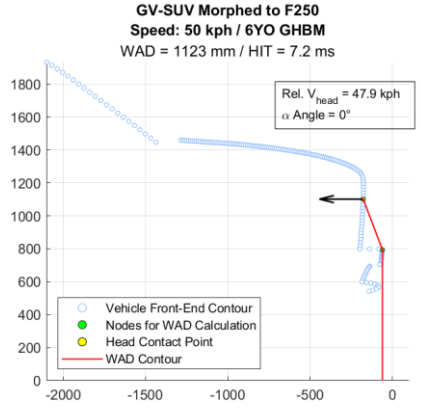	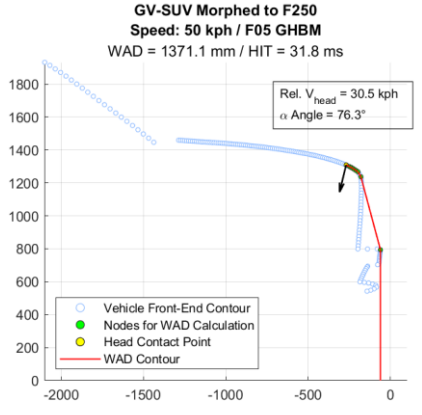

Ford F-250 (2006)

	M50	M95
30 kph	**Normal termination (Pedestrian knocked down without head contact)**	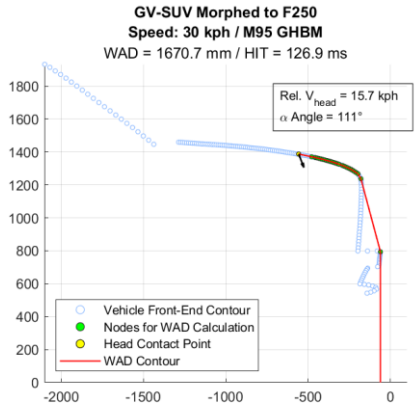
40 kph	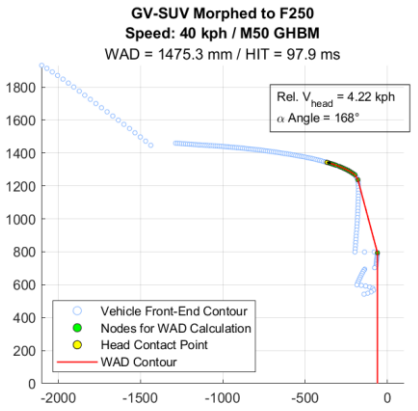	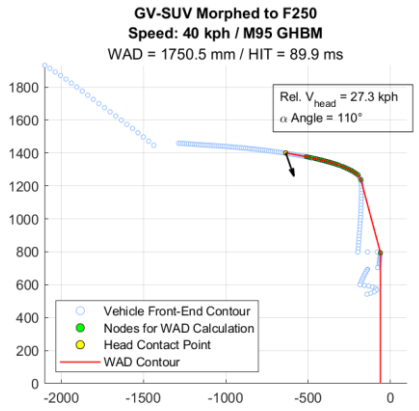
50 kph	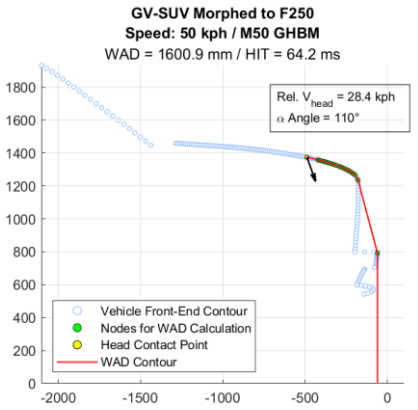	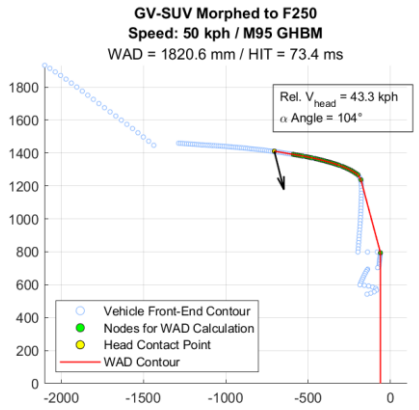

Ford Focus (2013)

	6YO	F05
30 kph	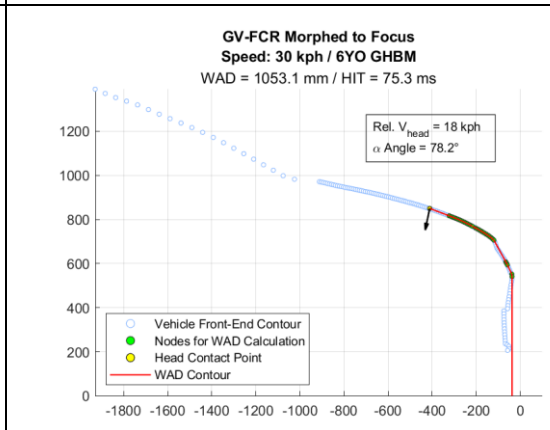	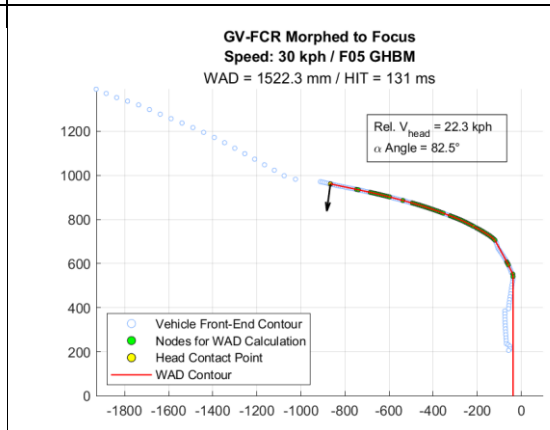
40 kph	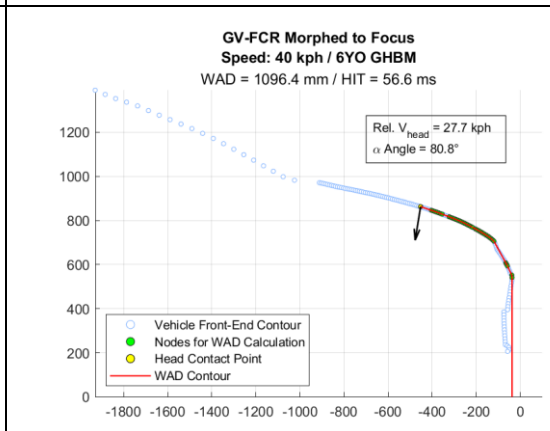	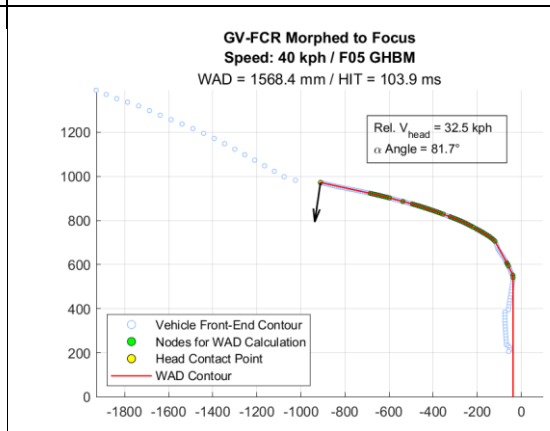
50 kph	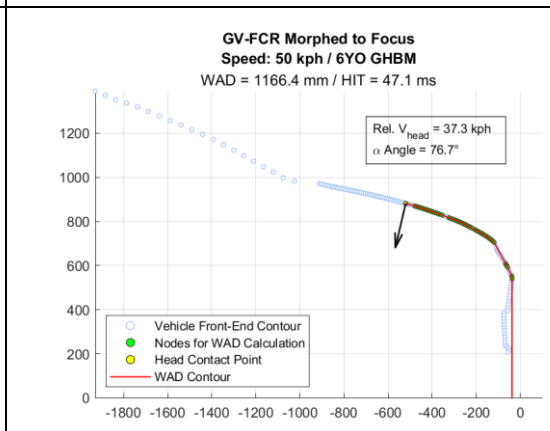	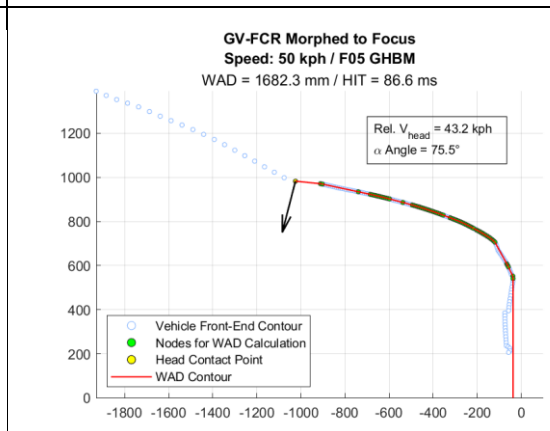

Ford Focus (2013)

	M50	M95
30 kph	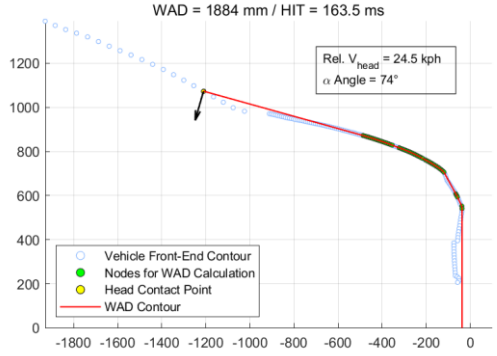	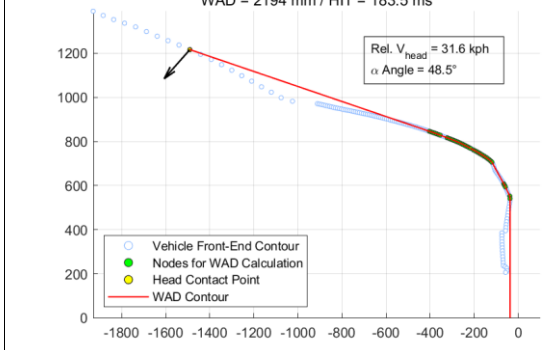
40 kph	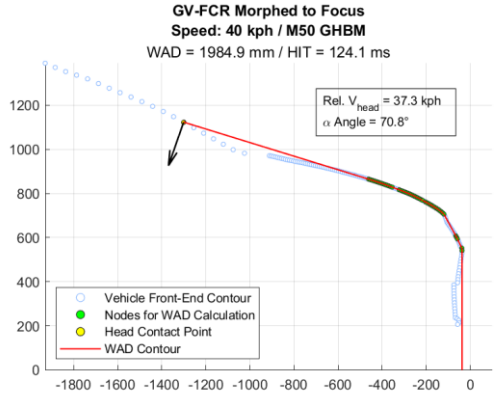	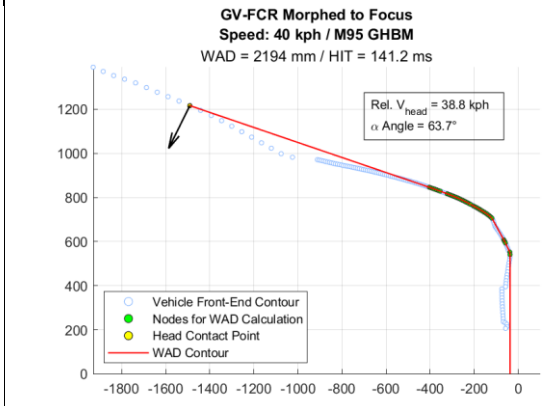
50 kph	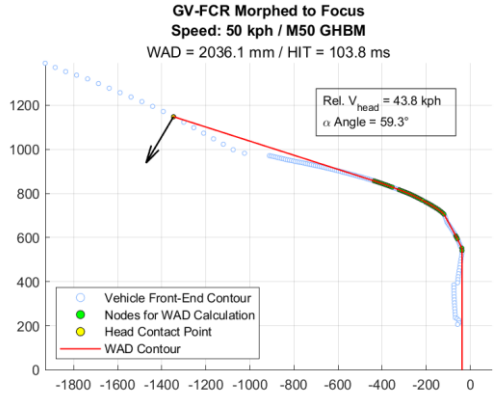	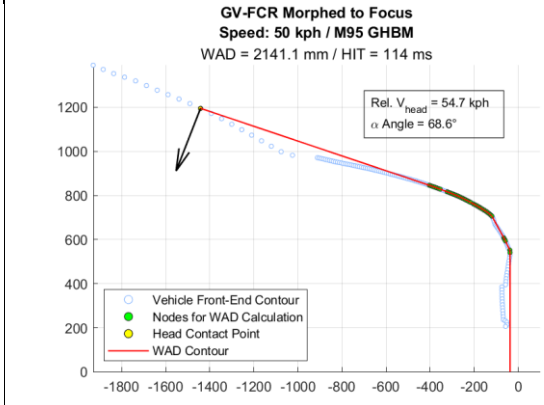

Toyota Highlander (2019)

	6YO	F05
30 kph	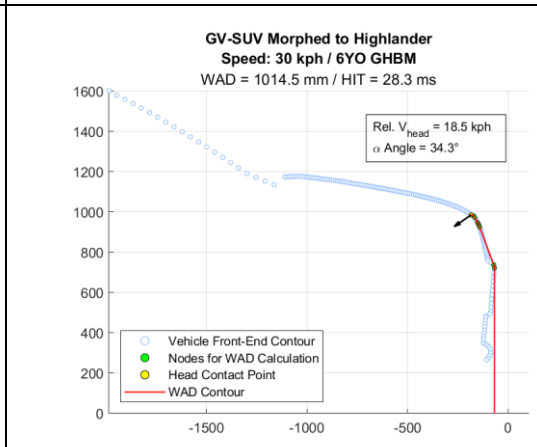	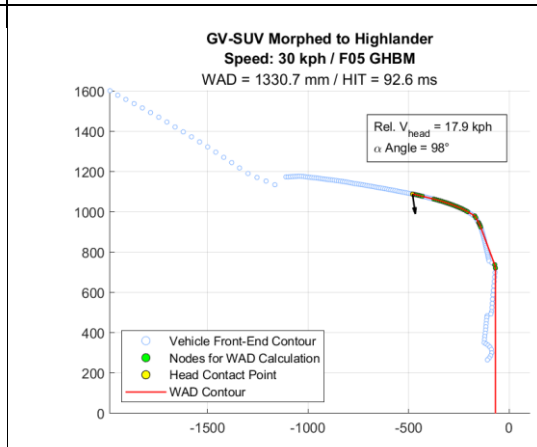
40 kph	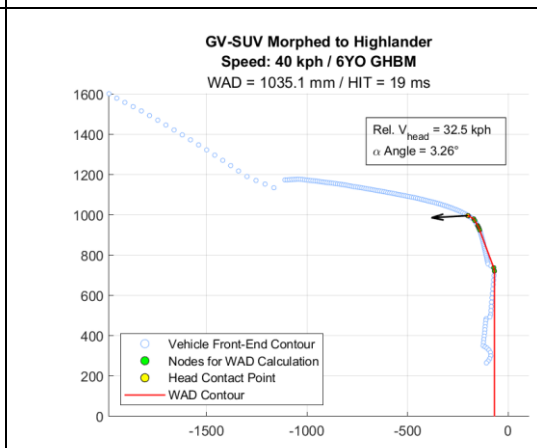	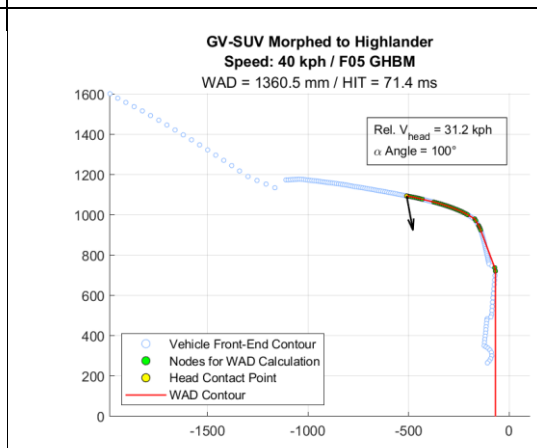
50 kph	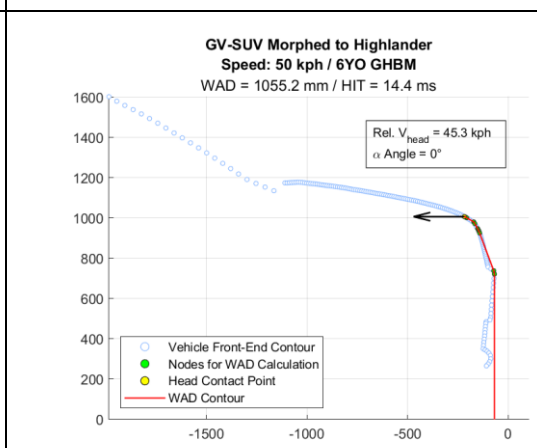	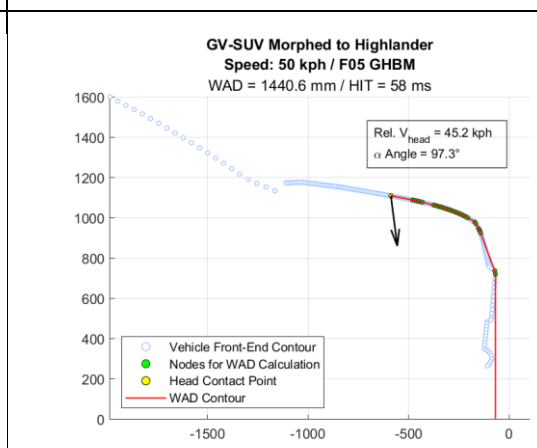

Toyota Highlander (2019)

	M50	M95
30 kph	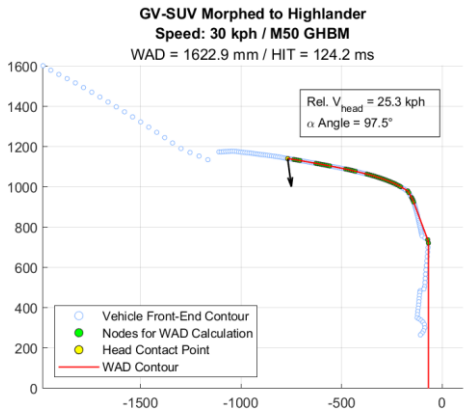	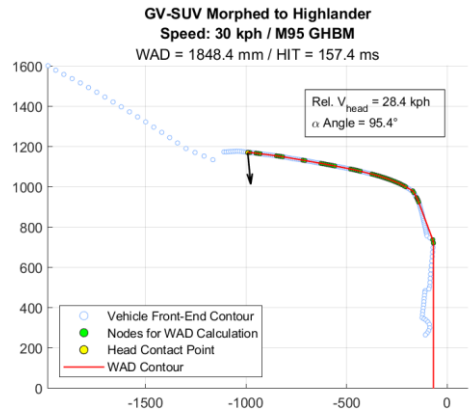
40 kph	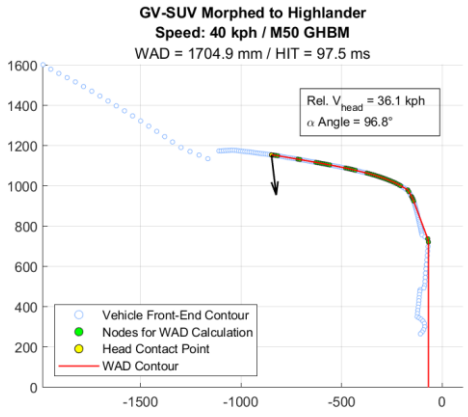	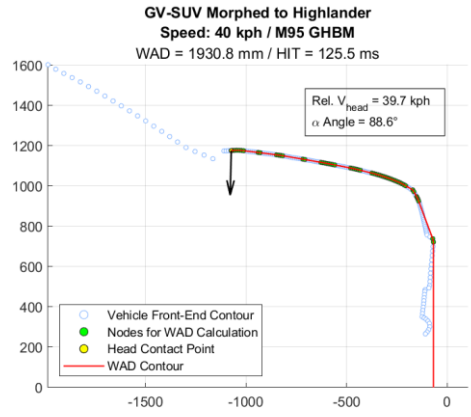
50 kph	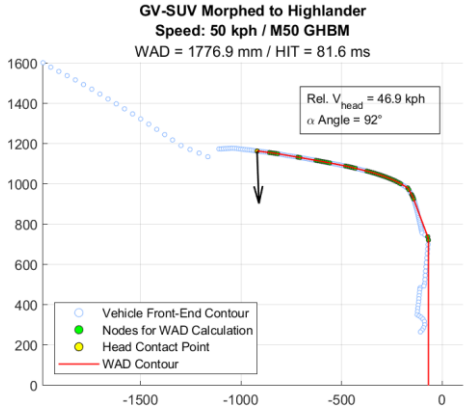	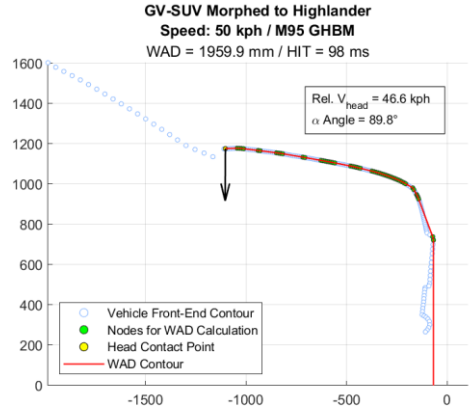

Dodge Neon (1996)

	6YO	F05
30 kph	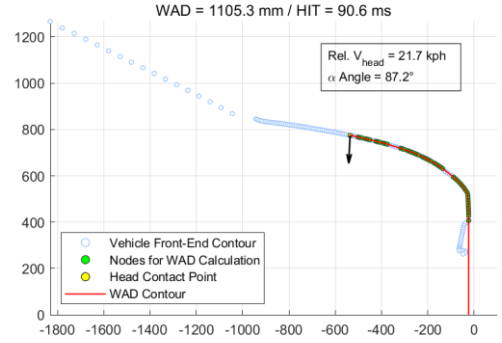	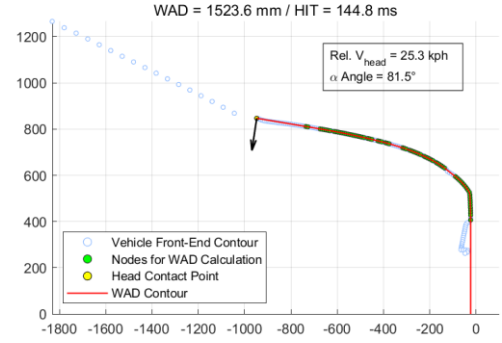
40 kph	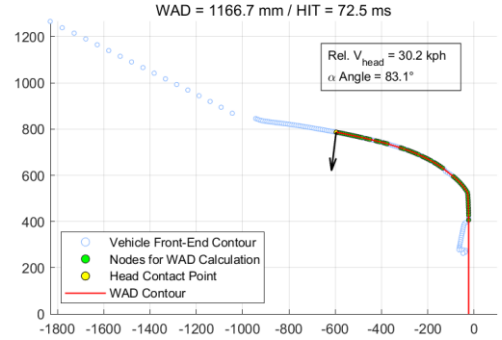	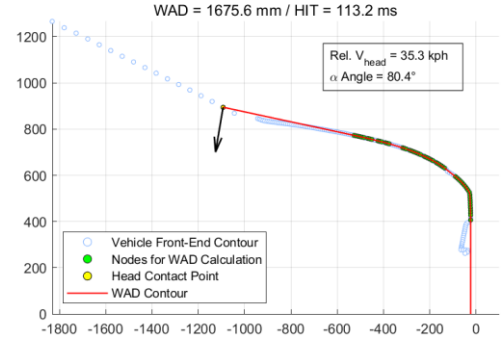
50 kph	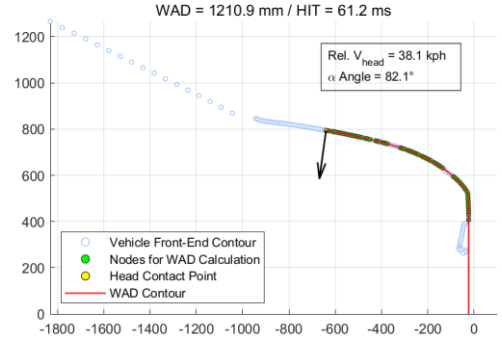	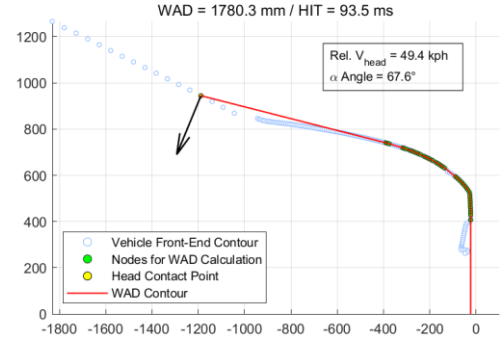

Dodge Neon (1996)

	M50	M95
30 kph	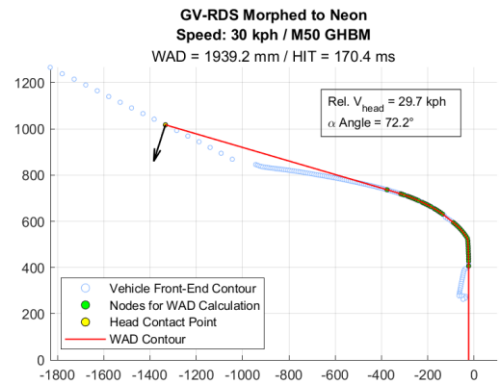	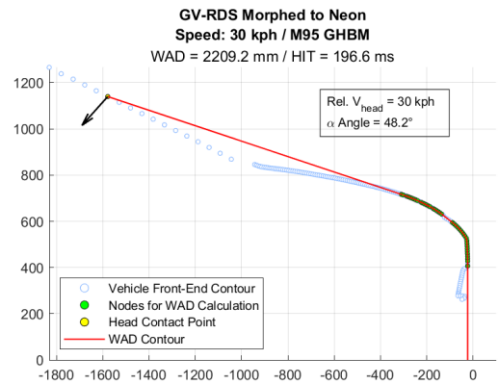
40 kph	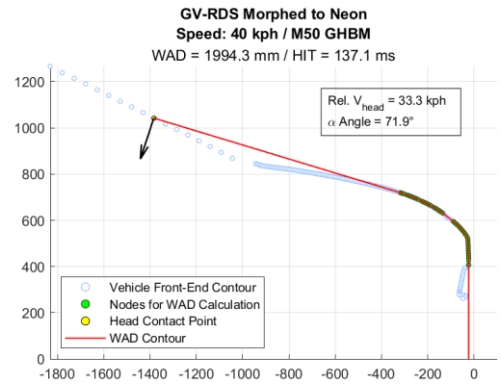	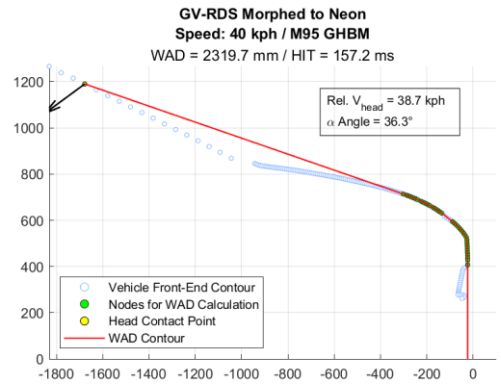
50 kph	**Error Termination** **(Negative volume in left armpit area)**	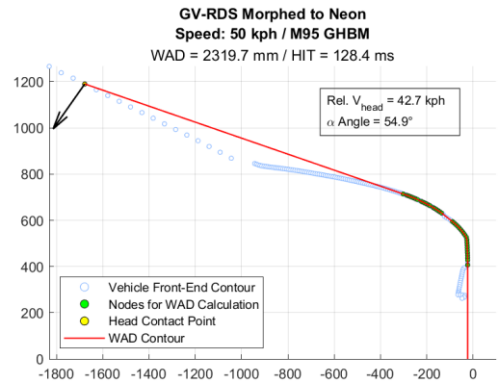

Honda Odyssey (2018)

	6YO	F05
30 kph	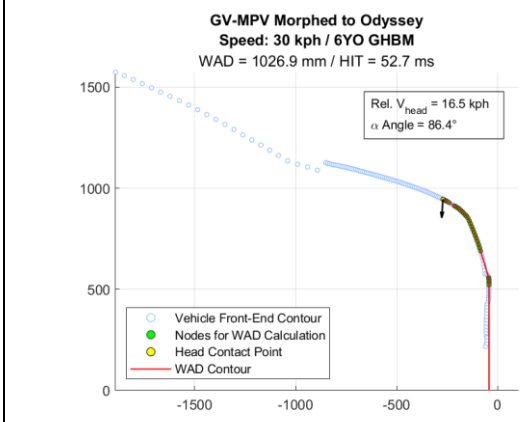	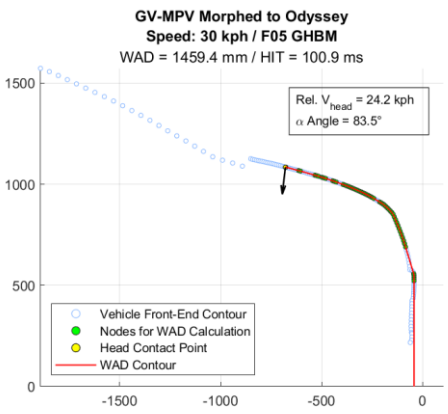
40 kph	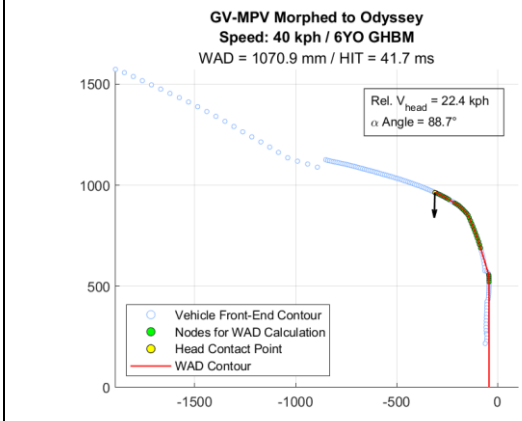	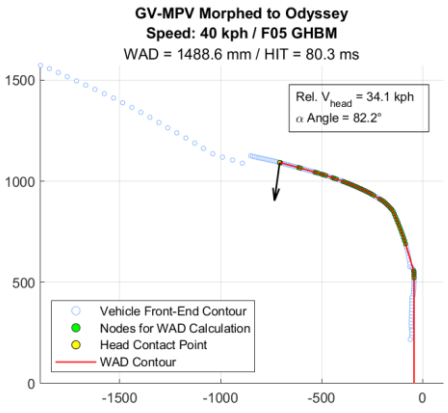
50 kph	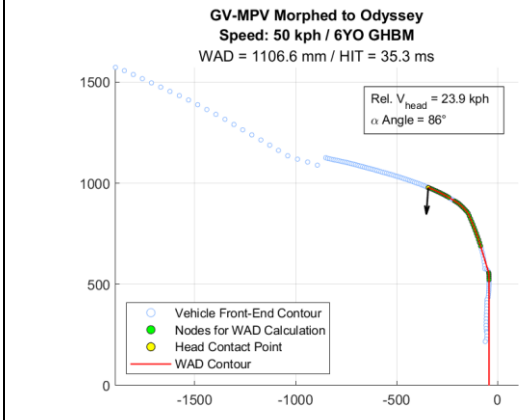	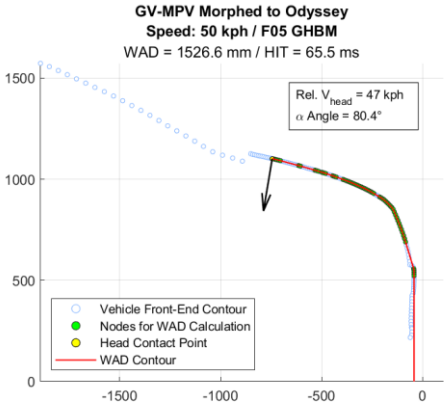

Honda Odyssey (2018)

	M50	M95
30 kph	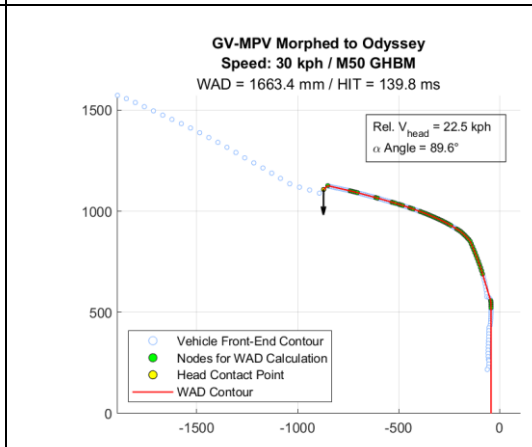	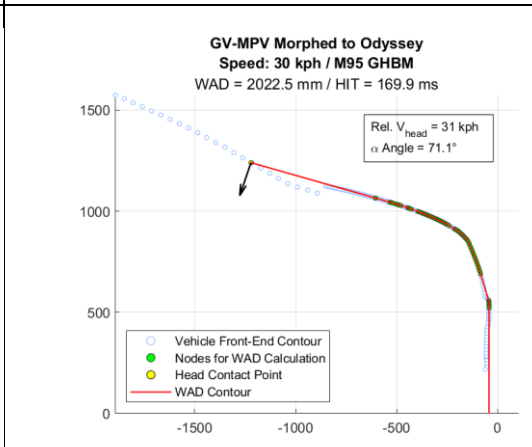
40 kph	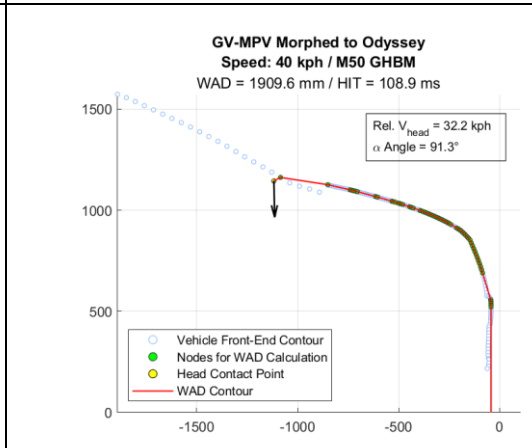	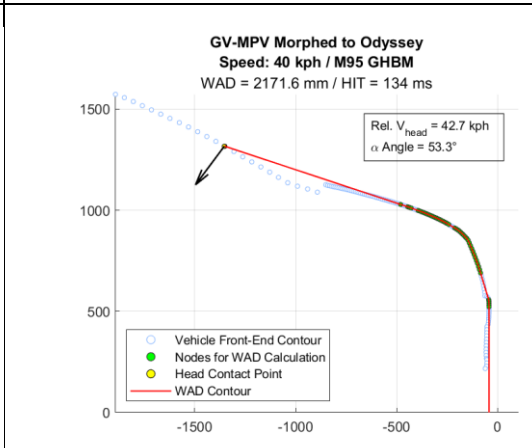
50 kph	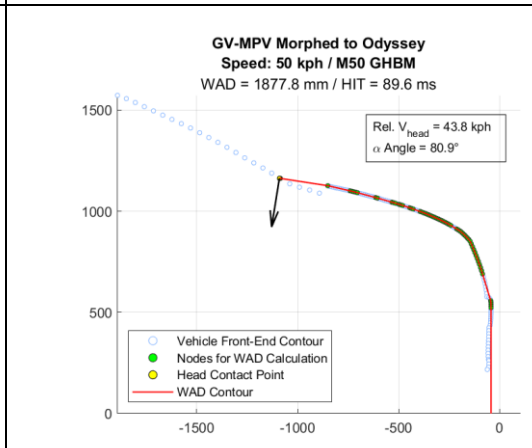	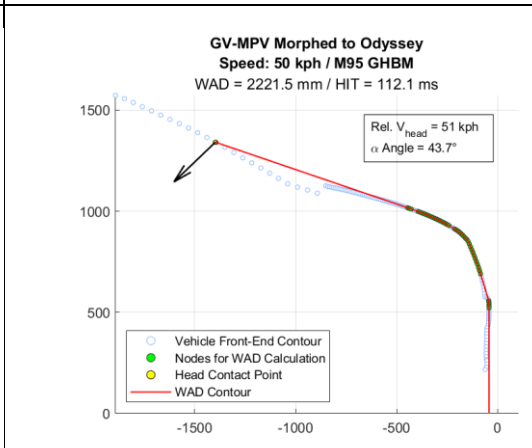

Chrysler Pacifica (2019)

	6YO	F05
30 kph	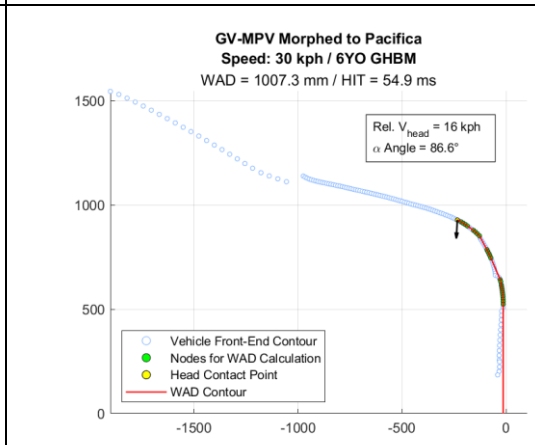	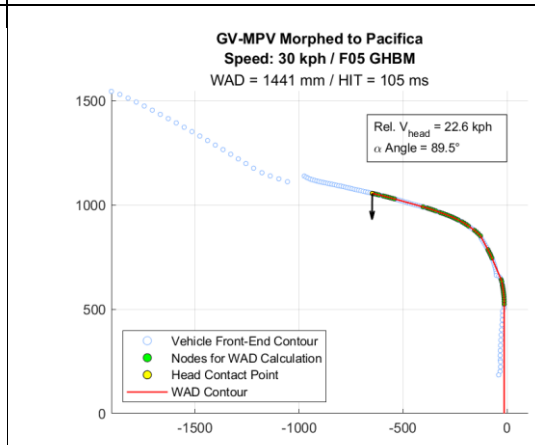
40 kph	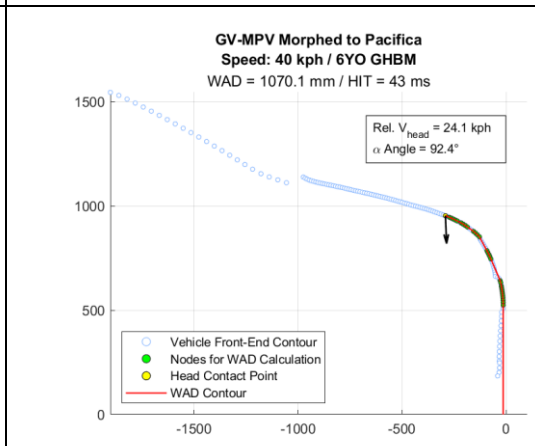	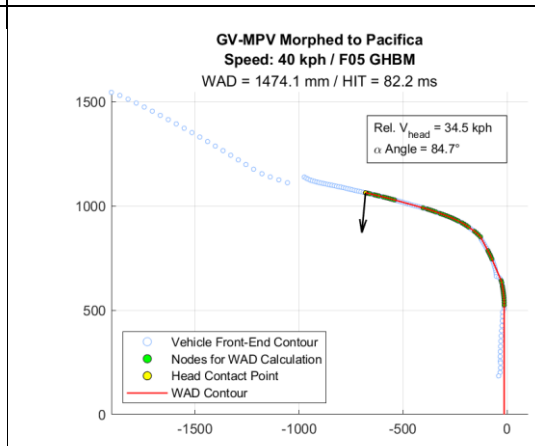
50 kph	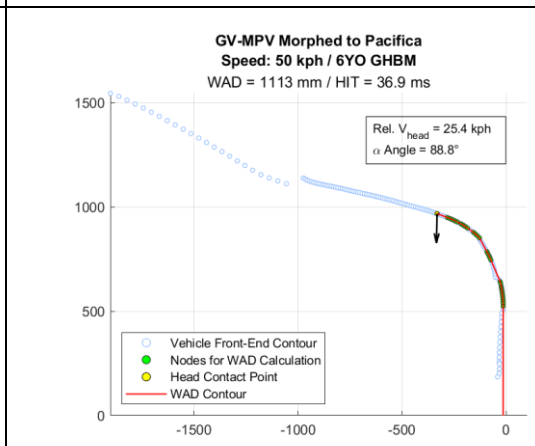	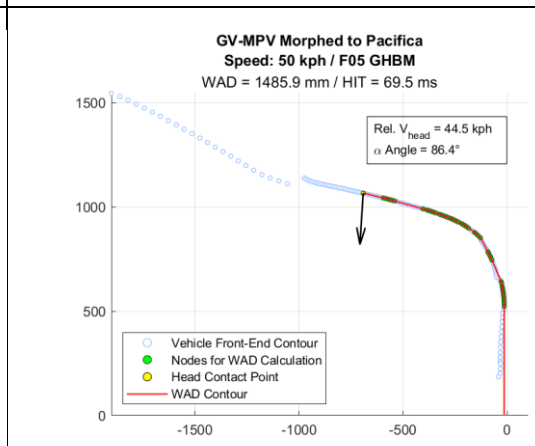

Chrysler Pacifica (2019)

	M50	M95
30 kph	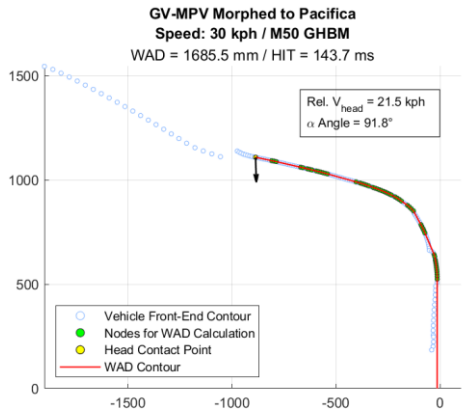	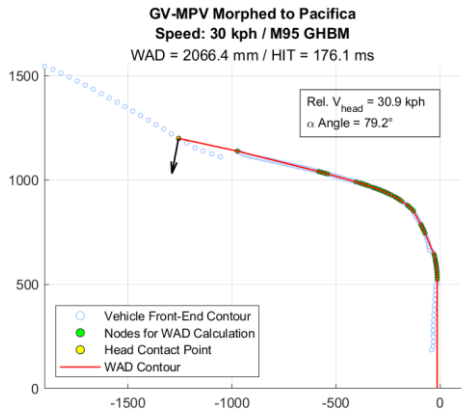
40 kph	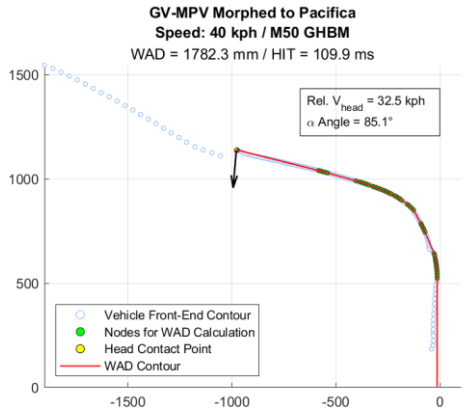	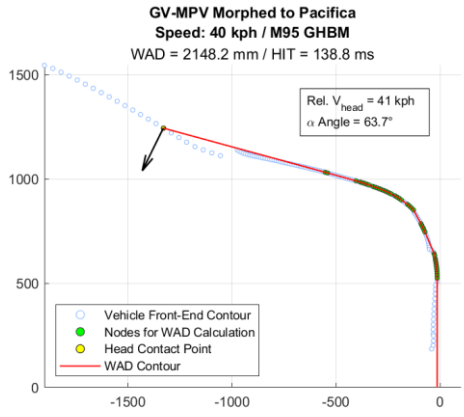
50 kph	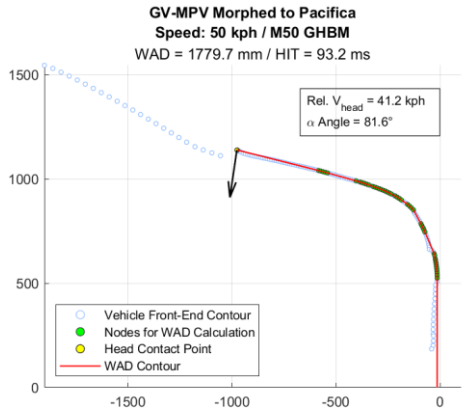	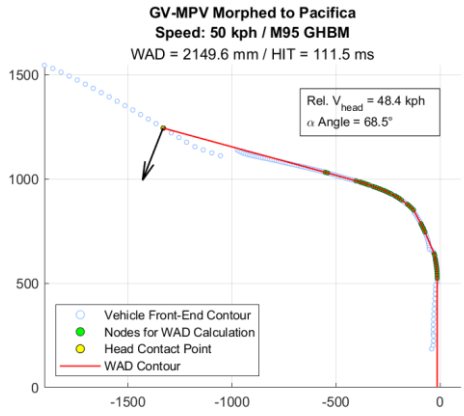

Toyota RAV4 (1997)

	6YO	F05
30 kph	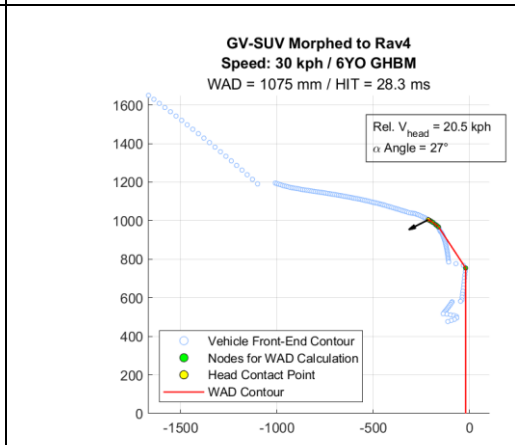	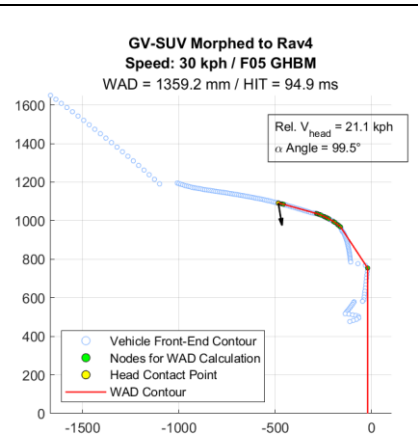
40 kph	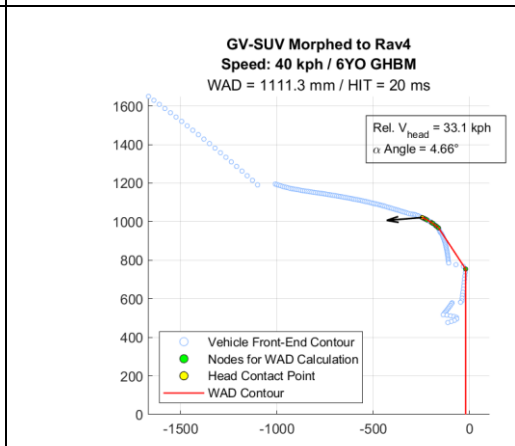	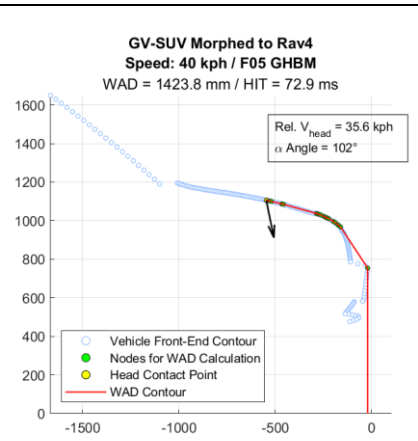
50 kph	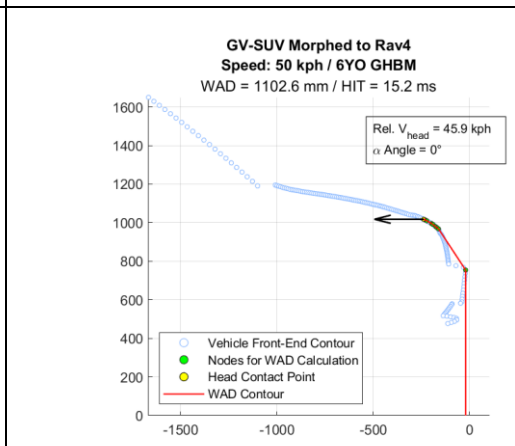	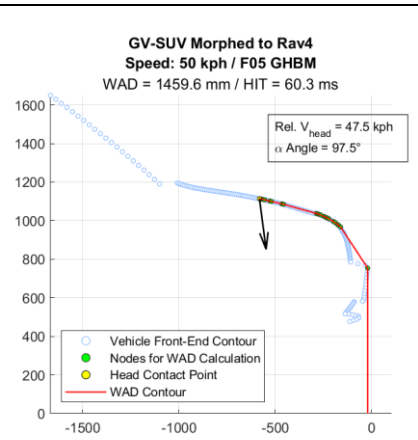

Toyota RAV4 (1997)

	M50	M95
30 kph	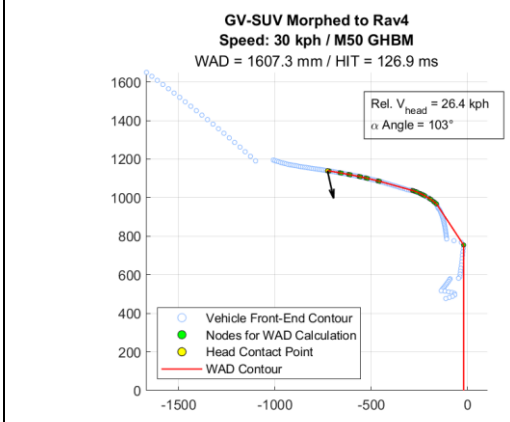	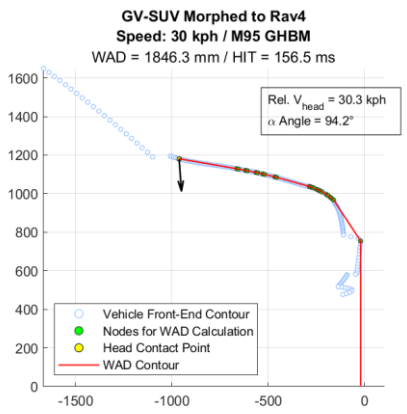
40 kph	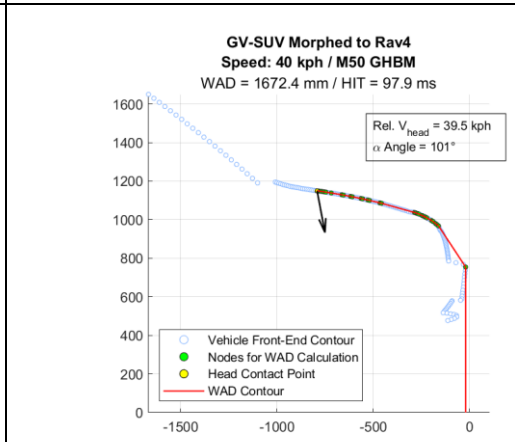	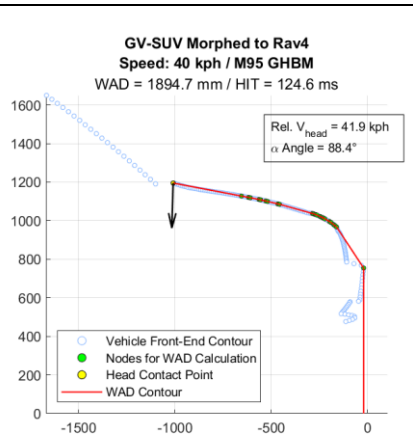
50 kph	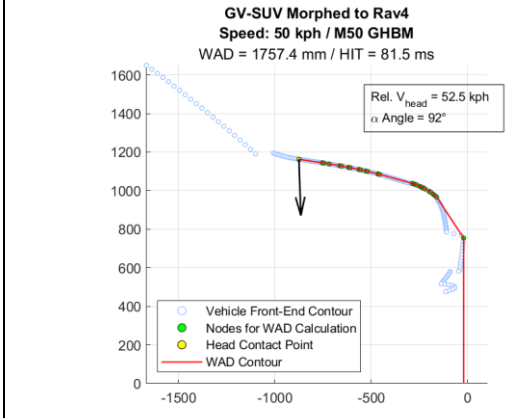	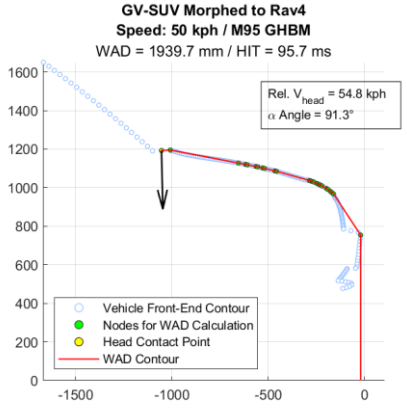

Nissan Rogue (2020)

	6YO	F05
30 kph	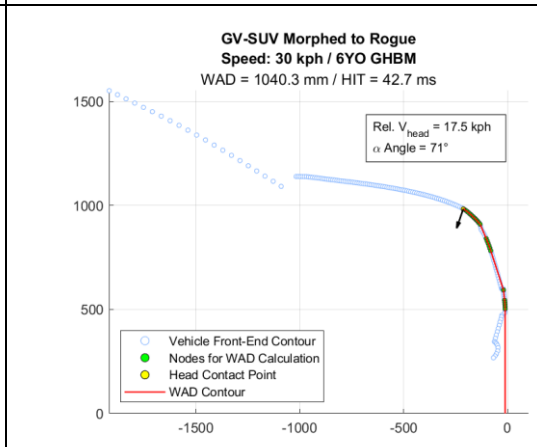	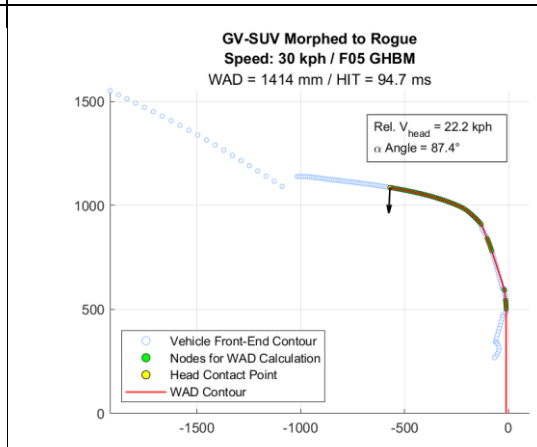
40 kph	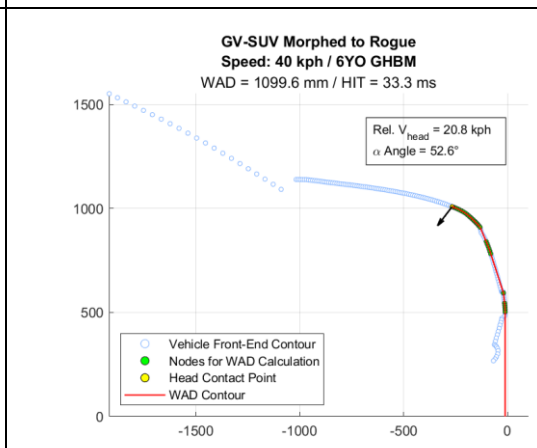	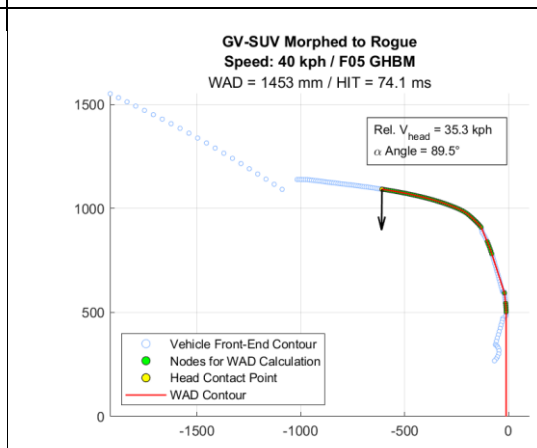
50 kph	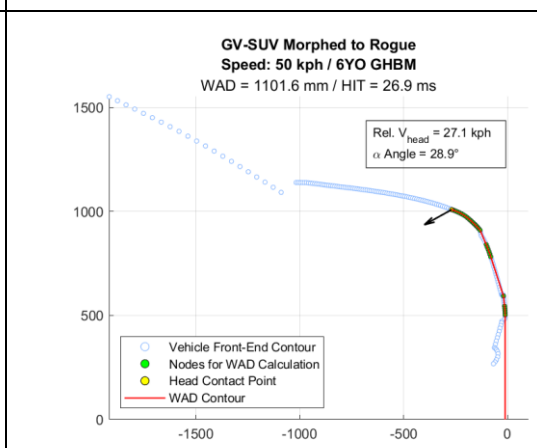	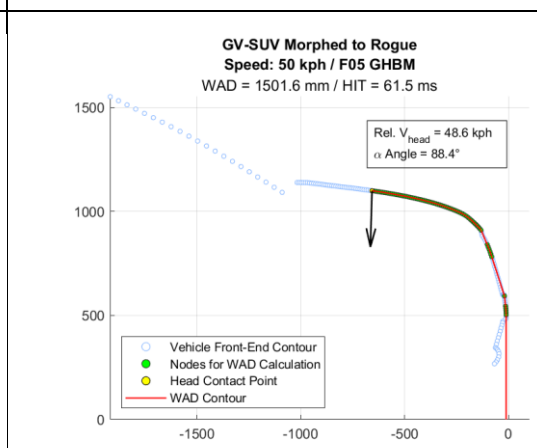

Nissan Rogue (2020)

	M50	M95
30 kph	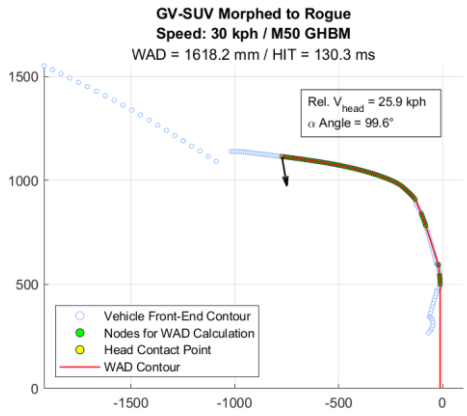	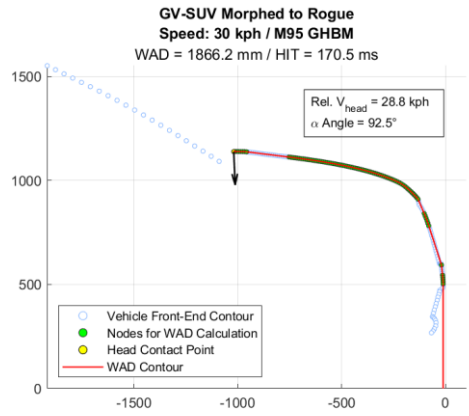
40 kph	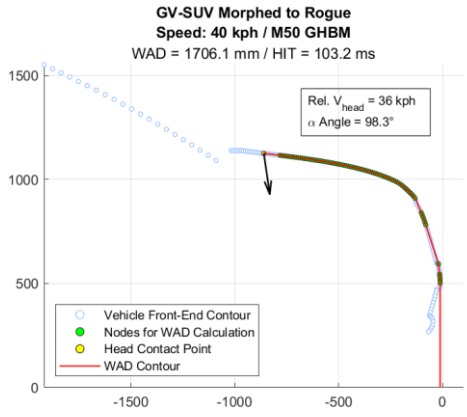	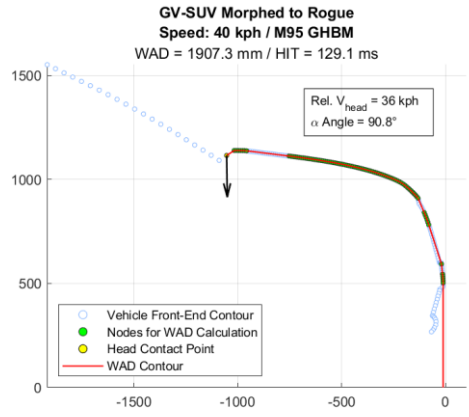
50 kph	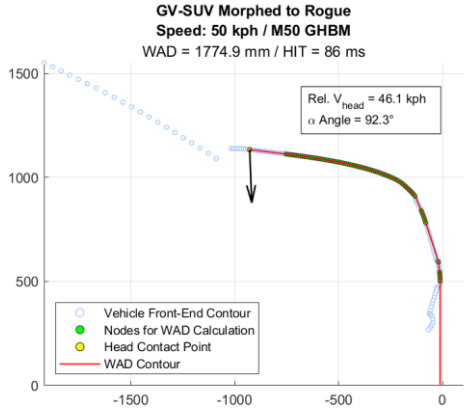	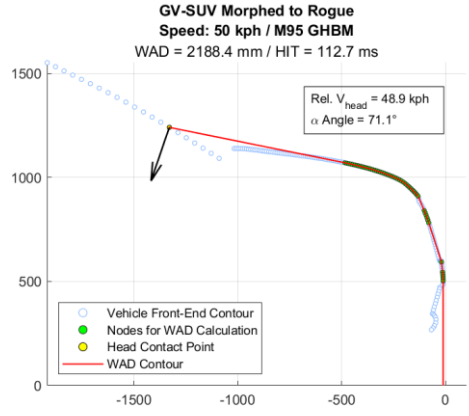

Toyota Sienna (2016)

	6YO	F05
30 kph	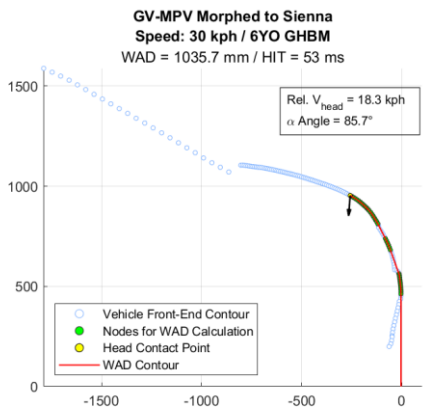	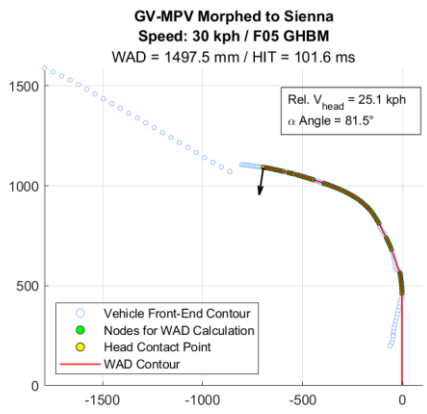
40 kph	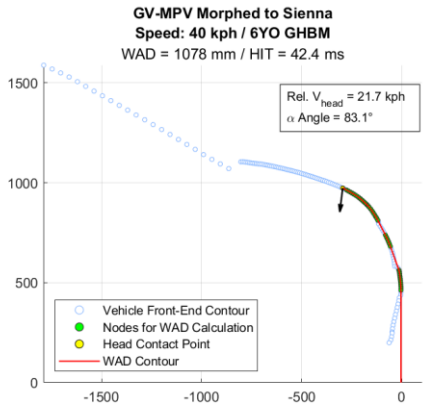	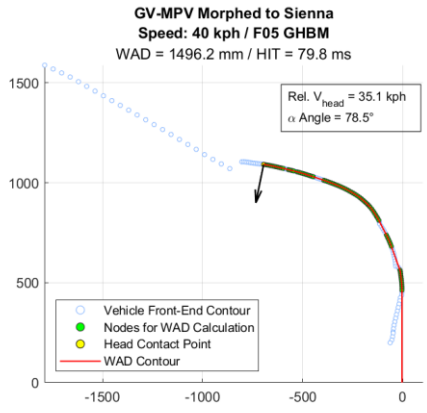
50 kph	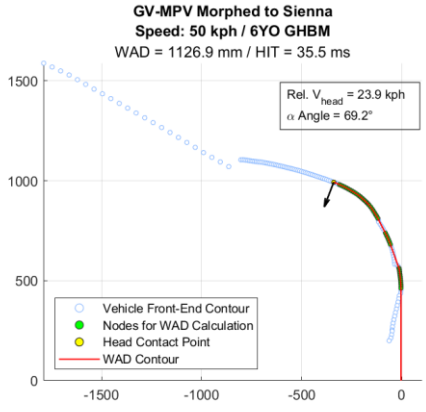	**Error Termination** **(Negative volume in lower leg flesh)**

Toyota Sienna (2016)

	M50	M95
30 kph	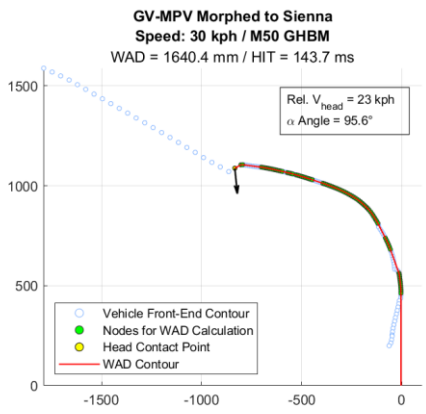	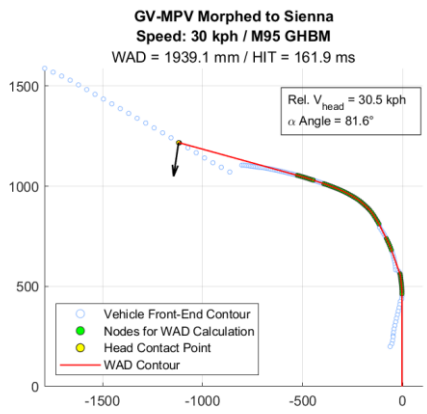
40 kph	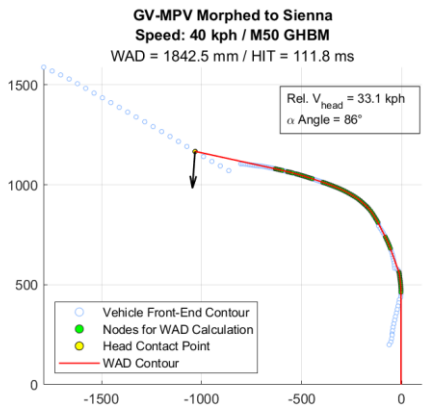	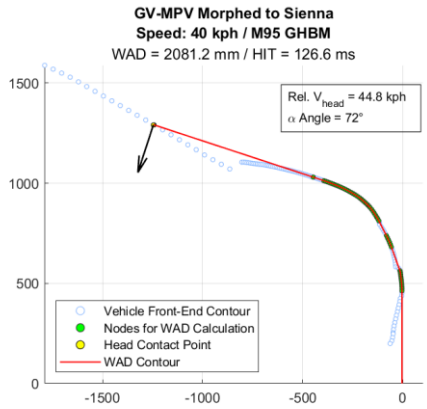
50 kph	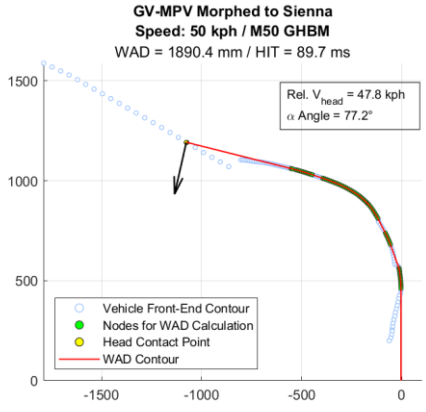	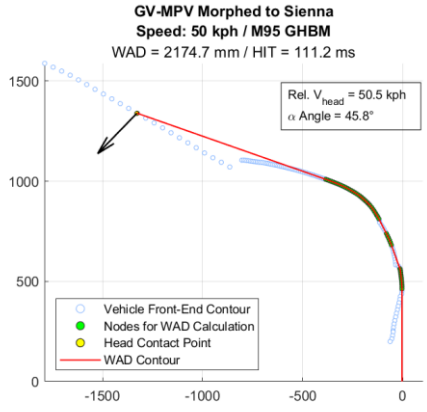

Chevrolet Silverado (2014)

	6YO	F05
30 kph	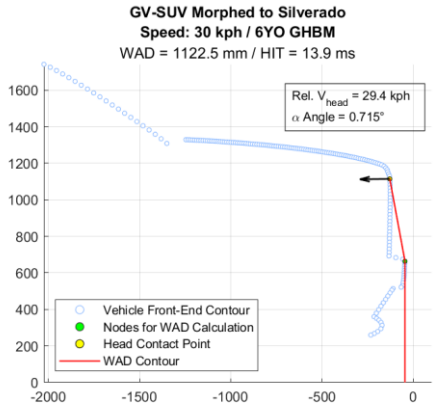	**Normal termination (Pedestrian knocked down without head contact)**
40 kph	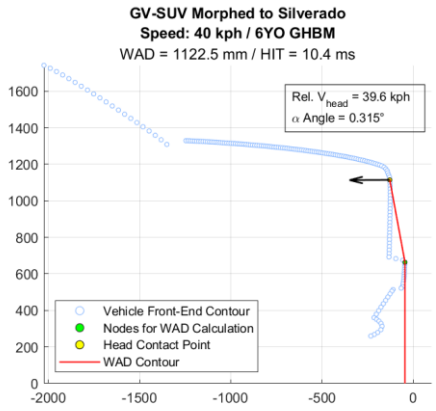	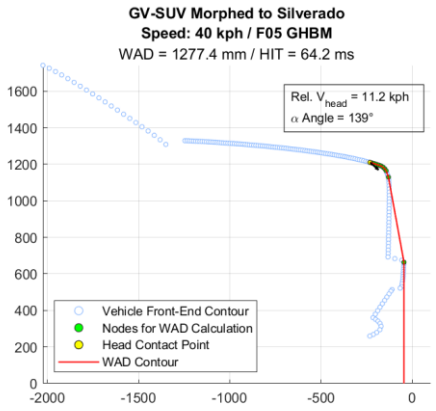
50 kph	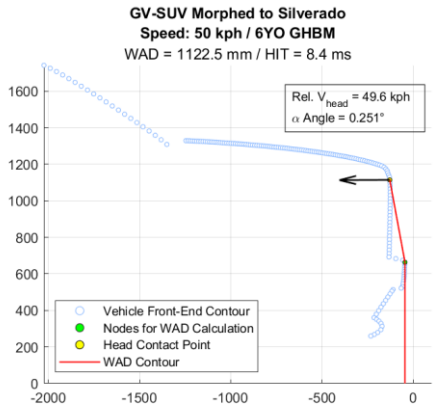	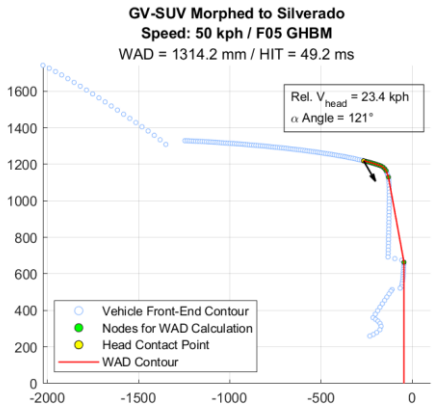

Chevrolet Silverado (2014)

	M50	M95
30 kph	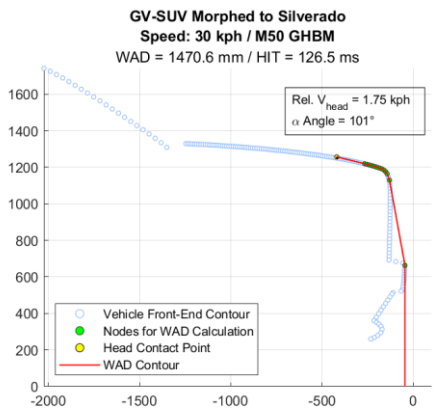	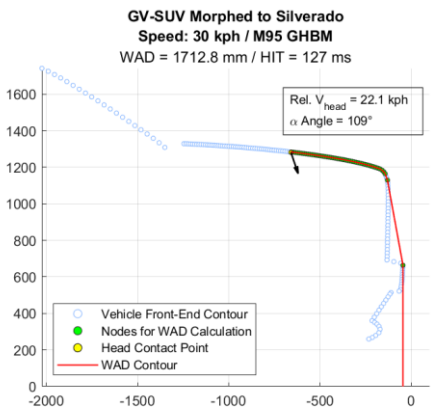
40 kph	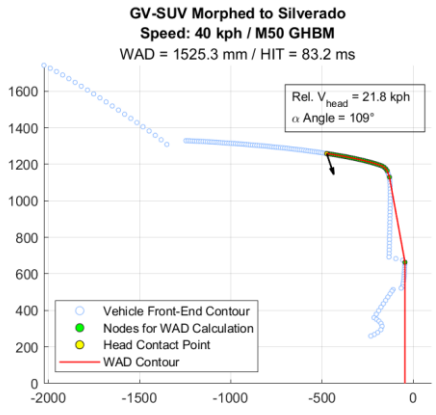	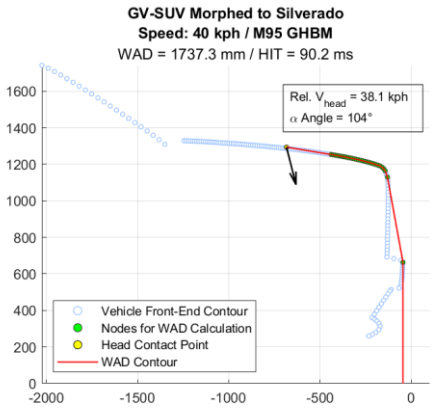
50 kph	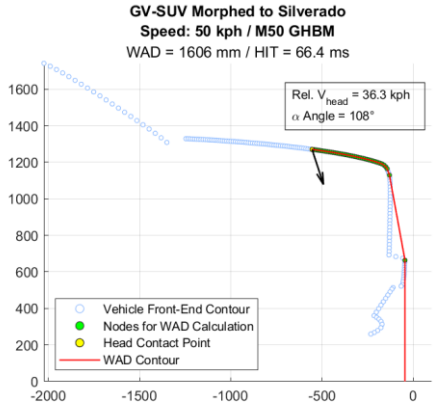	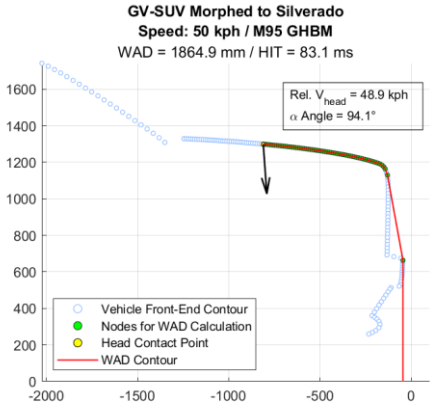

Ford Taurus (2001)

	6YO	F05
30 kph	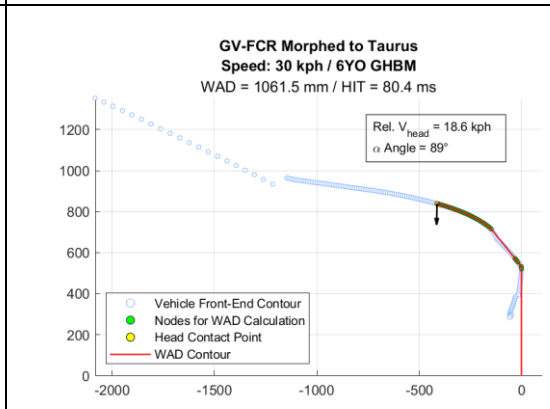	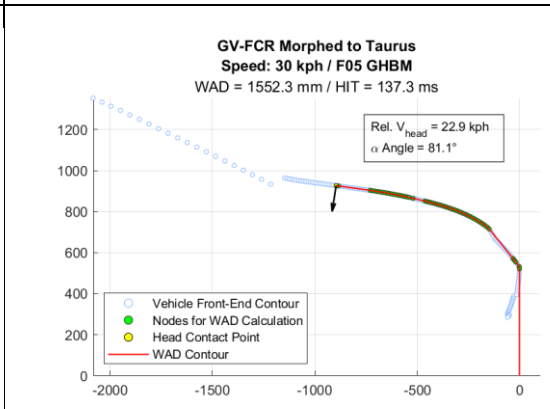
40 kph	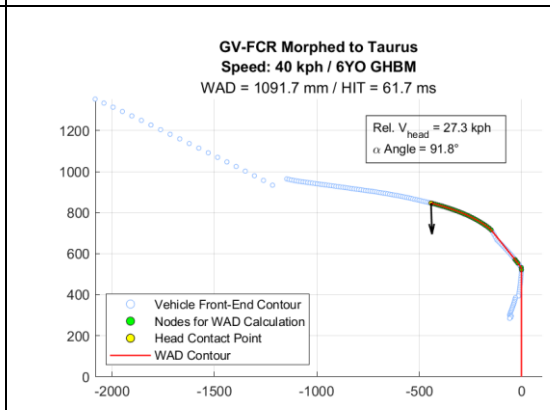	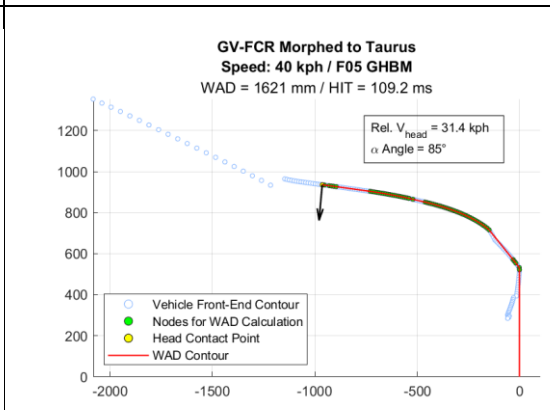
50 kph	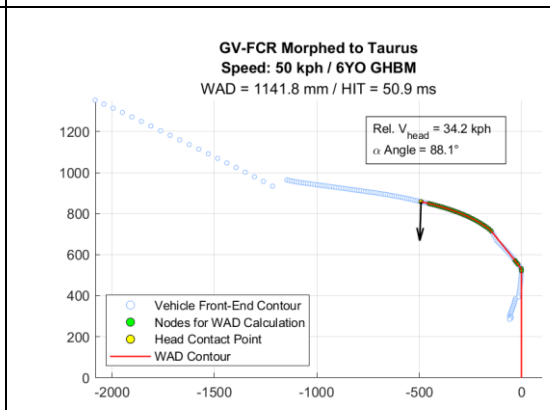	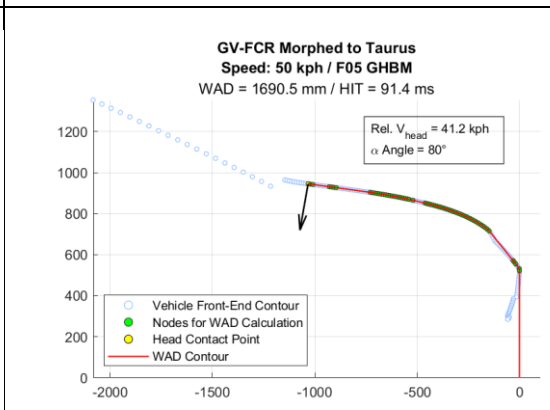

Ford Taurus (2001)

	M50	M95
30 kph	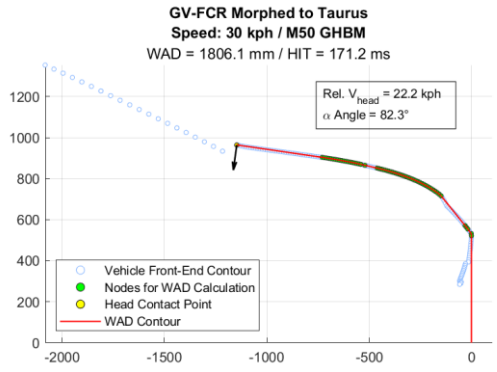	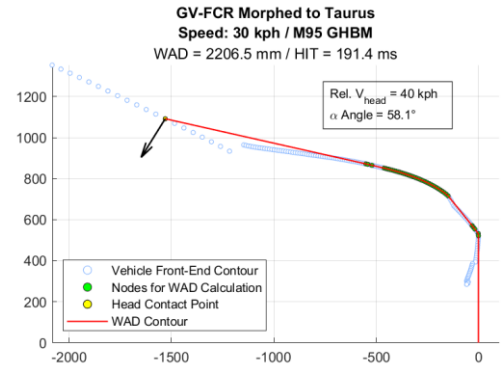
40 kph	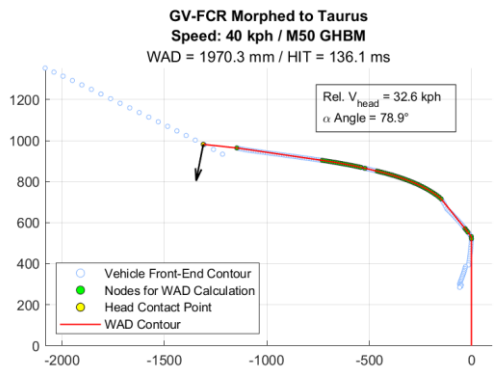	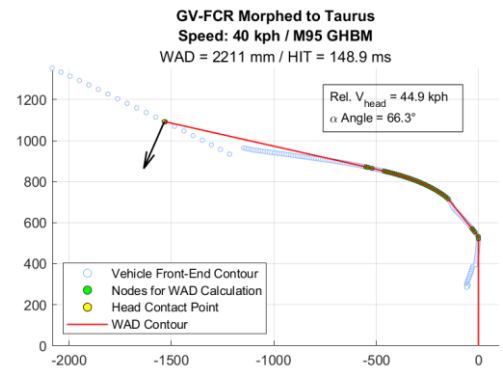
50 kph	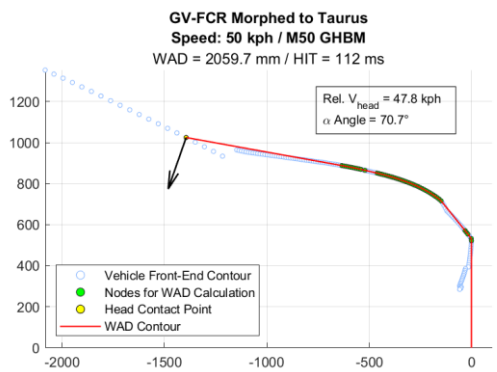	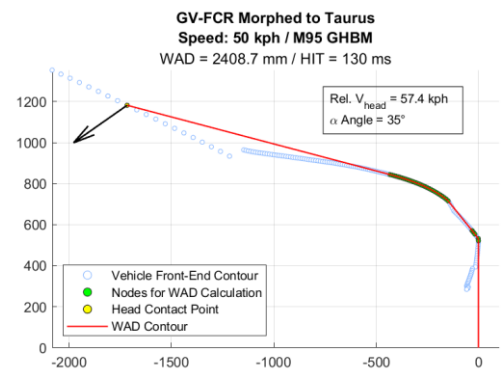

Ford Yaris (2010)

	6YO	F05
30 kph	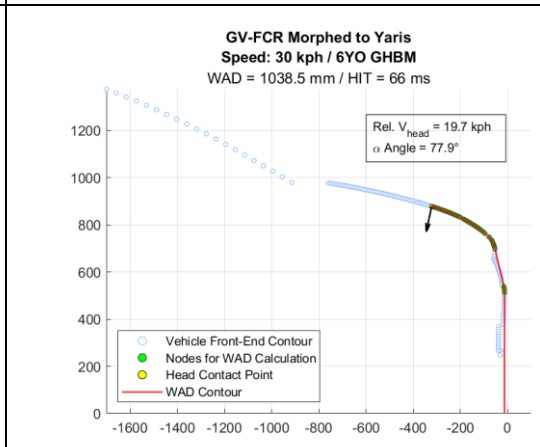	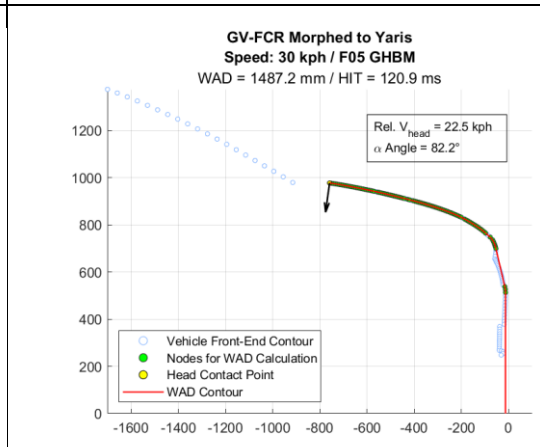
40 kph	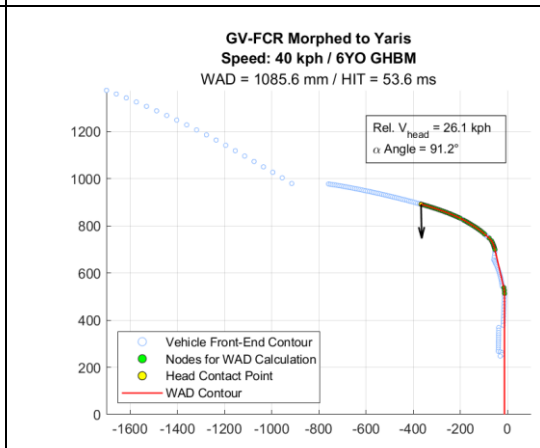	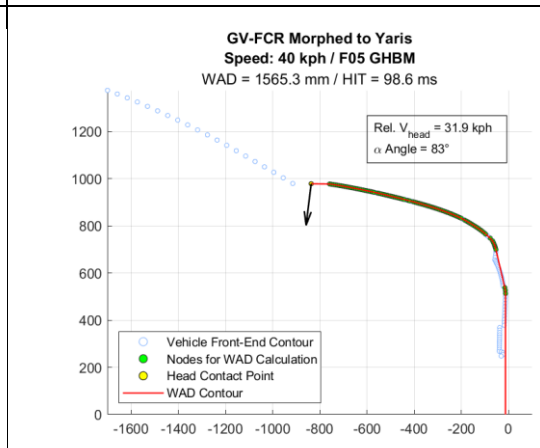
50 kph	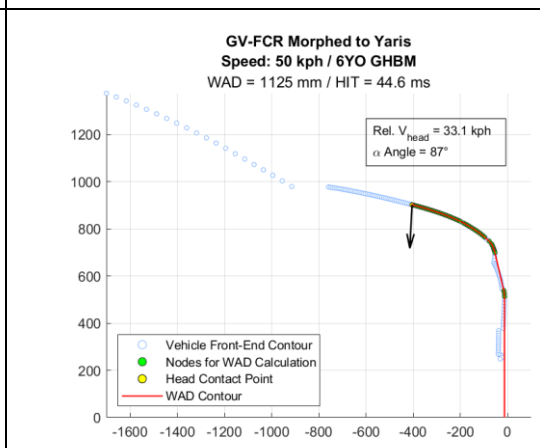	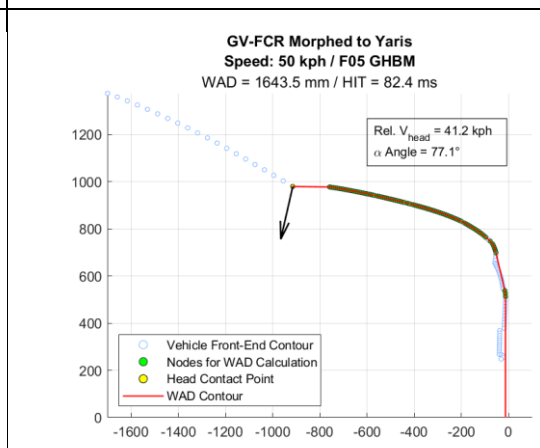

Ford Yaris (2010)

	M50	M95
30 kph	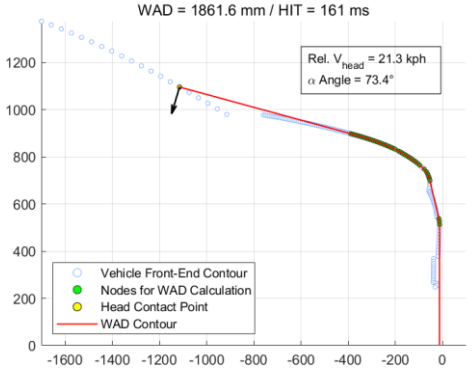	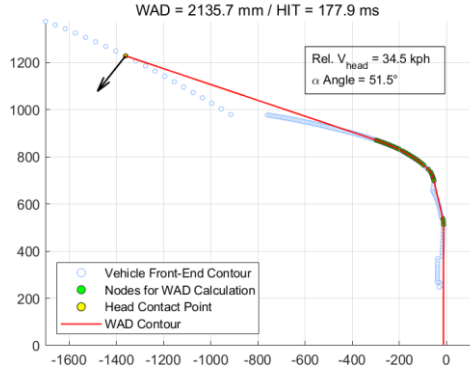
40 kph	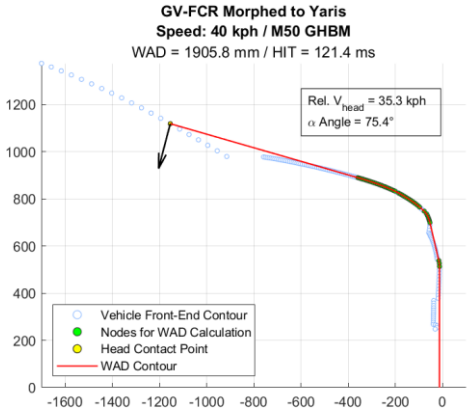	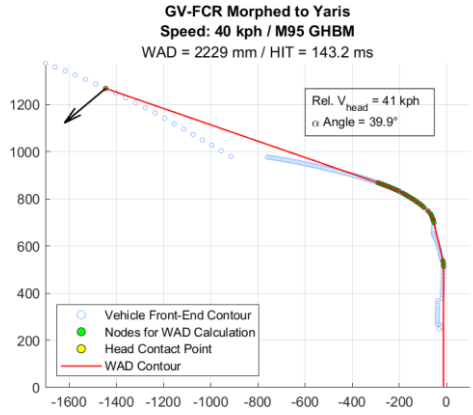
50 kph	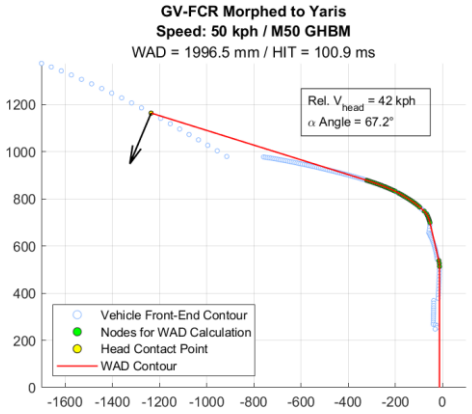	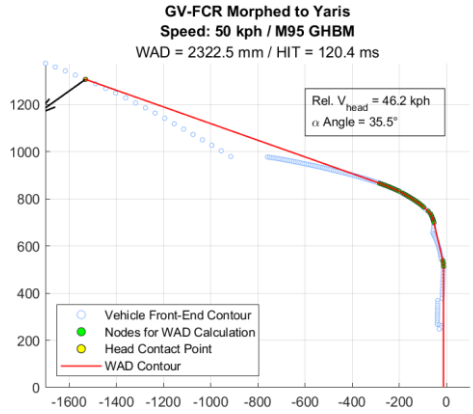

DOT HS 813 518
November 2023

U.S. Department
of Transportation

**National Highway
Traffic Safety
Administration**

16077-102523-v1a